Nouveaux peptides chélateurs du Cu(I) comme candidat potentiel pour le traitement de maladie de Wilson

Edit Mesterhazy

Communauté UNIVERSITÉ Grenoble Alpes

THÈSE

Pour obtenir le grade de

DOCTEUR DE LA COMMUNAUTÉ UNIVERSITÉ GRENOBLE ALPES

DOCTEUR DE L'UNIVERSITE DE SZEGED

Spécialité : Chimie inorganique et Bio inorganique

Arrêté ministériel : 25 mai 2016

Présentée par

Edit MESTERHAZY

Thèse dirigée par **Pascale DELANGLE**, CEA

préparée dans le cadre d'un co-tutelle au sein du **Laboratoire Systèmes Moléculaires et Nano Matériaux pour l'Énergie et la Santé**
dans **l'École Doctorale Chimie et Sciences du Vivant**

Nouveaux peptides chélateurs du Cu(I) comme candidat potentiel pour le traitement de maladie de Wilson

New peptidic Cu(I) chelators as potential candidates for the treatment of Wilson's disease

Thèse soutenue publiquement le **12 décembre 2018**,
devant le jury composé de :

Madame PASCALE DELANGLE
CHERCHEUSE, CEA GRENOBLE, Directeur de thèse
Madame KATALIN VARNAGY
PROFESSEUR, UNIVERSITE DE DEBRECEN - HONGRIE, Rapporteur
Monsieur MARIUS REGLIER
DIRECTEUR DE RECHERCHE EMERITE, CNRS DELEGATION PROVENCE ET CORSE, Rapporteur
Madame CATHERINE BELLE
DIRECTRICE DE RECHERCHE, CNRS DELEGATION ALPES, Examinateur
Monsieur JANOS WOLFLING
PROFESSEUR, UNIVERSITE DE SZEGED - HONGRIE, Président
Monsieur GABOR SCHUSZTER
PROFESSEUR ASSISTANT, UNIVERSITE DE SZEGED - HONGRIE, Examinateur

UNIVERSITY OF SZEGED

Doctoral School of Chemistry

UNIVERSITÉ GRENOBLE ALPES

Doctoral School of Chemistry and Life Science

New peptidic Cu(I) chelators as potential candidates for the treatment of Wilson's disease

Doctoral (Ph.D.) Dissertation

Edit Éva Mesterházy

SUPERVISORS

Dr. Attila Jancsó
Assistant professor

Dr. Pascale Delangle
Principal Investigator

Szeged & Grenoble

2018

Table of content

List of abbreviations

ACN	acetonitrile
BAL	British anti-Lewisite = dimercaprol
BCA	bicinchoninate anion
BCS	bathocuproin disulfonate
CD	circular dicroism (spectroscopy)
COSY	correlation spectroscopy (NMR)
Cys	cysteine
DOSY	diffusion-ordered spectroscopy (NMR)
D-Pen	D -penicillamine
GSH	glutathione
His	histidine
HSAB	hard-soft acid-base theory
LH_x	different protonation states of the peptides
LMCT	ligand to metal charge transfer
MD	Menkes disease
Met	methionine
MT	metallothionein
NOESY	nuclear Overhauser effect spectroscopy (NMR)
P	general notation for the peptide, independent from the protonation state
ROESY	rotating-frame Overhauser spectroscopy (NMR)
ROS	reactive oxygen species
TOCSY	total correlation spectroscopy (NMR)
UV-vis	UV-visible (spectroscopy)
WD	Wilson's disease

INTRODUCTION

I. Introduction

Copper is a transition metal found in group 11 of the periodic table, along with silver and gold (Figure 1). The name copper and symbol Cu are related to the Island of Cyprus, which was the main source of this metal in the Roman era. The phrase *aes cyprium* meaning the metal of Cyprus is believed to have evolved to cuprum and finally to copper.[1]

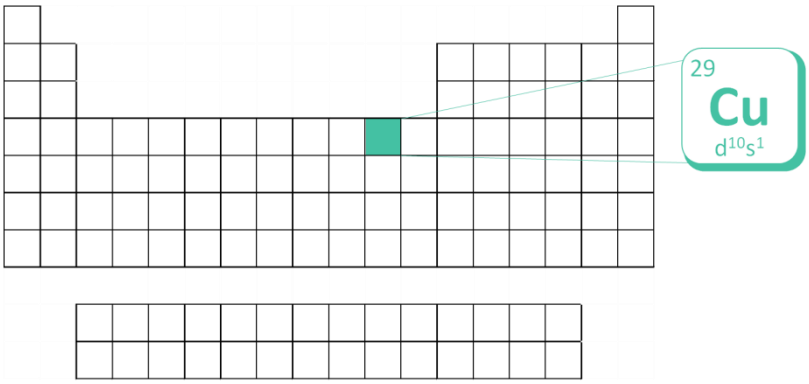

Figure 1. The place of copper in the periodic table

Copper was one of the first metals used and played an important role during history, because it can be found in elemental form, besides the various compounds, and it possesses useful physical properties, such as good ductility, malleability, strength, corrosion resistance, and high thermal and electrical conductivity, combined with an attractive appearance. From the primitive tools and weapons of prehistoric times, through the coinage and alloy formation to electrical wires and high-temperature superconductors in modern ages, there is a wide range of applications of copper and its compounds. They are also used as catalysts in both homogeneous and heterogeneous reactions, as fungicides, pesticides, wood preservatives, and as pigments for paints and glasses.[1]

Copper is also an important element from the biological point of view. It is an essential micronutrient participating in several vital processes. Since copper can alternate between the Cu(I) and Cu(II) oxidation forms, it mainly acts as a cofactor of redox enzymes. Some examples of copper proteins are cytochrome c oxidase, a member of the cellular respiratory chain, Cu/Zn superoxide dismutase, which plays an antioxidative defense role, lysyl oxidase, which is responsible for the collagen cross-link formation, dopamine beta-hydroxylase, that participates in catecholamine production and the two iron homeostatic proteins, hephaestin and ceruloplasmin.[2]

Nevertheless, this electrochemical activity makes the excess free copper as well harmful for the cell. It can promote the formation of reactive oxygen species (ROS) in

Fenton-like reactions. It is well-known that ROS can damage all cellular compartments from lipid membrane to nucleic acids. Therefore, cellular copper concentration is under strict control involving a sophisticated system of proteins.

Illnesses like Menkes or Wilson's diseases (MD and WD, respectively) can disturb this sensitive balance leading to copper deficiency or overload. WD is treated by chelation therapy. However, the nowadays-used drugs induce several adverse side effects. Thus, there is a substantial need for the development of safer therapeutics.

LITERATURE REVIEW

II. Literature review

1. Overview of human copper homeostasis

1.1. *Copper sources*

Nutrition is the main source of copper for the human body. Foods that are rich in copper are the seeds, grains, nuts, beans, potato, tomato, shellfish and liver. Drinking water also contributes to the daily intake, but in significantly smaller quantity (1 μg/day) depending on the characteristics of water like pH, hardness or copper availability in the water supply network. The recommended amount of ingested copper per day is around 0.8 mg, but the exact value depends on the geographical location, the age or sex.

In the proximity of industrial settlements such as mines or metal production plants, the copper level can be extremely high in the environment and it can be absorbed through the skin or by inhalation.[3]

1.2. *The route of copper in the body*

Dietary copper is absorbed by the enterocytes found in the wall of the small intestine. The enterocytes transfer copper to the portal circulation towards the destination of the liver. Liver is often called as the center of copper homeostasis, because copper is incorporated here into copper proteins and distributed to the other organs of the body. Excess copper is excreted through the bile in a form that cannot be reabsorbed and finally removed with the feces.[4]

1.3. *Coordination chemistry of copper in a living organism*

Copper has a $d^{10}s^1$ valence electron configuration and it is stable in Cu(I) and Cu(II) oxidation states. According to Pearson's hard-soft acid-base (HSAB) theory Cu(I) is characterised as a soft Lewis-acid,[5] and consequently, it is often coordinated by 2, 3 or 4 sulphur and nitrogen donors in linear, trigonal planar or tetrahedral geometry.[1] The borderline Lewis-acid Cu(II) can be coordinated by oxygen and nitrogen donors with coordination numbers 4–6 and in a square planar, (distorted) pentacoordinate or (distorted) octahedral geometries [1, 6]. In copper binding proteins these donor atoms are provided by the thiolate moieties of cysteines, the thioether groups of methionines, the carboxylate groups of glutamates and aspartates, the imidazole rings of histidines, and besides, the N- and O-atoms of the polypeptide backbone can also play a role in the coordination of Cu(II).

1.4. *Cellular copper trafficking*

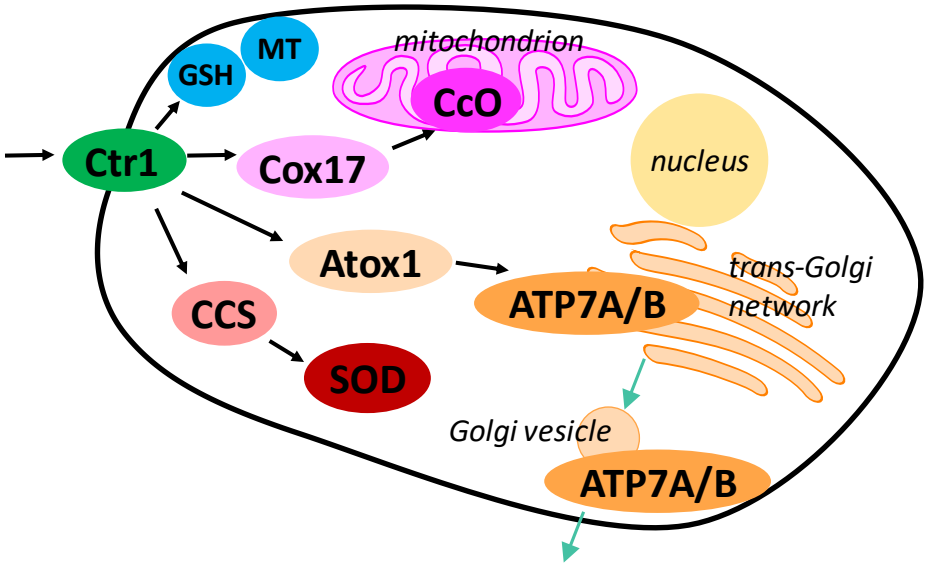

Figure 2. Cellular copper trafficking. Black arrows represent the route of copper; green arrows represent the movement of bigger units. Figure was made based on [4, 7].

Ctr1

Copper enters cells by the transporter protein Ctr1 (Figure 2). Ctr1 has three transmembrane regions that position the N-terminal domain on the extracellular side and the C-terminal domain in the cytosol. The extracellular domain is rich in methionines arranged in MXXM or MXM motifs, while the C-terminal domain contains conserved cysteines and histidines (Figure 3).[8]

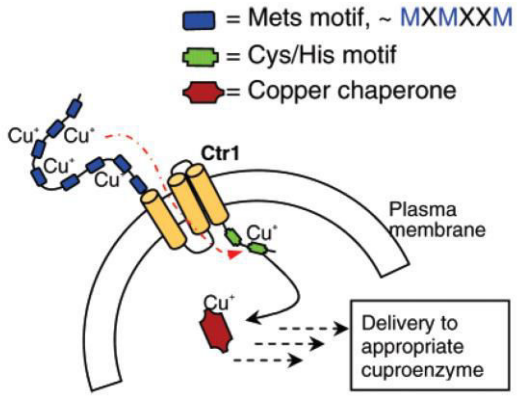

Figure 3. Schematic representation of cellular copper uptake[8]

A peptide modeling the first 14 amino acids of the extracellular N-terminal domain of Ctr1 (MDHSHHMGMSYMDS) is able to bind Cu(II) and Cu(I) with high affinity ($\log K_{Cu(II)}$ = 11.0 and $\log K_{Cu(I)}$ = 10.2) at pH = 7.4. Cu(II) is coordinated in square planar environment provided by the ATCUN motif formed by the amino nitrogen of the terminal

Met, the amide nitrogens of the following two peptide bonds and the imidazole nitrogen of the His residue. Interestingly, Cu(II) can be reduced in this complex by ascorbic acid, which is not typical at all for the ATCUN motif. The reduction leads to the rearrangement of the coordination site. Cu(I) is bound in a distorted tetrahedral geometry by two imidazole nitrogens and the carbonyl oxygen of the *bis*-His motif and by a thioether sulfur of one of the methionines.[9, 10]

Another peptide modelling the Met-rich motif of the N-terminal domain in the MXMXXM sequence was shown to coordinate Cu(I) in an all-methionine fashion. Dissociation constant of the 1:1 mononuclear complex was determined to be $K_D \sim 10^{-6}$ at pH = 3.5-4.5. The peptide displayed high selectivity for Cu(I) since no Cu(II) species could be detected.[8]

Based on UV-vis spectroscopic results, the cytosolic C-terminal domain of Ctr1 binds four Cu(I) ions and structural investigation by X-ray absorption spectroscopy showed the formation of a cluster with a Cu_4S_6 core (Figure 4). ESI-MS experiments revealed that this Cu_4 cluster was the only species formed, without the detection of any mono-, di- or tri-metalated complexes. The $K_D \sim 10^{-19}$ dissociation constant was determined by competition experiments.[11]

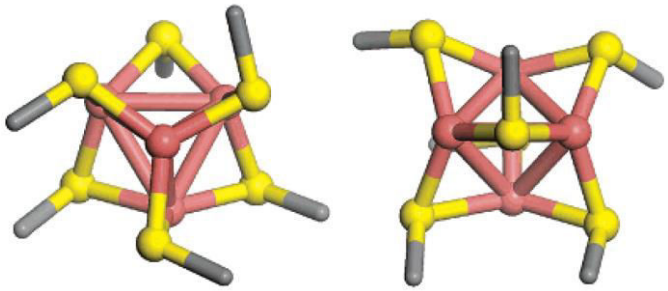

Figure 4. Model of the Cu_4S_6 cluster. Brown spheres represent copper atoms and the yellow ones represent the sulfurs[11]

Once copper is inside the cell, it binds to metallochaperones that incorporate it to copper dependent proteins, or to glutathione or metallothioneins for storage.

Cox17

Cox17 is one of the six chaperone proteins that transfer copper to the cytochrome c oxidase in the mitochondrion. It contains six conserved cysteines and exists in three oxidation forms, the fully reduced form with no disulfide bridges, the partially oxidized form with two disulfide bridges and the fully oxidized form with three disulfide bridges.

The fully reduced Cox17 binds four Cu(I) ions in a cooperative manner at neutral pH resulted in a tetranuclear cluster, where the metal ions are exclusively coordinated by the six cysteine thiolates. Decrease of pH leads to the dissociation of the Cu_4Cox17 complex starting at pH = 4.8. Other forms with one or five bound Cu(I) are also detectable, but the intermediate Cu_2Cox17 and Cu_3Cox17 are absent. Fully reduced Cox17 also can bind a maximum of two Zn(II) ions, but in a non-cooperative manner. This is explained by the different coordination preferences of Cu(I) and Zn(II). Although Ag(I) and Cu(I) have similar coordination properties, Cox17 cannot be reconstituted with Ag(I), possibly because of its larger size.

Partially oxidized Cox17 can bind one Cu(I) or Zn(II) at neutral pH. This Cu(I) complex decomposes at higher pH than the Cu_4S_6 cluster of the fully reduced form, indicating the participation of other amino acid residues, like histidine or methionine, in the coordination. No metal complexes of the fully oxidized protein have been detected.[12, 13]

Atox1

Atox1, also known as HAH1, is a human copper chaperone playing a similar role to Atx1 in yeast.[14, 15] These proteins contain a MxCxxC metal binding motif and transports copper to their target copper ATPases, namely ATP7A and ATP7B in humans.

The stoichiometry of the Cu(I)-Atox1 complex was determined by the addition of the protein to the solution of the $[Cu(BCA)_2]^{3-}$ complex (BCA = bicinchoninate anion). Spectroscopic results showed that protein bound one equivalent of Cu(I). A similar experiment with $[Cu(BCS)_2]^{3-}$ complex (BCS = bathocuproin disulfonate) led to the determination of the $K_D = 3.9 \times 10^{-18}$ dissociation constant at pH = 7.0.[16]

The interaction of Atox1 with Hg(II) was also studied by means of ^{199}Hg NMR, ^{119m}Hg PAC, UV-vis spectroscopy and gel-filtration. It was shown that at pH = 7.5 Hg(II) was bound to the monomeric protein via the two Cys residues in a linear geometry. At pH = 9.4 Hg(II) promoted the dimerization of the protein leading to the formation of a mixture of T-shaped HgS_3 and a distorted HgS_4 species.[17]

ATP7A and ATP7B copper-transporter

ATP7A and ATP7B are copper transporter P-type ATPases. These transmembrane proteins use the energy obtained from the hydrolysis of ATP for the transport of copper across the cell membrane. They are localized in the membrane of the trans-Golgi network. Their main function is to distribute copper to the main enzymes such as ceruloplasmin by

transferring copper from the cytosol to the Golgi, and to help maintaining the optimal intracellular copper concentration. In case of increased copper concentration, vesicles are formed from at Golgi membrane and migrate to the cell membrane to expel Cu from the cell. ATP7A is expressed in all types of cells except liver and ATP7B is expressed in the liver and the brain. ATP7A present in the enterocytes of the small intestine is responsible for the regulation of copper absorption by trafficking copper from the intestine to the blood. ATP7B participates in the excretion of excess copper to the bile.[4]

ATP7A and ATP7B display 54% identity in their amino acid sequence. They both contain six MxCxxC metal binding motifs at the cytosolic N-terminal domain. The overall structure of these domains are similar, each of them bind one Cu(I) ion by the two cysteine residues in a solvent exposed loop.[18] The increase of Cu(I) concentration does not affect Cu(I) binding. The linear geometry, ideal for the two-coordinate binding mode is distorted with a S-Cu-S bond angle between 120° and 180°.[19] A model peptide, involving the 5th and 6th metal binding domains, was shown to bind two Cu(I) ions separately by a similar experiment like in the case of Atox1. Nevertheless, only one dissociation constant, $K_D = 4.0 \times 10^{-18}$could be determined at pH = 7.0, indicating a similar affinity of the two metal binding domains for Cu(I).[20]

Glutathione

Glutathione (GSH) is a ubiquitous tripeptide (Figure 5). It plays an essential role in cellular redox regulation, detoxification and signaling functions. Besides, with its thiol groups it often acts as a ligand for soft transition metal ions. It was shown that GSH forms a Cu_4S_6 type cluster with Cu(I) under physiological concentration. The stability of the cluster permits only femtomolar concentration of free Cu(I) in the cell. In other words, the existence of an intracellular Cu(I) pool that are buffered to the upper femtomolar or picomolar concentration range is precluded by normal physiological level of GSH.[21]

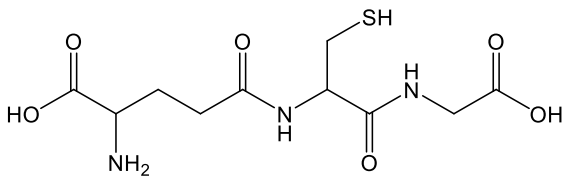

Figure 5. Schematic structure of glutathion

Metallothioneins

In 1957 Margoshes and Vallee identified a small, cysteine rich Cd(II) binding protein in horse kidney.[22] Later it turned out, that this was the first member of the superfamily of metallothioneins (MT). MTs are found from bacteria to humans in several isoforms showing diversity in the amino acid sequences and therefore in metal binding properties, three dimensional structures and functions. Characterizing features are the followings:

- low molecular mass combined with high cysteine content arranged in the typical CxC, CxxC or CCxxCC motifs. Figure 6 shows the position of cysteines in the sequence of a rabbit liver MT as an example.
- binding to Zn(II) and/or Cu(I) under physiological conditions, but also displaying high affinity for non-essential d^{10} metal ions.
- high thermodynamic stability combined with kinetic lability.
- the three dimensional structure is dictated by the bound metal ions, while the ApoMTs lack any secondary structure.
- formation of characteristic metal clusters with typical spectroscopic features.
- the absence or scarcity of aromatic amino acids.[23, 24]

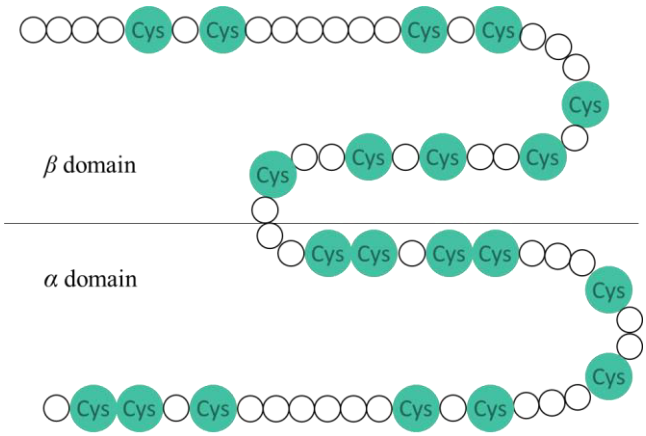

Figure 6. The position of cysteines in the sequence of a metallothionein from rabbit liver adapted from the figure of Stillman[25]

Different MT isoforms are expressed in different tissues under different conditions and therefore it is hard to define their function. As Blindauer claims the "enigmatic unified function of MTs does not exist".[23] MTs participate in the regulation of the essential Zn(II) and Cu(I) ions and in the detoxification of the toxic Hg(II) and Cd(II). They can be also related to anti-inflammatory, anti-apoptotic, antioxidant, proliferative and angiogenic processes.

The structures of the divalent metal ions complexes of metallothioneins are well-characterized. Generally, seven Zn(II) or Cd(II) ions are bound per metallothionein protein in an $M_4(S_{Cys})_{11}$ cluster in the α domain and in an $M_3(S_{Cys})_9$ cluster in the β domain (Figure 7). The metal ions display a tetrahedral coordination in both clusters. The α domain cluster can be described as two fused six-membered ring sharing two M(II)-S_{Cys} bonds. Thus, there are five bridging and six terminal cysteine thiolates. In the $M_3(S_{Cys})_9$ cluster three metal ion and three bridging thiolates form a six-membered ring in a distorted chair conformation, while the other six thiolates act as terminal ligands.[24]

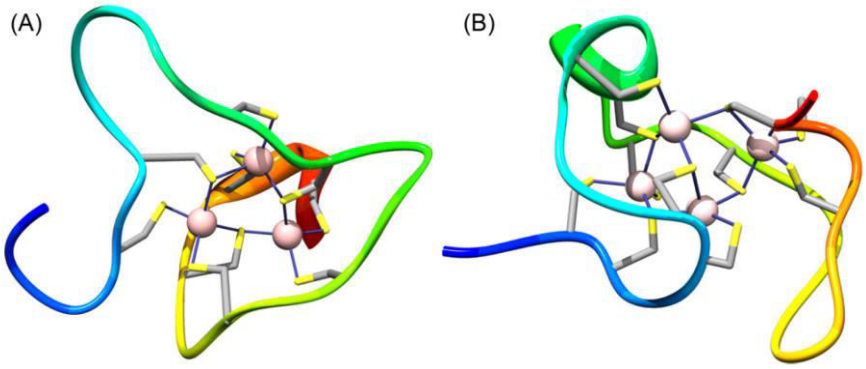

Figure 7. 3D structure of the human Cd_7-MT2 showing the β domain enclosing the $Cd_3(S_{Cys})_9$ cluster (A) and the α domain with the $Cd_4(S_{Cys})_{11}$ cluster (B).[24]

The formation of several Cu(I)-thiolate complexes of metallothioneins was evidenced by spectroscopic experiments. Cu(I) ions are coordinated digonally or trigonally. The thiolates act as bridging or terminal ligands. A metallothionein, isolated from rat liver was shown to bind 12 equivalents of Cu(I) per MT, which were distributed in two M_6 clusters of the α and β domain.[26] Yeast metallothionein formed a $Cu_8(S_{Cys})_{12}$ cluster in all-or-nothing manner.[27] Cu_8-MT and Cu_{12}-MT species were evidenced in MT-1 isolated from rabbit liver depending on the Cu(I):MT concentration ratio. These two complexes are built up by two $Cu_4(S_{Cys})_{6\text{-}7}$- and $Cu_6(S_{Cys})_{10}$ clusters, respectively.[28] Neuronal growth inhibitory factor (GIF) is a brain specific metallothionein. It forms a Cu_4Zn_3-GIF species. The study of the N-terminal (β) domain showed the formation of two well-defined Cu(I) clusters involving nine cysteine thiolates and 4 or 6 Cu(I) ions.[29] The Roman snail metallothionein is saturated by 12 Cu(I) ions.[30] As an explanation for such a diverse Cu-cluster formation, the possibility of different types of bound Cu(I) was proposed based on the results of a competition study with Cu(I) chelators. This experiment indicated that two of the eight Cu(I) ions of the yeast MT cluster were easily removable.[31] Later, it was shown that the formation and the structure of the Cu(I) complex of rabbit liver MT were

temperature dependent. At low temperature, the MT is relatively constrained and only the formation of a Cu_{12}-MT species is favored. In contrast, at higher temperature it becomes flexible enough to form a Cu_9Zn_2-MT complex.[32]

Although Cu(I) metallothioneins are widely studied, only the crystal structure of the truncated yeast Cup1 is available (Figure 8),[33] because of the relatively high flexibility of the protein backbone. The largest Cu(I)-thiolate cluster in biology was identified in Cup1 with the participation of six trigonally and two digonally coordinated Cu(I) bound by ten cysteine residues. The two digonally coordinated Cu(I) are located at the opposite site of the cluster which perhaps have a role in copper transfer to other proteins.

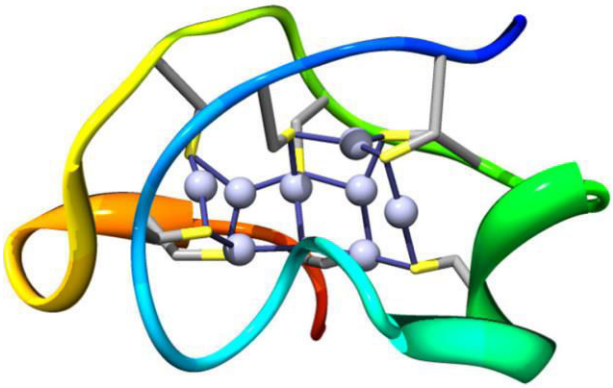

Figure 8. 3D structure of the Cu complex of a truncated form of Cup1 from S. cerevisiae, showing the $Cu_8(S_{Cys})_{10}$ cluster[24, 33]

The interaction between metallothioneins and metal ions, including Cu(I) is often studied by complementary spectroscopic methods. CD spectroscopy can be efficiently used because MTs do not contain aromatic amino acids or disulfide bonds, which have CD contribution in the wavelength range of thiolate-metal ion charge transfer (LMCT) transitions (230-400 nm). Besides, MTs are large enough to have a secondary structure in the presence of metal ions, but they are small enough to avoid possible compensation of the CD contributions of chromophores. The thiolate-Cu(I) LMCT has characteristic absorption in the UV region around 260 nm. However, it depends only on the net increase of Cu-S bonds and thus it is a good indicator for the formation of new Cu-S bonds.[34] The UV absorption spectrum of a Cu-MT system can be divided into the two distinct low- and high-energy regions. This latter one belongs to the electric dipole allowed thiolate to Cu(I) charge transfer (LMCT) occurring around 260 nm. The lower energy absorption is attributed to formally spin-forbidden 3d → 4s metal cluster centered transitions.[28]

2. **Copper related disorders**

2.1. *Copper toxicity*

Substances can be characterized as essential or toxic depending on the biological response that they induce. Essential elements have an optimal concentration range for a normal functioning, which varies from element to element. Concentration outside this optimal range causes health problems. The dashed line in Figure 9 shows that toxic substances have only negative effects, however it can also be seen that the body can cope with a small amount of the given element before toxic effects become apparent.[35]

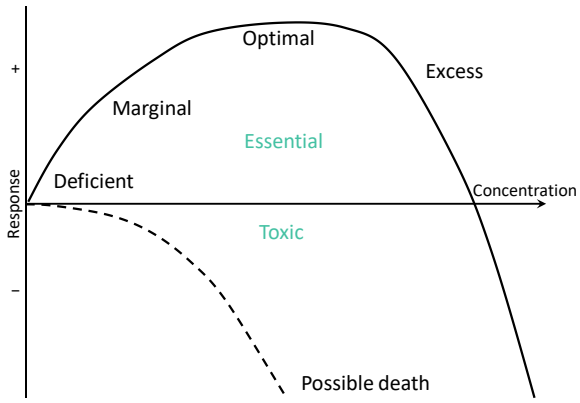

Figure 9. Dependence of biological response on concentration of an essential nutrient (solid line) and of a toxic substance (dashed line) in tissues.[35]

Copper toxicity is originated from unspecific interactions with proteins that disturb or inactivate the protein functioning. Toxicity may result from: (I) binding to sulfhydryl groups in proteins, thereby inhibiting enzyme activity or protein function; (II) initiating the deficiency of other essential ions; (III) impaired cell transport processes; and (IV) oxidative damage.[6] Among these, the main problem is attributed to the production of strong oxidizing agents. For a long time, it was supposed that these oxidants were ROS produced mainly in Fenton like reactions [36, 37]:

$$Cu^{+} + H_2O_2 \rightleftharpoons Cu^{2+} + OH^{\bullet} + OH^{-}$$

$$Cu^{2+} + H_2O_2 \rightleftharpoons Cu^{+} + HOO^{\bullet} + H^{+}$$

The reactions of Cu(I) and Cu(II) with H_2O_2 in the presence of O_2 at pH = 8.0 have been studied.[38] The results showed that, on one hand, Cu(II) reacted with H_2O_2 in the classical free radical mechanism producing Cu(I) and $O_2^{\bullet-}$. The formed Cu(I) was able to react with excess H_2O_2 to produce $OH^{\bullet}$. On the other hand, a well-known hydroxyl radical indicator did not show the formation of $OH^{\bullet}$ in reaction between Cu(I) and H_2O_2. However, the involvement of an intermediate species of copper in a higher oxidation state (Cu(III))

was assumed, but its reaction with the substrates was several orders of magnitude slower than $OH^{\bullet}$. Formation of $OH^{\bullet}$ from the dissociation of Cu(III) was determined to be extremely slow at pH 8.0. This result showed that $OH^{\bullet}$ was not an important oxidant in this system.

2.2. *Alzheimer's disease*

Alzheimer's disease (AD) is the most common neurodegenerative disorder. It is associated with the misfolding of the amyloid-β peptide forming fibrils and plaques in brain tissue. In the development of AD, a key role is attributed to ions of metals such as copper, zinc or iron, which can affect the aggregation and redox properties of the amyloid-β peptide. Metal binding sites of amyloid-β are found between the 1-16 amino acids of the sequence. The coordination of Cu(II), Cu(I) and Zn(II) is presented in Figure 10. Two different binding modes of Cu(II) are known, component I is favored at lower pH, while component II is present at higher pH. Both are characterized by a distorted square planar geometry and by the participation of amino nitrogen of Asp1 at the N-terminus. In component I, Cu(II) is also bound to the carbonyl oxygen of the Asp1-Ala2 peptide bond and two histidine nitrogen atoms of the His6 residue and one of His13 and His14 which are in equilibrium. In component II, the deprotonated amide nitrogen of the Asp1-Ala2 peptide bond, the carbonyl oxygen of the Ala2-Glu3 bond and a histidine nitrogen bind to the Cu(II) ion. Cu(I) is coordinated in a linear fashion by two of the imidazole nitrogen atoms from the dynamic equilibrium of His6, His13 and His14 with a preference for the His13-His14 couple. Zn(II) is tetrahedrally coordinated by two histidine residues (His6 and His13 or His14) and two carboxylate residues from Asp1, Glu3 or Asp7, where the Asp1 is favored. Stability constants were determined in the range of 10^9-10^{10} for Cu(II), 10^7-10^{10} for Cu(I) and 10^5 for Zn(II).[39]

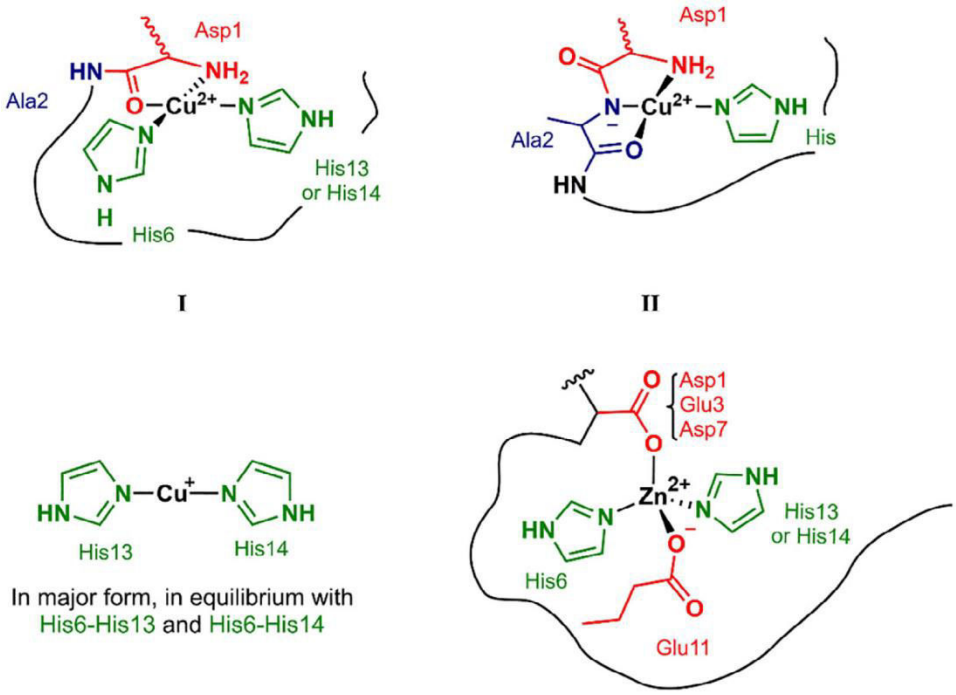

Figure 10. The main coordination modes of amyloid-β peptide with Cu(II), Cu(I) and Zn(II)[39]

2.3. *Menkes disease*

Menkes disease (MD) is due to the mutations of the ATP7A gene found on the X chromosome. This induces dysfunctions of the ATP7A copper transporter, and copper cannot be absorbed and hence patients suffer from copper deficiency. Clinical symptoms usually appear in boys at the age of 2-3 months with a subsequent loss of previously obtained developmental milestones.[40] Children die in their early childhood. All patients gain very little weight following birth. The clinical symptoms of MD can be traced back to the deficiency of developmentally important copper enzymes. The impairment of lysyl oxidase, a protein needed for crosslink formation in connective tissues, causes the weakening of connective tissues that leads to arterial ruptures or skin laxity. Low levels of cytochrome c oxidase cause temperature instability and the absence of tyrosinase explains the hair depigmentation.[41] MD is also characterized by mental retardation and neurodegeneration.

The current treatment is copper supplementation, which can be highly effective depending on the type of the ATP7A mutation and the timing of treatment.[40, 42] Far perspective is the adeno- associated virus-mediated gene therapy.[40, 43]

2.4. *Wilson's disease*

Wilson's disease (WD) is induced by the monogenic, autosomal recessive mutation of ATP7B presented in a high variety of point or splice junction mutations (more than 500 are identified).[40] The mutations lead to the loss of ATP7B function, and hereby to the accumulation of copper in the liver, and later, in the central nervous system. There are three phases in the progression of WD. In the first phase copper starts to accumulate in the cytoplasm of hepatocytes. The increased copper concentration induces the expression of high amounts of metallothioneins in the second phase and the formation of copper storages in the liver, which cause cell death and the release of copper to the blood stream. In the third phase, copper accumulates in other organs, such as brain, kidney and eyes.[41] WD is characterized by three groups of symptoms: (I) hepatic, like jaundice, acute hepatitis, liver failure, cirrhosis[1]; (II) neurological, like movement disorders or tremor; (III) psychiatric e.g. personality changes, paranoia, depression and schizophrenia[44]. Symptoms usually appear in the age between 5 and 35 years, but there were patients who became symptomatic when they were older than 70 years.[40] Generally, children are diagnosed with WD by the manifestation of liver problems, while adults by neurological symptoms. It is assumed that patients with neurological disorders also have asymptomatic liver disease. WD is characterized by the Kayser-Fleisher rings of copper deposition in the eyes and low serum ceruloplasmin concentration.[44] Wilson's disease is treated by chelation therapy. In case of fulminant liver failure, transplantation is required. Without treatment, WD is lethal.

2.5. *Further disorders associated with copper overload*

Copper accumulation is associated with other liver damages than Wilson's disease. Indian childhood cirrhosis, Endemic Tyrolean infantile cirrhosis and Idiopathic copper toxicosis were found to be identical,[45] but they were present in different places, in India and different regions of Austria. It was caused by the high copper exposure originated from the consumption of milk stored and heated in copper or copper-alloy utensils. After the instruction of the population to avoid the use of such containers in 1974, no new cases were reported. The collected data suggest that the development of cirrhosis is a result of the synergy of excess copper intake and non-Wilsonian genetic susceptibility for impaired copper metabolism.[3, 46]

[1] Liver damage that is characterized by the replacement of normal liver tissue by scar tissue.

3. Strategies in the treatment of Wilson's disease

3.1. *Historical and current treatments*

Chelation therapy is widely used for the treatment of toxic metal poisoning and in diseases related to metal overload. In general, chelation therapy refers to the administration of a chemical agent to remove heavy metal ions from the body (Figure 11).

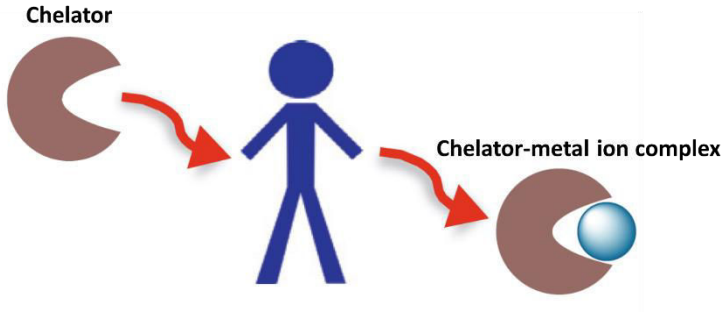

Figure 11. Schematic representation of the mode of action of a chelator[47]

This chemical agent is a so-called chelator, originated from the Greek word "chele" for claw, because as the molecule binds to the metal ion, it resembles to how the lobster catches its prey. A chelator possesses more than one donor group and therefore it forms a ring around the metal ion during the coordination. This provides higher complex stability than monodentate ligands of the same donor atom and it is called chelate effect. Chemical properties like charge, solubility, lipophilicity, redox potential, geometry and pH dependence, kinetics and thermodynamics of the exchange of the ligand or the metal ion can all influence the behavior of a chelator and its metal complex in biological conditions.[47]

Drugs used for the treatment of Wilson's disease are presented in Figure 12. Dimercaprol (British anti-Lewisite, BAL) and its derivatives, dimercapto-propanesulfonic acid (DMPS) and dimercapto-succinic acid (DMSA) are general chelating agents that were first applied against copper overload in Wilson's disease. Later, they were replaced by D-penicillamine (D-Pen) and triethylenetetramine (trien). Tetrathiomolibdate (TTM) is currently under investigation. Besides chelation, Wilson's disease is treated by zinc therapy, which limits the copper absorption in the intestine.

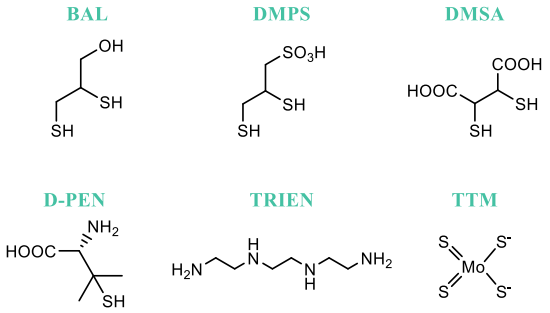

Figure 12. Schematic structure of the drugs used for the treatment of Wilson's disease

An ideal treatment for Wilson's disease should consist of two phases. First, it has to be started with an aggressive de-coppering phase to decrease the amount of copper accumulated in the body. This should be followed by a maintenance therapy of reduced doses to control a normal copper homeostasis. Refinement and adjustment of this second phase could also be necessary to avoid copper deficiency caused by overtreatment.[40]

BAL

Dimercaprol, also called as British anti-Lewisite or BAL, was developed against arsenic poisoning caused by the warfare gas Lewisite in the Second World War. Later it was also used for the intoxication of mercury, gold, lead, antimony, bismuth, copper and nickel. After the identification of the relationship between the Wilson's disease and copper overload, BAL was the first drug proposed for the treatment. BAL is an oily, highly hydrophobic substance and therefore it has to be administered by the painful intramuscular injection. It was usually mixed with the highly allergenic peanut oil. As a result of the treatment, patients showed remarkable improvements and increased urinal copper excretion. However, BAL induces many side effects, such as the increase of blood pressure, nausea and vomiting, headache, burning feeling of the lips, mouth or throat and painful irritation at the injection site.[48] The orally administrable BAL derivatives DMSA and DMPS were used only in China for the treatment of Wilson's disease.[49]

Interestingly, although BAL has been used for several decades, its interaction with copper ions was just recently described.[50] The reaction between copper ions and thiols usually occurs in the following way:

$$2Cu(II) + 2RSH \rightleftharpoons 2Cu(I) + RSSR + 2H^+$$

$$Cu(I) + RSH \rightleftharpoons Cu\text{-}SR + H^+$$

Reaction between BAL and $CuSO_4$ or $CuCl_2$ results in the formation of a dark blue to grey, solvated suspensions of a mixture of species with stoichiometries of 2 Cu(I)/oxidized

dimeric BAL and Cu(II)/BAL 1:1. Because of the empty coordination site of Cu(I), polynuclear species were suspected, but their nature could not be revealed. Reaction of BAL with CuCl in methanol gave the $Cu(I)_2$-BAL salt as a dark green solid, insoluble in organic solvents, displaying the same IR spectrum than the product of the reaction with $CuCl_2$. Solubilization of these solids failed indicating that the urinary extraction of copper by BAL proceeded through another mechanism than the formation of a simple binary complex.

D-Penicillamine

D-Penicillamine (D-Pen) is a metabolite of penicillin. It was first used for WD treatment in 1955 according to the proposal of Walshe.[51] Since then, it is still the first drug of choice. The great advantage of D-Pen compared to BAL is that it can be orally administered, making it more convenient and more effective. However, D-Pen has also side effects, like fever, rash or renal toxicity.[3] It causes pyridoxine (vitamin B_6) deficiency and interference in collagen and elastin formation leading to skin lesions and immunological problems.[52] Furthermore, worsening of neurological problems was registered in a significant number of patients after the treatment with D-Pen.[2]

D-Pen is characterized by three protonation constants belonging to the thiol ($\log K$ = 10.8), the NH_3^+ ($\log K$ = 8.1) and the carboxyl groups ($\log K$ = 2.2). The dominant species at physiological pH is the zwitterionic form.[53] D-Pen can bind Cu(II) as a bidentate ligand via the thiol and amino groups and a redox reaction occurs between the metal ion and thiol group. The reduction of the metal ion induces changes in the preference of the coordination geometries. If D-Pen coordinates to a Cu(II) bound to a protein and the protein is not flexible enough to follow this change, the copper-protein interaction becomes weak and the metal ion is more readily removable.[54] Based on potentiometric and spectroscopic results, the formation of a stable and red-violet colored, mixed-valance species was proposed (Figure 13).[3, 55] This species was suspected to have a key-role in urinary copper extraction by D-Pen.

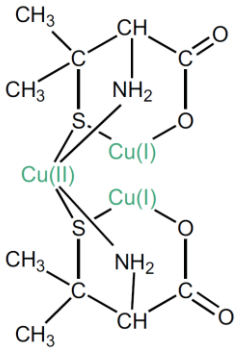

Figure 13. The proposed mixed-valance copper–D-Pen complex[3, 55]

When D-Pen was added to the copper-albumin complex, the formation of a yellow brown species was observed. However, after a few minutes the solution became red-violet, indicating that the ternary complex transformed into the mixed-valance complex (Figure 13).[3, 56]

The interaction of the disulfide derivative of D-Pen with Cu(II) was also studied.[3, 57] The monomeric CuLH and dimeric Cu_2L_2 complexes were formed with stability constants of $\log\beta_{CuLH}$ = 15.8 and $\log\beta_{Cu_2L_2}$ = 27.9 determined by pH potentiometric measurements. Cu_2L_2 dominated over pH = 3.5. Cu(II) ions were bound via the oxygen and nitrogen atoms of the ligand, but the sulfurs of the disulfide bridge did not participate in the metal ion coordination (Figure 14).

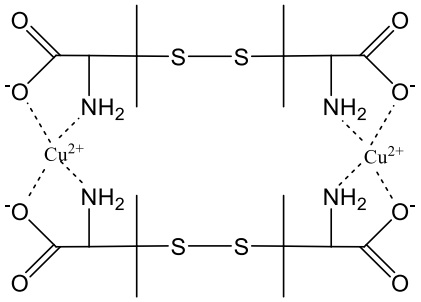

Figure 14. Schematic structure of the Cu_2L_2 complex of the disulfide D-Pen[57]

It was also stated that D-Pen could participate in copper detoxification by inducing the synthesis of metallothioneins in the liver.[49]

Triethylenetetramine

Triethylenetetramine, also known as trientine or trien also acts by increasing urinary copper extraction. It was first used in patients who intolerated D-Pen.[58] This drug has fewer side effects compared to D-Pen.[52, 59] In cases when the treatment with D-Pen had to be suspended, it could be efficiently continued with trien.[60]

Trien contains four amino nitrogen donor groups allowing the binding of copper in Cu(II) form. The interaction between trien and its metabolites (mono- and diacetylated) and Cu(II) and Zn(II) was studied by potentiometric and photometric studies.[61] Cu(II) complex formation resulted in the appearance of two bands on the UV-vis spectra, one centered at 250 nm and one at 580 nm with lower intensity. Data analysis revealed the formation of a CuLH complex at low pH, which completely transformed into the CuL complex at pH ~ 3.0. Cu(II) was coordinated by the four nitrogens of trien in a planar ring. Zn(II) complexes also formed but with significantly lower stability. ZnL formation occurred at a ~ 2.5-unit higher pH relative to the formation of the CuL complex. The acetylated metabolites formed the same type of metal complexes, but they displayed lower stabilities.

Sarkar and coworkers analyzed ternary systems of Cu(II), human serum albumin and trien or D-Pen. They found that trien efficiently removed the metal ion from the Cu(II)-albumin complex at neutral pH forming small membrane-diffusible, low molecular weight complexes. In contrast D-Pen was unable for such a Cu(II) removal. These results lead to the conclusion that the two kinds of chelators targeted different copper pools. Trien reduced the Cu(II) concentration in the blood stream, while D-Pen mobilized copper from the tissues.[62]

To increase the efficiency of trien, it was encapsulated into surface modified liposomes.[63] Such a colloidal carrier can penetrate the blood-brain barrier and the copper overload in the central nervous system can be treated by the released trien.

Improvement after the treatment of either D-Pen or trien was significant in patients with hepatic problems, but the therapy was less effective in the case of neurological symptoms. Both drugs induced the worsening of neurological problems in 20% of the cases. This deterioration was attributed to the initial large dose of the chelating agent and led to the hypothesis of the presence of two different kind of copper pools, the high-affinity bound copper (bound to ceruloplasmin) and free copper (not bound to ceruloplasmin). A plausible mechanism of the paradoxical neurological deterioration could be the overmobilisation of copper by chelation therapy, leading to an increased free copper pool with toxic effects.[40]

Tetrathiomolybdate

TTM has a high affinity for both Cu(I) and Cu(II) forming polymetallic clusters.[64] Solution equilibrium speciation and stability data, however, have not been reported yet, because of the complexity of the system. For instance, Mo, Cu and S can be present in different oxidation states, Cu and Mo can precipitate as sulfide and the hydrolysis of MoS_4^{2-}

and Cu(II) can occur.[3] Nevertheless, X-ray absorption spectroscopy showed the formation of different species of Cu/ MoS_4^{2-} stoichiometry ranging from 1:1 to 4:1 (Figure 15).

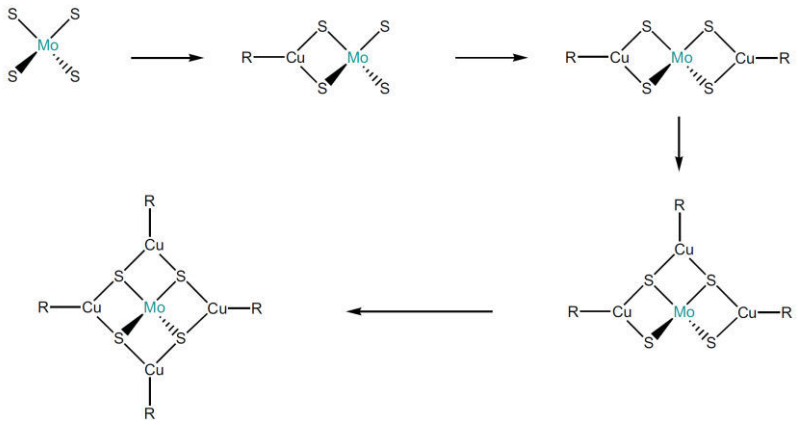

Figure 15. The formation of different Cu-TTM complexes with increasing Cu concentration.[3, 65]

TTM has two ways of action. When ingested with food, TTM forms complexes with dietary copper and thereby prevents the absorption of metal ion. When TTM is added between meals, it can be absorbed and forms ternary complexes with copper and proteins like albumin or metallothioneins in the blood stream. In this way copper becomes unavailable for the body and is excreted through the urine or the bile.[3, 52]

Originally, TTM was used to treat animals with copper toxicosis and later it was applied for patients who were intolerant for D-Pen. The application of TTM does not cause the worsening of neurological problems and it has fewer side-effects. These side-effects are probably related to the extensive copper removal. Nevertheless, clinical data about TTM is limited and the drug is not commercially available.[3]

The effectiveness of BAL, D-Pen, trien and TTM was compared according to their demetallation ability of two Cu(I)-binding proteins, the copper chaperone Cox17 and a metallothionein.[66] All of the drugs were able to remove Cu(I) from CuCox17, but in different concentrations. D-Pen was necessary to be applied in the highest amount followed by trien and BAL, while TTM was found to be 1000 times more efficient than the others. Demetallation of Cu_{10}MT was more complicated. Cu(I) withdrawal started only after the binding of four TTM molecules, that probably opened the cluster and Cu(I) could dissociate from the protein. TTM was still the most efficient since 1000x higher concentration of the other drugs had to be applied to reach the same result.

Zinc therapy

Administration of zinc-acetate to WD patients limits the intestinal copper absorption. Zn(II) stimulates the synthesis of metallothioneins in the intestinal epithelial cells. MTs bind dietary copper therefore prevent further copper accumulation.[40] MT-bound copper is excreted through peeling of enterocytes within some days via the feces.[2, 67] Since zinc and copper are uptaken by the same carriers of the enterocytes, saturation of these carriers with Zn(II) can block the absorption of Cu(II).[68] Zinc therapy has significantly fewer side effects than chelating agents. Nevertheless, the proposed daily dose of zinc (600 mg)[69] is notably higher than the normal dietary uptake, which can induce adverse gastrointestinal effects. Zinc is recommended as a maintenance therapy after the initial chelation therapy and for the treatment of asymptomatic or presymptomatic family members of Wilson's disease patients.[64]

3.2. *New perspectives*

Targeting intracellular Cu(I) of hepatocytes

In modern drug research, it is a rule of thumb to develop specific treatments for the different diseases to reduce the side-effects. Two basic concepts for the achievement of this goal are the so-called drug targeting and the use of pro-drugs. When a drug is targeted to a specific organ, it is functionalized in a way that it can be absorbed only by cells of this organ. A pro-drug is an inert compound where the functions responsible for the curative effect are inactivated.[70] It becomes active only at the required site through metabolism.[71] In chelation therapy it is also important that the chelating agent should be highly selective for the metal ion to be removed in order to avoid disturbance in the homeostasis of other essential metal ions, like Zn(II) or Ca(II).

In the case of Wilson's disease these concepts can be realized by means of targeting Cu(I) in liver cells because of the following reasons.[4, 72] Copper taken up by the cells is in the Cu(I) oxidation state and the millimolar intracellular concentration of gluthation (GSH) [73] makes its oxidation to Cu(II) very unlikely.

$$2\ Cu^{2+} + 2\ GSH \rightleftharpoons 2\ Cu^{+} + GSSG + 2\ H^{+}$$

Accordingly, an efficient chelator has to be selective for this Cu(I) form. The HSAB theory [5] and the metal binding sites of proteins may provide some hints on how to choose an optimal set of donor groups for Cu(I). The thiol functions of cysteines, as soft bases, often participate in the ligation of the Cu(I) ion, also possessing a soft character. Further advantage

of cysteines is the fact that they easily form disulfide bridges, which are inactive in metal ion chelation. These disulfide bridges can be broken in the reducing intracellular medium and thus the active chelator is released. In this way, cysteines also fulfill the pro-drug concept.

Finally, since liver is the center of copper homeostasis and therefore mostly affected in Wilson's disease, an efficient drug targeting strategy could be if the new product was targeted to this organ.

The Delangle group aims to find an efficient Cu(I) chelator and then functionalize this ligand to target the liver cells. Their first tested ligands were inspired by the metal binding sequence of the Atx1 [14, 15] copper chaperone protein.[74] Both the linear Ac-MTCSGCSRPG-NH_2 and the cyclic c(MTCSGCSRPG) peptides displayed an outstanding selectivity towards Cu(I) over Zn(II), Cd(II) and Pb(II). The peptides formed the mononuclear CuL complex under ligand excess conditions with logβ = 16-17 apparent stabilities at pH = 7, which is in the same range as the native Atx1 protein (logβ = 18 at pH = 7.4).[11] However, at higher Cu(I) concentration, the formation of polynuclear species was observed. These experiments showed that the insertion of the xPGx motif and the cyclization of the peptide backbone did not disturb the complex formation, moreover, the complexes of the cyclic peptide displayed systematically higher stabilities with all the metal ions. This effect was attributed to the preorganization of the binding loop positioning the two cysteine side chains on the same side of the macrocyclic peptide.

The other direction in Cu(I) chelation research was based on the use of tripodal pseudopetide ligands. In this kind of ligands three derivatives of cysteine [75, 76], D-penicillamine [77], methionine or methyl cysteine [78] were anchored on a nitrilotriacetic acid (NTA) scaffold to mimic the high S-density of metallothioneins (Figure 16). A great advantage of this scaffold is that all the metal binding arms were oriented to the same direction forming a metal binding cavity.

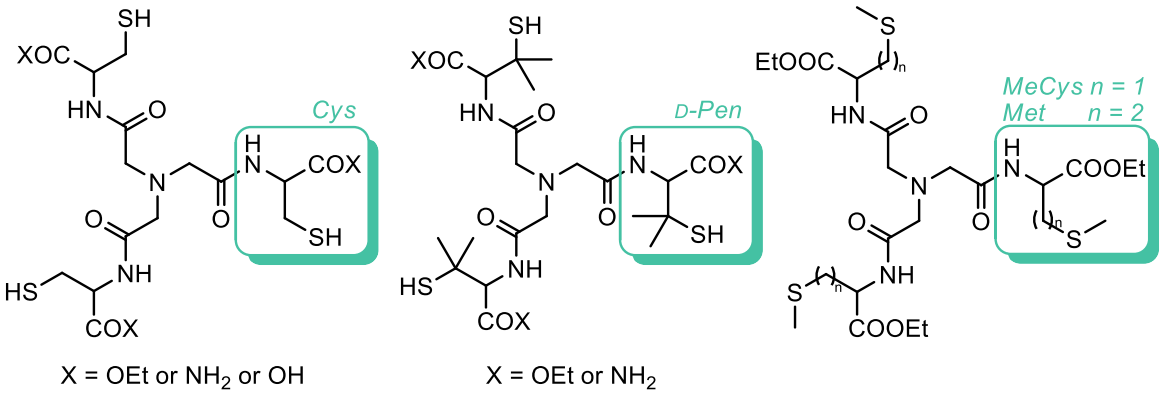

Figure 16. Schematic structures of the tripodal ligands [76-78]

Three cysteine-based ligands were investigated. These molecules differed in the nature of the carbonyl function and this difference was proved to have a great effect on the complexation properties.

The ligand bearing three carboxylate functions only formed non-defined $(Cu_2L)_x$ polymetallic Cu(I) species of low stability. This destabilizing effect was probably due to the large electrostatic repulsion between the negative charges of the three carboxylate groups at physiological pH, which were brought closer to each other in the complex. The mononuclear Cu(I) complexes of the two other ligands with ester and amide groups were the first described water soluble CuS_3 species. The Cu(I) ion was bound in symmetrical trigonal planar geometry in these complexes suggesting that the cavity of these NTA based ligands was perfectly adapted to the coordination of Cu(I).[79] Temperature dependent NMR measurements proved that the cavity was stabilized by a network of hydrogen bonds in the upper cavity involving the NH of one arm and the C=O of the next arm.[76]

In excess of Cu(I), the mononuclear CuL complex transformed into the Cu_6L_3 cluster, as presented in Figure 17. The amide derivative showed the greatest tendency to form the cluster from the mononuclear complex.

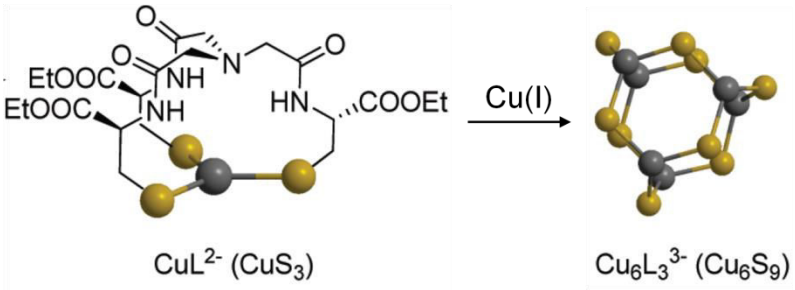

Figure 17. Structure of the Cu(I) complexes of the tripodal ligands [75]

The stability constants $\log\beta_{11}^{pH\ 7.4} \sim 19$ obtained for the mononuclear complexes are in the range of those reported for metallothioneins.[80] The molecules displayed an 8-9 orders of magnitude larger affinity towards Cu(I) with respect to Zn(II).

D-Pen, as the most frequently used drug for Wilson's disease, was also an interesting candidate to be anchored on the NTA scaffold. The two D-Pen based ligands with amide and ester groups on the carbonyl functions showed significantly different complexation behavior with Cu(I), probably due to the different size of these groups. The ligand bearing the bulkier ester group formed exclusively the well-defined Cu_4L_2 cluster with the Cu_4S_6 core, while the other compound formed the mononuclear CuL complex in the presence of ligand excess and the same type of Cu_4L_2 cluster under Cu(I) excess conditions. Trigonal planar coordination around Cu(I) was proved with the participation only of the sulfur donors and Cu-S distances characteristic for the CuS_3 geometry. The ligands bound Cu(I) tightly with affinities of $\log\beta$ = 16-17, which were lower than those determined for the cysteine derivatives, but significantly higher than the affinity reported for the D-Pen alone.[81] The studied ligands also displayed remarkable selectivity in favor of Cu(I) relative to Zn(II).

The thioether derivatives were inspired by the methionine rich motifs of the Ctr1 protein. The ligands exclusively formed mononuclear complexes with Cu(I) even in the presence of excess metal ion. The obtained $\log\beta$ = 10-11 stabilities were significantly lower than those of the thiolate ligands, but higher than the $\log\beta$ = 5-6 values reported for linear peptides mimicking isolated methionine-only binding sites found in Ctr1 sequences.[8, 82]

As a second step in the research, the two most promising ligands, the peptides and the cysteine based tripodal pseudopeptides were functionalized for drug targeting as presented in Figure 18. Since the drug should be selectively absorbed in hepatic cells, the asialoglycoprotein receptor (ASGP-R) was chosen as a target.[83-85] The ASGP-R is predominantly expressed on the surface of hepatocytes [86, 87] and recognizes terminal galactose (Gal) and *N*-acetylgalactosamine (GalNAc) with higher affinity.[88] The ASPG-R mediated targeted drug strategy was successfully applied for the specific delivery of antiviral [89, 90] and anticancer drugs [91-93], and gene therapeutic agents [94-98] to hepatocytes *in vivo*.

The glycocyclodecapeptide ligand was designed by the regioselectively addressable functionalized template (RAFT) concept [99] to distinguish the Cu(I) chelating unit with two cysteine side chains hidden in a disulfide bridge and the ASPG-R recognition unit with a cluster of four GalNAc carbohydrates on two independent faces.[100] In the sulfur tripod

glycoconjugate, the thiol functions were masked by tethering one GalNAc with an ethylene glycol spacer to each arms through disulfide bonds (Figure 18).[101]

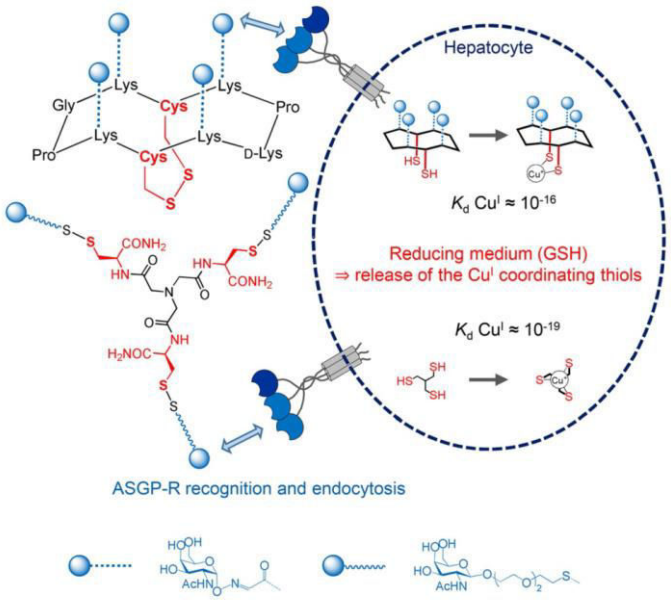

Figure 18. Design and mechanism of action of the two glycoconjugates

The efficiency of the targeting units was proved by the uptake of a fluorescent analogue of both ligands by various hepatic cell lines.[100, 101] The peptide based product was better internalized than the triopdal one.[102] The disulfide bridges hid the chelating binding sites and, as expected the ligands did not show Cu(I) chelating properties. When the disulfide bridges were reduced in the intracellular medium, the ligands lowered the Cu(I) concentration which was monitored by the trafficking of the copper ATPase ATP7B.[100, 101] The intracellular Cu(I) chelating efficiency of the two glycoconjugates was similar, although the affinity of the released chelators for Cu(I) differed by three orders of magnitude in favor of the tripod derivative.[102]

All in all, these glycoconjugates can be considered as pro-drugs that release copper chelators only in the reducing intracellular medium of hepatocytes.

Reduction of the copper uptake by an indigestible biopolymer

Another promising therapy can be if an efficient copper chelator is grafted to an indigestible carrier. A system like this can bind copper ions obtained by food in the gastro intestinal tract and hereby reduces the amount of the absorbed copper ions. Meanwhile, the chelator does not enter the blood stream or other organs and therefore it does not induce side effects. Cu(II) complexes of 8-hydroxyquinoline are formed in a wide pH range.

Furthermore, the ligand displays high selectivity for Cu(I) ions over Zn(II). 8-hydroxyquinoline was covalently bound to microcrystalline cellulose and crosslinked chitosan. The covalent bond prevents the release of the ligand in the body. These biopolymers are non-digestible, because human body lacks the cellulolytic enzymes and thus they go through the body without degradation or reaction with bio-compartments and therefore they are supposed to be harmless.[103]

α-lipoic acid, as a new candidate

Recently, α-lipoic acid (Figure 19) was proposed as a new drug candidate for the treatment of Wilson's disease.[66]

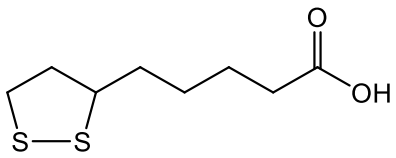

Figure 19. Schematic structure of α-lipoic acid

This compound is an essential cofactor of several enzymes that participate in aerobic metabolism. It mainly acts by transferring acyl or methylamine groups. α-lipoic acid has some advantageous features with regard to the treatment of WD. α-lipoic acid is reduced in the intracellular environment to dihydrolipoic acid, which has two free thiol groups and displays higher affinity for Cu(I) than D-Pen or trien. α-lipoic acid has good membrane and blood brain barrier permeation ability. Finally, it is a well-tolerated food supplement. Preliminary experiments on hepatic cells showed that α-lipoic acid could protect the cells from a copper concentration 1,5x higher than its LD_{50} value.

Aims and Objectives

III. Aims and Objectives

Due to the drawbacks of the currently used drugs, there is a substantial need of new copper chelators for the treatment of Wilson's disease. In chapter 3.2 a new strategy was described where excess Cu(I) in hepatocytes is targeted. To improve the efficiency of the chelators, it is necessary to identify the factors that play a role in the affinity towards Cu(I). Peptides are easily tunable tools in metal ion chelation thanks to the diverse functional groups of the essential amino acids. In peptide design aiming at the chelation of the soft Cu(I) ion,[5] cysteines are obvious choices as potential binding sites. The goal of my PhD project was the design of new, cysteine-containing peptides as potential drug candidates and the investigation of their Cu(I) binding properties.

Three series of peptides were designed from three different approaches.

1) Peptides mimicking the metal binding loop of the bacterial Cu efflux regulator protein (CueR) were chosen to take advantage of the outstanding sensitivity and selectivity of CueR.
2) In three cysteine containing peptides we wanted to combine the advantageous features of the ligands previously developed in Pascale Delangle's lab, namely the large Cu(I) binding affinity of tripodal pseudopeptides and the better internalization by the hepatocytes of peptide based molecules.
3) Finally, the advantages of a highly preorganized peptide structure were exploited in a short, rigid tetrapeptide where two cysteines were linked by a turn motif

The Cu(I) binding properties of these peptides were studied by solution equilibrium and structural methods, i.e. UV-visible, circular dichroism and nuclear magnetic resonance spectroscopies and mass spectrometry to evidence the influence of the peptide length, the amino acid sequence, the backbone structure and the number of the Cys residues on Cu(I) complexation properties in water at physiological pH. Complexes with Hg(II), a soft divalent ion often taken as a model non redox-active metal ion for Cu(I), have also been studied for comparison. Since Zn(II) is present in relatively high concentration in the body and it is a potential competitor of Cu(I), the interaction with Zn(II) was therefore also tested.

EXPERIMENTAL SECTION

IV. Experimental section

1. Peptide synthesis and purification

The peptides were synthesized by solid phase peptide synthesis (SPPS) following the Fmoc strategy. The application of SPPS was established by Robert B. Merrifield in 1963.[104] In this protocol, the growing polypeptide chain is attached to a solid support during the whole synthesis, and therefore the reagents and by-products are easily removable by simple filtration and washing. Over the years, SPPS underwent several optimization in the solid support, the protecting groups, etc. to reach its present state.[105] The protocol consists of the repeating cycles of deprotection/washing/coupling/washing/capping/washing as graphically summarized in Figure 20. The peptide chain grows from the C-terminus to the N-terminus, contrary to the protein synthesis *in vivo*. The amino acid building blocks are protected by the base labile 9-fluorenylmethyloxycarbonyl group (Fmoc) at the amino function and by different acid labile protecting groups at the side chains.

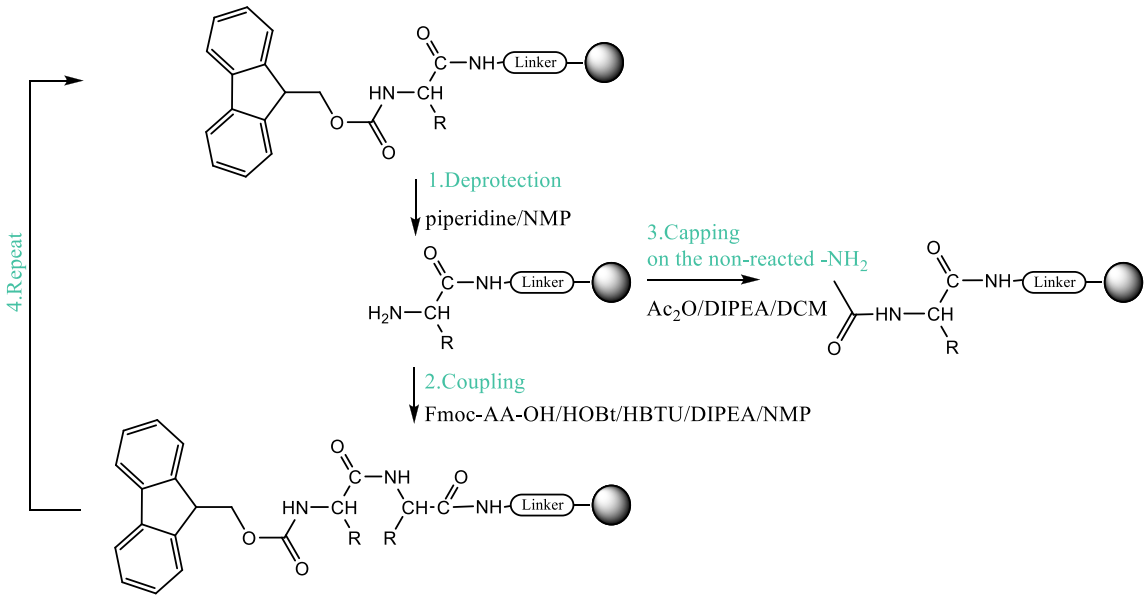

Figure 20. The main steps of the Fmoc solid phase peptide synthesis

For the synthesis of linear peptides Rink Amide AM resin (200-400 mesh) was used as solid support with 0.67 mmol/g loading, which gives an $-NH_2$ protected C-terminal function after cleavage. The first step of the cycle, after swelling the resin in NMP (N-Methyl-2-pyrrolidone), was the removal of Fmoc by 20% piperidine solution in NMP for 3+3+10 minutes. The coupling mixture contained 4 times excess of amino acid building block, HOBt (Hydroxybenzotriazole), HBTU (2-(1H-benzotriazol-1-yl)-1,1,3,3-tetramethyluronium hexafluorophosphate) and 8 times excess of DIPEA (N,N-

Diisopropylethylamine) in NMP. The reaction time was 1h. The incomplete coupling was checked by Kaiser's test using phenol, pyridine and ninhydrin solutions.[106] After each coupling, the resin was treated with the mixture of 10 % (in volume) acetic anhydride and 10 % DIPEA in dichloromethane (DCM) to acetylate the unreacted amino groups (2×15 min), this is called as capping. These steps were repeated until the peptide reached the desired sequence. After the last amino acid coupling, the Fmoc group was removed and the free amino groups were acetylated as described above. Then the resin was washed by DCM and MeOH and dried in a dessicator.

The protecting groups of the side chains and the peptide from the resin were cleaved in one step by the mixture of 92% TFA (trifluoro acetic acid), 1% TIS (triisopropylsilane), 2.5% EDT (ethanedithiol), 2.5% water and 2% phenol. After 4h of reaction, the mixture was filtered and TFA was removed by evaporation. The cleaved peptide was precipitated in ice cold ether and then centrifuged with 6000 rpm for 15 min. The step of washing with ether was repeated two more times. The crude product was lyophilized.

Side chain protected linear precursors of the cyclic peptides were synthesized on pre-loaded H-Gly-2-Cl-trityl (0.54 mmol/g, 0.5 g) resin following the same protocol. The cleavage of the peptide from this resin leaves the C-terminus free (acid form) to enable the cyclization. The precursor was cleaved from the resin by TFA in DCM (1/99 v/v) in a short time (2×5 min) in order to avoid the deprotection of the side chains. The filtrate was neutralized in MeOH/pyridine 8/2. After filtration, evaporation and precipitation, the product was dissolved in DCM in 0.5 mM concentration. A mixture of 3 equiv. of PyBOB (benzotriazol-1-yl-oxytripyrrolidinophosphonium hexafluorophosphate) and 4 equiv. of DIPEA was added, and stirred for 2h. DCM was removed by evaporation followed by precipitation and centrifugation. Then the product was treated in the same way like described before to cleave the protecting groups and obtain the crude product.

The products were purified by reversed phase HPLC on a Shimadzu LC-20 instrument equipped with a Phenomenex Synergi 4 μm fusion-RP 80 Å semi-preparative column using H_2O and acetonitrile eluents containing 0.10% TFA at 3 mL/min flowrate. ESI-MS and analytical RP-HPLC using an analytical column (Chromolith® performance RP-18e 100-4.6 mm) at 1 mL/min flowrate (gradient 0-60% of AcN in 30 min) were performed to check the purity. For the detailed description of the synthesis and the analytical data of **EC**, **VC** and **HS** peptides see reference [107, 108] and of $\mathbf{P^{3C}}$ see [109]. The references of the 3 cysteine containing and the tetrapeptides are summarized in Table 1.

Table 1. Analytical HPLC and (+) ESI MS references of the studied peptides

Name	t_r (min)	Chemical formula	Molecular weight (g/mol)	m/z $[M+2H]^{2+}$	m/z $[M+H]^{+}$
1^L	10.5	$C_{36}H_{62}N_{14}O_{14}S_3$	1010.37	506.3	1011.4
1^C	10.7	$C_{34}H_{57}N_{13}O_{13}S_3$	951.34	476.8	952.3
2^L	10.4	$C_{36}H_{62}N_{14}O_{14}S_3$	1010.37	506.7	1011.4
2^C	10.9	$C_{34}H_{57}N_{13}O_{13}S_3$	951.34	476.7	952.3
3^C	10.8	$C_{37}H_{62}N_{14}O_{14}S_3$	1022.37	512.3	1023.3
CDPPC	14.3	$C_{18}H_{29}N_5O_5S_2$	460.2	–	460.2
CPGC	10.0	$C_{15}H_{25}N_5O_5S_2$	420.1	–	420.0

2. Sample preparation for physicochemical studies

Solution of the peptides

Cysteine containing peptides and Cu(I) are sensitive to oxidation, therefore all the sample manipulations were performed in a glovebox under inert atmosphere and the solvents were degassed with argon. Peptide solutions were freshly prepared for each experiment in the appropriate buffer solution. When experiments with Cu(I) were performed, the peptide solution was prepared in the presence of acetonitrile (10% in volume) to overcome the disproportionation of Cu(I) in water.[110] The final peptide concentration was determined by Ellman's procedure, based on the reaction of DTNB (5,5-dithio-bis(2-nitrobenzoic acid)) with the free thiols forming TNB (2-nitro-5-thiobenzoate) (Figure 21), which has intensive absorption at λ = 412 nm with ε^{412nm} = 14 150 $M^{-1}cm^{-1}$.[111, 112]

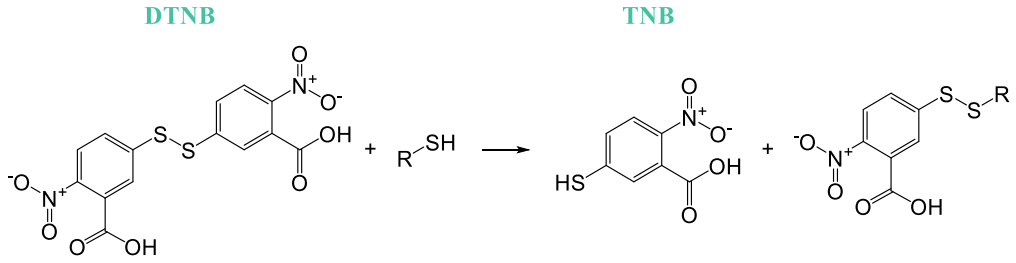

Figure 21. Reaction between DTNB and the free thiols

According to the protocol, 2.5 mL of phosphate buffer (100 mM, pH = 7.25) was transferred to a UV cell (l = 1 cm) and 200 µL of DTNB solution (~ 10 mM) in the same buffer was added (V_0) and the absorbance was recorded at λ = 412 nm (A_0). After the addition of x mL

aliquot of the peptide solution ($V_{peptide}$), the absorbance was recorded again at the same wavelength (A_1). The concentration was determined according to the following equations.

$$c_{SH} = \frac{A_1 - A_0 \frac{V_0}{V_0 + V_{peptide}}}{14150 \cdot l}$$

$$c_{peptide} = \frac{c_{SH}}{n} \cdot \frac{V_0 + V_{peptide}}{V_{peptide}}$$

c_{SH}: concentration of free thiols

n: number of thiols

Solutions of the metal ions

Cu(I) solution (c ~ 3 mM) was prepared from $Cu(CH_3CN)_4PF_6$ in acetonitrile. The final concentration was determined by adding BCS (bathocuproin disulfonate) in excess and measuring the absorbance of the $[Cu(BCS)_2]^{3-}$ complex (ε^{483nm} = 13 300 $M^{-1}cm^{-1}$).[20] 1.8 mL of phosphate buffer, 20 mM, pH = 7.4 was transferred to a UV cell (l = 1 cm) and 200 µL of BCS solution (c ~ 10 mM) in the same buffer was added (V_0). The absorbance was measured at λ = 483 nm (A_0,). Then x mL aliquot of the metal solution ($V_{Cu(I)}$) was added and the absorbance was recorded again (A_1, λ = 483 nm). The concentration was determined according to the following equation.

$$c_{Cu(I)} = \frac{A_1 - A_0 \frac{V_0}{V_0 + V_{Cu(I)}}}{13300 \cdot l} \cdot \frac{V_0 + V_{Cu(I)}}{V_{Cu(I)}}$$

Zn(II) and Hg(II) solutions (c ~ 3 mM) were prepared from precise weights of $ZnCl_2$ and $HgCl_2$, respectively, dissolved in water.

Solutions of the competitors used for determining the stability constants of the metal-peptide complexes

BCS and BCA (bicinchoninate anion) solutions (c ~ 10 mM) were prepared by dissolving appropriate amounts of sodium bathocuproin disulfonate or sodium bicinchoninate, respectively, in phosphate buffer (20 mM, pH =7.4). For the determination of the concentration of these solutions, they were first diluted by 100 times in the same buffer and then titrated by a Cu(I) solution with known concentration (c ~ 3 mM). The plot of the absorbance at 412 nm as a function of the volume of the added Cu(I) solution gave two straight lines and the intersection point (V_{eq}) indicated the total formation of the ML_2 complex. The concentration was then calculated according to the following equation.

$$c = \frac{2 \cdot V_{eq} \cdot c_{Cu(I)}}{V_0}$$

The zincon solution (c ~ 3 mM) was prepared by dissolving zincon monosodium salt in DMF. The concentration was similarly determined as above. After a 100× dilution in HEPES buffer, the sample was titrated by a Zn(II) solution with known concentration (c ~ 3 mM). The plot A^{620nm} = f($V_{Zn(II)}$) gave the two straight lines and from the intersection point (V_{eq}) the concentration could be easily calculated according to the following equation.

$$c = \frac{V_{eq} \cdot c_{Zn(II)}}{V_0}$$

Iodide solutions (c ~ 0.01 M, 0.1 M and 0.5 M) were prepared by dissolving precise weights of KI in water.

3. **UV-visible spectroscopy**

UV-vis spectra were recorded on a Varian Cary50 spectrophotometer equipped with optical fibers connected to an external cell holder in the glovebox. Generally, 2.5 mL freshly prepared peptide solution in phosphate buffer ($c_{peptide}$ ~ 30 μM, c_{buffer} = 20 mM, pH = 7.4) was transferred into a quartz optical cell with 1.0 cm path length (Hellma Analytics). Then aliquots of the appropriate metal solution (c ~ 3 mM) were added corresponding to 0.1 equivalents. In case of the 3 Cys containing decapeptides, titration with Cu(I) was performed in independently prepared samples due to long equilibration times. Aliquots of the Cu(I) solution corresponding to 0.0-3.0 equivalents were added to the peptide solutions. Samples were equilibrated for at least 2 h. Spectra were recorded regularly until stabilization.

For pH titrations 2.0 mL of the peptide solution (c ~ 30 μM) was transferred into the quartz UV cell and then 0.9-1.0 equivalent of a metal ion was added. The desired pH values were adjusted with KOH and HCl solutions of appropriate concentrations (e.g. 0.1 M, 0.01 M). The pH was measured by a Metrohm 702 SM Titrino system equipped with a Mettler Toledo InLab ® Microelectrode.

4. **CD spectroscopy**

CD spectra were acquired on an Applied Photophysics Chirascan spectrometer. The instrument was calibrated with (1S)-(+)-10-camphorsulfonic acid. The spectra were recorded in the 190-400 nm wavelength range with 1 nm steps and a dwell time of 2 s per points. Data were acquired and treated by Pro-Data and Pro-Data Viewer programs (Applied Photophysics). For each sample 3 parallel spectra were recorded and the average of these

spectra were smoothed. CD spectra are reported in molar ellipticity ([Θ] in units of deg cm^2 dmol^{-1}). [Θ] = θ_{obs}/(10lc) where θ_{obs} is the observed ellipticity in millidegrees, l is the optical path length in cm and c is the peptide concentration in mol/dm^3. Generally, 2.5 mL freshly prepared solution in phosphate buffer ($c_{peptide}$ ~ 30 μM, c_{buffer} = 20 mM, pH = 7.4) were transferred into a quartz optical cell with 1.0 cm path length (Hellma Analytics). Then aliquots of the Cu(I) solution (c ~ 3 mM) were added corresponding to 0.25 equivalents. Titrations of the 3 Cys containing decapeptides with Cu(I) were performed in the same batch samples as described above for the UV titrations.

5. **NMR spectroscopy**

NMR experiments were performed on Bruker Avance 400 MHz and 500 MHz spectrometers equipped with 5 mm inverse broadband probes with Z-gradients. For spectrum acquisition and evaluation TopSpin 3.2 program was applied. All sample manipulations were performed in the glovebox. Peptide concentration was ~ 1 mM. Samples were transferred into tubes with J. Young screwcap to avoid contact with air.

Assignment of the resonances in CDPPC and CPGC peptides

Complete assignment of the proton resonances in the free and Cu(I) bound peptides were achieved by the combination of COSY, TOCSY, NOESY and ROESY experiments. Samples for NMR spectroscopic measurements were prepared in phosphate buffer in D_2O (20 mM, pD = 7.4). Amide protons were identified on the spectra recorded for the samples prepared for the determination of the temperature coefficient as described later.

Cu(I) titration

^{1}H NMR spectra were recorded at 298 K in a 12 ppm window size and 32k time domain. Peptide solutions were prepared in phosphate buffer in D_2O (20 mM, pD = 7.4) titrated with a Cu(I) solution in CD_3CN (c ~ 30 mM).

Diffusion coefficient measurement

Diffusion coefficient measurements were performed using the bipolar stimulated spin echo sequence (PGSE).[113-115] Diffusion coefficients were obtained by TopSpin 3.2 using the following equation: $I = I_0 \exp\left(-D\sqrt{2\pi\gamma g_i \delta}\left(\Delta - \frac{\delta}{3}\right)10^4\right)$, where I and I_0 are the intensities detected with and without gradient pulses of strength g_i, respectively The length of the bipolar gradient pulse is δ/2, Δ is the diffusion delay, and γ is the gyromagnetic ratio

(for protons, γ_H = 4 258 Hz/G). Δ = 149.9 ms and δ = 2 ms values were used in the diffusion coefficient measurements. In the experiments, g was incremented from 2.31 to 43.81 G/cm.

Temperature coefficient measurement

The temperature coefficient of the amide protons of the free ligands and the Cu(I) complexes were measured by recording ^{1}H NMR spectra over the temperature range 278-318 K. Temperature coefficients of the free peptides were compared by recording the spectra in H_2O/D_2O, 9/1, v/v. The spectra of the Cu(I) complexes were recorded in phosphate buffer (20 mM, pH = 7.4, H_2O/D_2O, 9/1, v/v). Residual water signals were suppressed by presaturation.

6. **ESI MS experiments**

Mass spectra were acquired on a LXQ-linear ion trap (THERMO Scientific) instrument equipped with an electrospray source. Electrospray full scan spectra in the range of m/z = 50-2000 amu were obtained by infusion through a fused silica tubing at 2-10 µL/min. The samples were analyzed in the negative mode. The LXQ calibration (m/z = 50-2000) was achieved according to the standard calibration procedure from the manufacturer (using a mixture of caffeine, MRFA and Ultramark 1621). The temperature of the heated capillary for the LXQ was set in a range of 200-250 °C, the ion-spray voltage was adjusted to 3-6 kV and the injection time varied between 5-200 ms. The ligand solution ($c \sim 100$ µM) was prepared in ammonium acetate buffer (pH = 7.0, c_{buffer} = 20 mM). Samples for Cu(I) experiments contained 10% of AcN in volume. Different equivalents of the appropriate metal ion solution ($c \sim 3$ mM) were added to the peptide samples.

7. **Determination of stability constants**

Stabilities of the metal complexes at given pH values were determined in the presence of well-known competitors. The displacement of the metal ions from their peptide complexes by the competitor, or the reverse, was followed by UV spectroscopy in all cases.

Stability of copper(I) complexes

Two competitors, namely BCS (bathocuproin disulfonate) and BCA (bicinconinate anion), presented in Figure 22, were used depending on the stability of the studied Cu(I)-peptide complex.

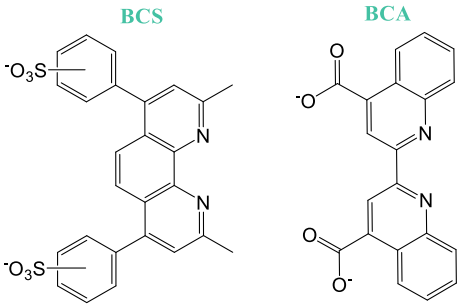

Figure 22. Schematic structure of the competitor BCS and BCA

Both of these ligands form CuL_2 complexes with known stability and spectroscopic properties. [20]

$$Cu^+ + 2\ BCS^{2-} \rightleftharpoons [Cu(BCS)_2]^{3-} \qquad \log\beta_2 = 19.8$$

$$Cu^+ + 2\ BCA^{2-} \rightleftharpoons [Cu(BCA)_2]^{3-} \qquad \log\beta_2 = 17.2$$

$[Cu(BCS)_2]^{3-}$ is an orange complex with absorption maximum at λ_{max} = 483 nm and ε = 13 300 $M^{-1}cm^{-1}$. The purple $[Cu(BCA)_2]^{3-}$ has maximal absorption at λ_{max} = 562 nm maximally with ε = 7 900 $M^{-1}cm^{-1}$.

Different strategies were applied depending on the characteristics of the studied system. In the first attempt, parallel samples were prepared by adding 0.9 equiv. of Cu(I) to 2.5 mL of the peptide solution in phosphate buffer ($c_{peptide}$ ~ 30 µM, c_{buffer} = 20 mM, pH = 7.4). After the formation of the Cu(I)-peptide complex, different amounts of the appropriate competitor were added. Samples were equilibrated until the absorbance stabilised. The calculation of the stability constants was based on the measured absorbance at the wavelength where the absorption is maximal according to the following equations. Charges are omitted for simplicity.

$$[Cu(BCS)_2] = \frac{A}{\varepsilon}$$

$$[BCS] = c_{BCS} - 2[Cu(BCS)_2]$$

$$[Cu] = \frac{[Cu(BCS)_2]}{10^{19.8}[BCS]^2}$$

$$[CuL] = c_{Cu} - [Cu(BCS)_2] - [Cu]$$

$$[L] = c_L - [CuL]$$

$$\beta = \frac{[CuL]}{[Cu][L]}$$

A reverse another strategy was applied in case of CDPPC and CPGC peptides. The $[Cu(BCS)_2]^{3-}$ complex was titrated with the peptide solution. Samples, which were prepared

in phosphate buffer (20 mM, pH = 7.4), contained Cu(I) in $c \sim 30$ μM concentration and BCS in 10-fold excess. Then aliquots of peptide solution were added. Samples were equilibrated until the stabilization of the absorbance. The recorded spectra were fitted with SpecFit program to obtain the apparent stability constant.[116-119]

Stability of mercury(II) complexes

Stabilities of the mercury(II) complexes were determined by competition with I^- ions. Mercury(II) forms consecutively four iodo complexes with known stabilities. Data presented in Table 2 were determined at $I = 0.5$ M ionic strength.[120] In our application these stability constants were recalculated to $I = 0.1$ M by the SIT model.[121, 122]

Table 2. Stability constants of the Hg(II) – I^- complexes previously determined at $I = 0.5$ M ionic strength and the data recalculated for the applied conditions.

	$\log\beta$ (I=0.5 M)[120]	$\log\beta$ (I=0.1 M)
$[HgI]^+$	12.87	13.05
$[HgI_2]$	23.82	24.09
$[HgI_3]^-$	27.60	27.84
$[HgI_4]^{2-}$	29.83	29.91

As a first step, the molar absorption spectra of the Hg(II)-iodo complexes were determined under the conditions used in the subsequent competition with the peptides. Hg(II) solution ($c \sim 30$ μM, $I = 0.1$ M $NaClO_4$) were transferred to a UV cell. The pH was adjusted to 2.0 by a 1.0 M HCl solution. The pH was controlled throughout the whole titration. This Hg(II) sample was titrated with KI solution ($c \sim 0.01$, 0.1; 0.5 M). The recorded spectra were fitted with SpecFit [116-119] where the stability constants were fixed to values given in Table 2.

Afterwards, 1.0 equivalent of Hg(II) was added to 2.0 mL of the peptide solution ($c \sim 30$ μM, pH = 2.0, $I = 0.1$ M $NaClO_4$). This sample was then titrated with KI solution. In the fitting procedure the stabilities and the molar absorption spectra of the Hg(II)-I^- complexes were fixed.

Stability of zinc(II) complexes

The apparent stability constants of the Zn(II) complexes were determined in the presence of zincon (ZI) as a competitor (ZnZI $\log\beta_{11} = 4.9$, $\varepsilon^{620nm} = 23\ 200\ M^{-1}cm^{-1}$) by UV-vis spectroscopy.[123]

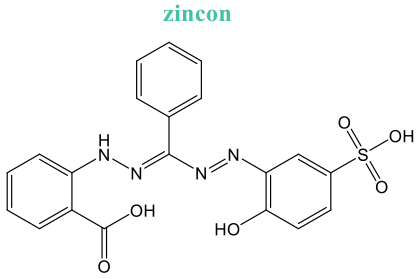

Figure 23. The schematic structure of zincon

The peptide solution was prepared in ca. 30 μM concentration in HEPES (4-(2-hydroxyethyl)-1-piperazineethanesulfonic acid) buffer (c_{buffer} = 20 mM, pH = 7.4) and 1.0 equiv. of Zn(II) was added. The Zn(II)-complexes were then titrated with zincon solution (~ 3 mM in DMF). The stability of the absorbance at λ = 620 nm was controlled before any further addition. The stability constants were calculated by considering the exclusive formation of a mononuclear complex according to the following equations.

$$[ZnZI] = \frac{A}{\varepsilon}$$

$$[ZI] = c_{ZI} - [ZnZI]$$

$$[Zn] = \frac{[ZnZI]}{10^{4.9}[ZI]}$$

$$[ZnL] = c_{Zn} - [ZnZI] - [Zn]$$

$$[L] = c_L - [ZnL]$$

$$\beta = \frac{[ZnL]}{[Zn][L]}$$

RESULTS AND DISCUSSION

V. Results and Discussion

1. Cu(I) binding properties of model peptides of the metal binding loop of CueR proteins

1.1. *The background of the chosen peptide sequence*

The copper efflux regulator CueR protein [124-126] is a transcriptional factor and it belongs to the MerR family of metalloregulatory proteins.[127-130] It regulates the expression of proteins which take part in copper detoxification in bacteria. CueR is able to sense Cu(I) in zeptomolar (10^{-21} M) concentration and distinguishes +1 charged metal ions from +2 charged ones. The metal binding loop of CueR from *E. coli* is presented in Figure 24. As it is seen, the Cu(I) ion is coordinated by two cysteine residues, which are conserved throughout the MerR family, in linear geometry. This coordination geometry is rarely observed in protein metal binding sites but therefore it can be rather suitable for selective metal ion recognition.[131, 132]

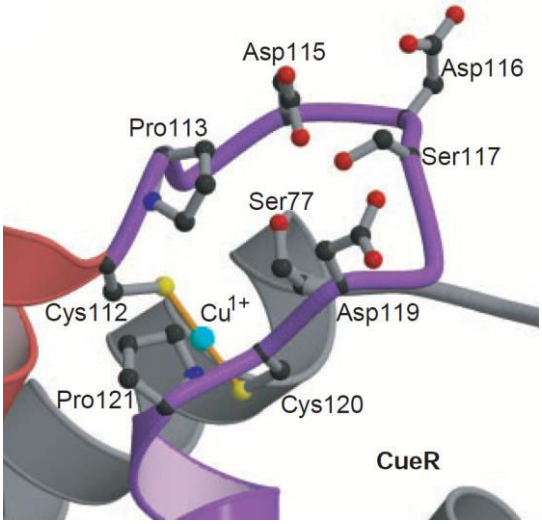

Figure 24. The metal-binding region in CueR [131]

To exploit the selectivity and sensitivity of CueR in Cu(I) chelation, peptides were designed to mimic the metal binding domain of this protein from different bacteria.

Figure 25 presents the schematic structures of the studied peptides. Two of them are identical to the native sequence of CueR in bacteria *E. coli* (Ac-A**C**PGDDSAD**C**PI-NH_2; **EC**) and *V. cholerae* (Ac-S**C**PGDQGSD**C**PI-NH_2; **VC**). The third one (Ac-S**C**HGDQGSD**C**SI-NH_2; **HS**) is the variant of **VC** where the prolines were replaced by a histidine and a serine to modify the flexibility and as well the metal binding properties of the

molecule. Indeed, histidine and proline can be found at the same positions in some other MerR family member proteins.[131]

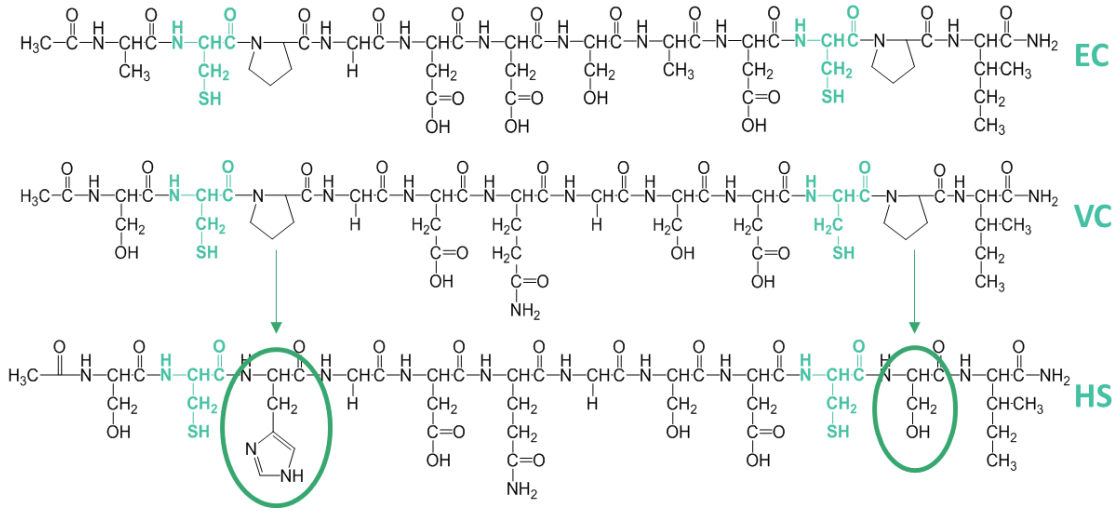

Figure 25. Schematic structures of the CueR model peptides

HS was demonstrated to be able to accommodate Cd(II), Hg(II) and Zn(II), which are metal ions with significantly different coordination preferences. **HS** formed a variety of species with Cd(II) depending on the pH and the metal ion availability.[133] Hg(II) was bound to the two cysteine residues of the peptide forming a loop-like structure. In contrast, in Zn(II) ligation the histidine moiety also participated in metal ion binding besides the cysteine thiolates, providing a more structured form of the peptide backbone with higher helical content.[134] Interestingly, **EC** and **VC** bound Ag(I) by a protonated thiol with a pK_a close to physiological pH. [108] Despite of the similar chemical characteristics of Ag(I) and Cu(I), the behavior of the peptides with Cu(I) cannot be predicted and therefore the study of the Cu(I)-**EC/VC/HS** systems is inevitable.

1.2. *Mononuclear Cu(I) complexes of the CueR mimicking peptides*

The interaction between Cu(I) and **EC**, **VC**, **HS** peptides was first studied by UV-vis spectroscopy. Aliquots of Cu(I) solution corresponding to 0.1 equivalent per ligand were added to the peptide solutions at pH = 7.4. As it can be seen in Figure 26, the increasing Cu(I) concentration results in the appearance of intense absorption bands at λ ~264 nm and λ ~300 nm. The first transition is characteristic for the charge transfer from thiolate to Cu(I) (LMCT) [133] indicating that the metal ion is coordinated to the ligand by the cysteine moieties.

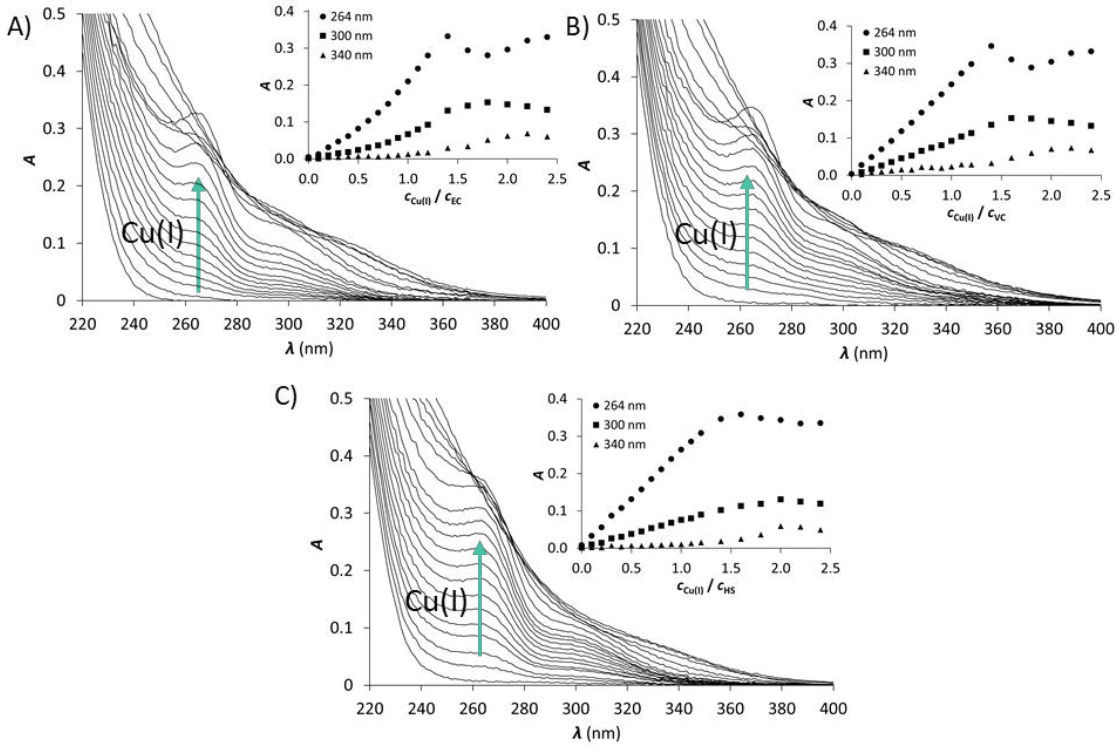

Figure 26. UV titration of **EC** (A), **VC** (B) and **HS** (C) peptides with Cu(I) at pH = 7.4 (phosphate buffer, 20 mM). The insets show the evolution of absorbance as a function of the $c_{Cu(I)}/c_{peptide}$ ratio. ($c_{peptide}$ = 30 μM)

The LMCT absorbance increases linearly in case of **VS** and **HS**, while in the titration of **EC** follow a non-linear trend. Lebrun and co-workers studied the Cu(I) binding of the CopZ protein [135] and observed a similar non-linear trend with intersections at 0.5 and 1.0 Cu(I) equivalents. The formation of two major forms of Cu(I)-CopZ complex was proposed. From 0.0 to 0.5 Cu(I) equivalent two protein bound one Cu(I) ion via one cysteine of each molecule. Between 0.5-1.0 equivalent, $Cu(I)_2(CopZ)_2$ formed where four cysteines took part in the Cu(I) coordination and two of them bridged the two metal ions. The formation of these two Cu(I)-CopZ complexes was more evident in the CD spectra, where two clear breakpoints were observed in the evolution of the LMCT bands.

A competition between Cu(I) and Hg(II) was conducted to determine whether the **EC** peptide forms a similar CuP_2 complex. A sample containing **EC** and 0.5 equivalent of Cu(I) was titrated with Hg(II). The RS^- to Cu(I) LMCT does not change significantly until 0.5 equivalent of Hg(II) is (Figure 27). Since the more thiophilic Hg(II) does not disturb the RS^- to Cu(I) LMCT, there must be free cysteines available to coordinate the added Hg(II) ions. The slight increase observed at 264 nm can be attributed to the overlapping effect of the RS^- to Hg(II) LMCT below 220 nm.[17, 74, 134, 136-138] Further addition of Hg(II) results in the collapse of the RS^- to Cu(I) LMCT and the continuous increase of the Hg(II) LMCT indicates the transformation of the Cu(**EC**) complex into the more stable Hg(**EC**)

species. Based on these observations it can be stated that the CuS_4 type Cu(**EC**) complex does not exist.

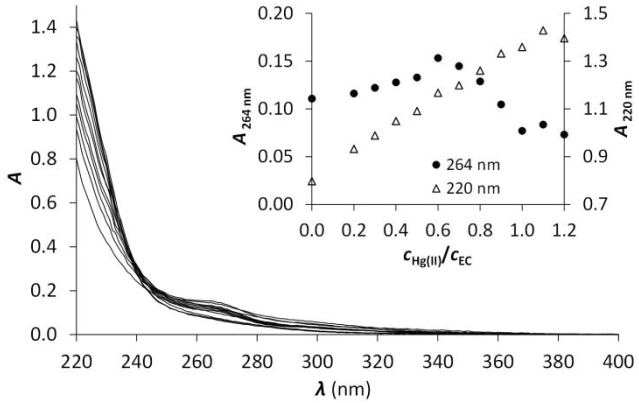

Figure 27. UV titration of the sample containing **EC** and Cu(I) in 1:0.5 ratio with Hg(II) at pH = 7.4 (phosphate buffer, 20 mM). The inset shows the evolution of the absorbance at 264 (•) and 220 (△) nm as a function of the $c_{Hg(II)}/c_{EC}$ ratio. ($c_{peptide}$ = 30 μM)

Molar absorbances of the LMCT $\varepsilon \sim 7000\ M^{-1}cm^{-1}$ per bound Cu(I) were calculated as the slope of the absorbance according to the Cu(I) concentration. This value is compatible with those determined for metallothioneins [28, 29] or other Cys containing ligands.[75, 100] The increase of the absorbance was terminated by a sharp breakpoint at 1.4 Cu(I) equivalents. Previously it was shown that the LMCT is not sensitive for the speciation only for the number of thiolate to Cu(I) bonds.[34] With these ligands the absorbance increase linearly up to 2.0 equivalents of Cu(I), even though it was demonstrated that two different species formed, the CuL mononuclear complex from 0.0 to 1.0 Cu(I) equivalent and Cu_4L_3 or Cu_6L_3 clusters in excess of Cu(I).

The lower energy band at $\lambda \sim 300$ nm was previously attributed to cluster formation in metallothioneins.[28] However it was also observed with other two cysteine containing peptides, where the exclusive formation of mononuclear complex until 1.0 Cu(I) equivalent was proved by DOSY NMR.[74]

CD spectroscopy was also applied to monitor the effects of the gradual addition of 0.25 equivalent of Cu(I) into the peptide solutions. The results are presented in Figure 28. The intense negative band below 220 nm is attributed to $\pi \rightarrow \pi^*$ and possibly overlapping n $\rightarrow \pi^*$ transitions of the amide bonds of the peptide backbone [34, 139] displaying an essentially disordered structure.[107, 134, 140] The gradual change of this band illustrates well the structural rearrangement promoted by Cu(I) binding. Besides, CD spectroscopy also gives information about the RS^- to Cu(I) LMCT bands. Along with the increasing Cu(I)

concentration, CD bands appear in the λ = 240-380 nm wavelength range. For all the three peptides the intensity of these bands increases linearly up to 1.0 equivalent of Cu(I) and isodichroic points are systematically observed.

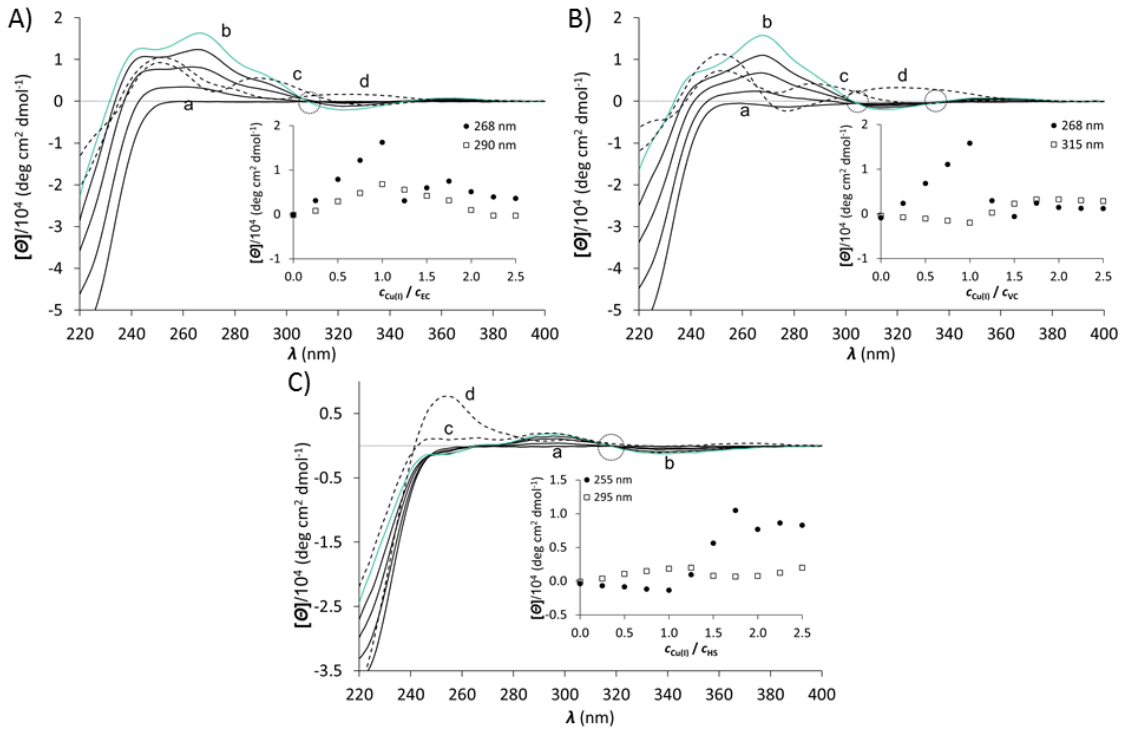

Figure 28. CD titration of **EC** (A), **VC** (B) and **HS** (C) peptides with Cu(I) from 0.0 (a) to 1.0 (b) equivalents (solid lines) at pH = 7.4 (phosphate buffer, 20 mM). Dashed lines represent spectra with 1.25 (c) and 2.0 (d) equivalents of Cu(I). The insets show the evolution of absorbance as a function of the $c_{Cu(I)}/c_{peptide}$ ratio. ($c_{peptide}$ = 30 μM)

These results clearly demonstrate the transformation of the free peptides into one single complex species up to reaching the 1:1 Cu(I):peptide ratio. In other words, only the CuP mononuclear complexes formed with all the three peptides, even in case of **EC** where a more complicated complex formation occurring in different steps was suspected based on the slight bend in the UV titration.

The comparison of the CD spectra of the three peptides in the presence of 1.0 equivalent of Cu(I) (highlighted in green in Figure 28) reveals that the Cu(**HS**) complex has a significantly different CD signature. Since the spectra of the free peptides are quite similar and the difference mainly emerges in the LMCT region, the Cu-thiolate interaction is somehow affected in Cu(**HS**) compared to the Cu(I) complexes of the two other peptides. The absence of the proline residues and the higher conformational flexibility in **HS** could explain this difference. However, the most likely explanation is the participation of the histidine residue in Cu(I) coordination, as it was demonstrated earlier for a few Cu(I)-binding

proteins and model peptides.[9, 10, 141, 142] The additional coordinating donor group besides the thiolates should modify the chiral environment around the Cu(I) and thereby the RS^--Cu(I) LMCT leading to a different shape of the CD spectrum.

(−)ESI MS spectra were also recorded for additional information about the complex speciation. The most intense signals arise from the free ligand as the negatively charged $[P-2H]^{2-}$ and $[P-H]^-$ ions (Figure 29). Mononuclear CuP complexes are also clearly observed with all the three peptides when 0.9 equivalent of Cu(I) is added. They are detected in the form of $[P-3H+Cu]^{2-}$ with m/z = 631.4 (Cu(**EC**)), 639.2 (Cu(**VC**)), and 654.1 (Cu(**HS**)). Cu(**EC**) and Cu(**HS**) complexes are also observed as monocharged species $[P-2H+Cu]^-$ with m/z = 1264.2 and 1309.2, respectively.

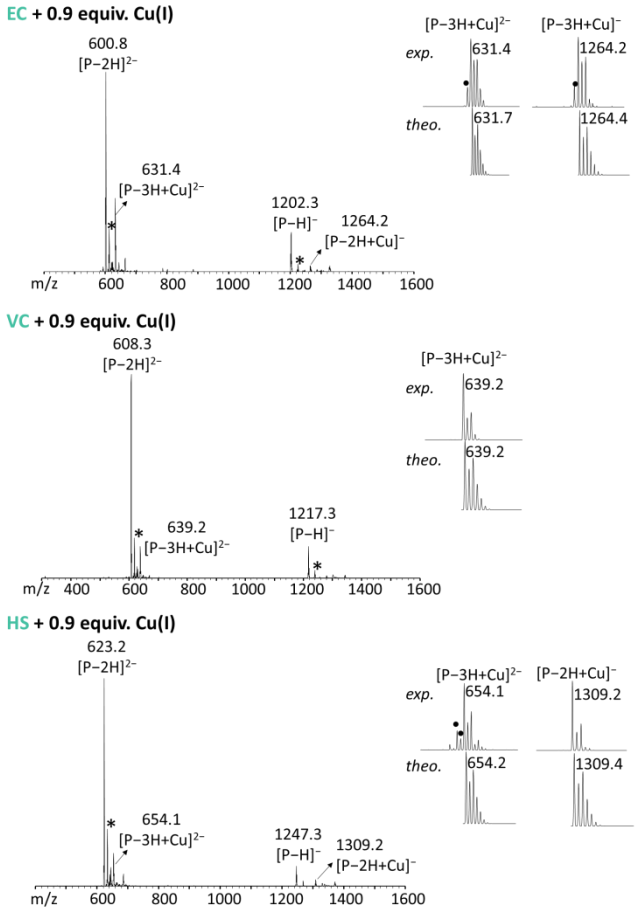

Figure 29. (−)ESI-MS spectra of the studied peptides in the presence of 0.9 equivalent of Cu(I) at pH = 6.9 (NH_4AcO buffer, 20 mM) with the experimental and theoretical isotopic patterns of the detected species. * indicates sodium adducts, • indicates peaks related to oxidized species. ($c_{peptide}$ = 100 μM)

1.3. *Polynuclear Cu(I) species evidenced in excess of the metal ion*

When more than 1.0 equivalent of Cu(I) is added, the complex formation becomes rather complicated. In the presence of Cu(I) excess, a third transition emerges in the UV spectra at λ ~ 340 nm representing a formally spin-forbidden 3d→4s metal to metal transition [28, 143] and indicating the formation of often-observed Cu(I)-thiolate clusters.[11, 75, 143, 144] The intensity of the LMCT bands in the UV spectra continue to increase up to 1.4 equivalents of Cu(I). However, the clear breakpoint at 1.0 Cu(I) equivalent observed in the CD titrations confirm that the LMCT is not sensitive to the nature of the different complexes (monometallic or polymetallic) but only to the number of the thiolate-Cu(I) bonds.

The CD spectra undergo significant changes when more than 1.0 equivalent of Cu(I) is added as represented by dashed lines in Figure 28. This indicates a rather complicated speciation, as a possible result of the formation of different clusters or polymetallic structures.

Figure 30 presents the (−)ESI MS spectra recorded for samples of the peptides with 2.0 equivalents of Cu(I). Several polynuclear species like Cu_2P, Cu_3P or Cu_4P_2 can be observed in all the three systems.

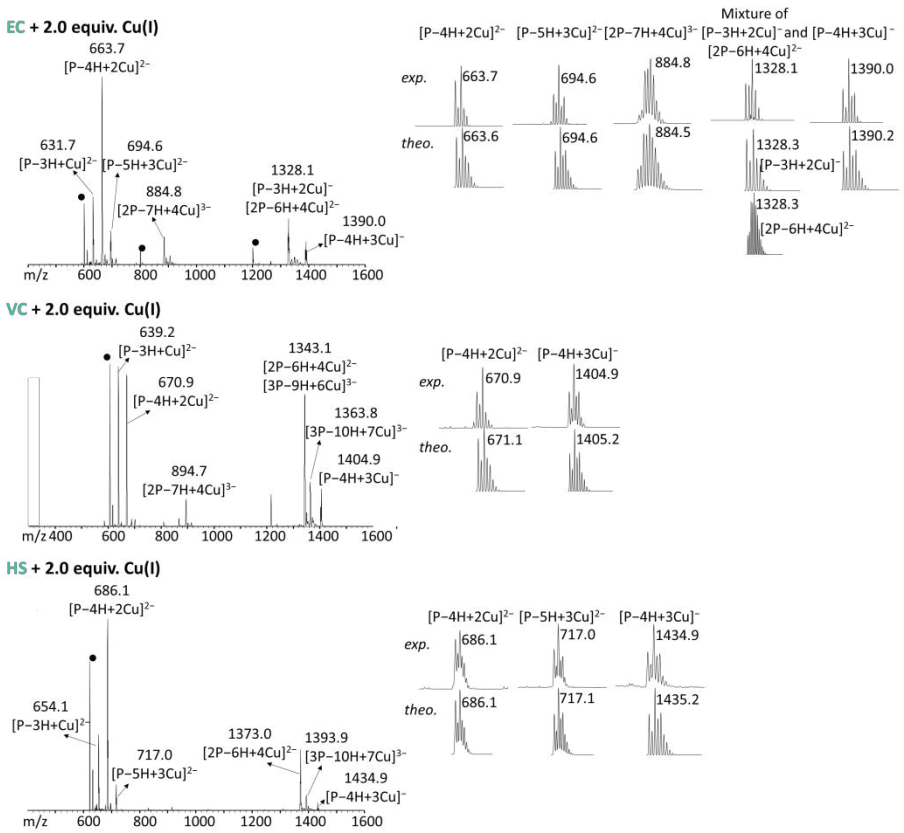

Figure 30 (−)ESI-MS spectra of the studied peptides with 2.0 equivalents of Cu(I) at pH = 6.9 (NH_4AcO buffer, 20 mM) with the experimental and theoretical isotopic patterns of the detected species. • indicates peaks related to oxidized species. ($c_{peptide}$ = 100 μM)

1.4. *Confirmation of the participation of the histidine residue in Cu(I) coordination by ^1H NMR spectroscopy*

The Cu(I)-coordination of the histidine residue in the **HS** peptide was suspected on the basis of the CD spectroscopic results. To obtain more information ^1H NMR measurements were conducted. Solution of **HS** was titrated by Cu(I) from 0.0 to 2.0 equivalents with 0.25 steps. The aromatic region of the recorded spectra is shown in Figure 31. As the results of the Cu(I) addition, the narrow $C_{\varepsilon 1}H$ and $C_{\delta 2}H$ signals of His are shifted to higher ppm values and new, broad signals appear. These findings clearly show that the His residue is involved in Cu(I) binding. However, the two different type of effects suggest different complex formation processes. The downfield shift of the $C_{\varepsilon 1}H$ and $C_{\delta 2}H$ resonances can be attributed the formation of the Cu(**HS**) mononuclear complex and these signals vanish in the presence of Cu(I) excess. Dynamic exchange between several species at the NMR timescale can lead to the broadening of the signals indicating the presence of polynuclear species. They can be seen even at low Cu(I) concentration, where the CD and MS experiments proved the formation only of the 1:1 complex up to 1.0 Cu(I) equivalent.

Nevertheless, the concentration applied in the NMR experiments (mM) is significantly higher than those used in other spectroscopic technics (30-100 μM) and the formation of polymetallic species is therefore strongly favored.

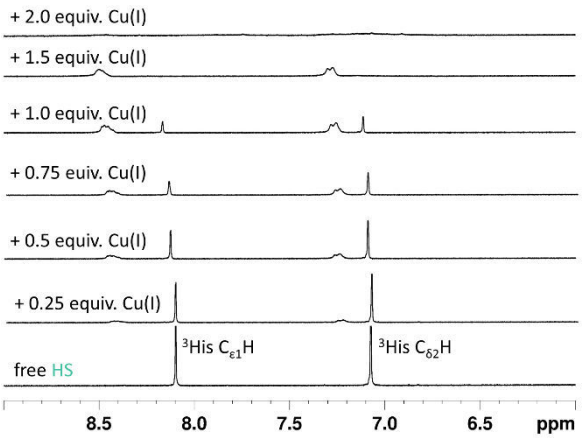

Figure 31. ^{1}H NMR resonances of the imidazole ring of the His residue in the **HS**-Cu(I) system in phosphate buffer in D_2O (20 mM, pD = 7.4). (c_{HS} = 1.5 mM)

1.5. *Effect of the pH on the coordination of the cysteine thiols*

UV-vis spectra of the peptides in the presence of 0.9 equivalents of Cu(I) per ligands were also recorded as a function of pH. As it can be seen in Figure 32, the absorbances attributed to the RS^- to Cu(I) LMCT bands are stable above pH = 7 in all the three studied system and the ε ~ 7 000 $M^{-1}cm^{-1}$ values showed that the complex formation is complete.

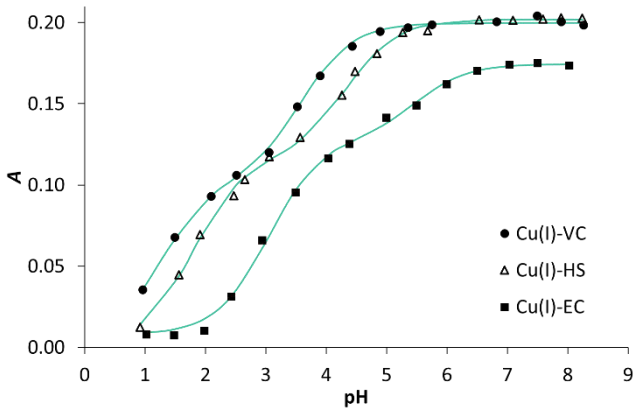

Figure 32. Absorbance recorded at λ = 264 nm in the Cu(I):peptide 0.9:1 systems as a function of pH. The continuous lines represent the fitted values for the same wavelength. Data fitting was performed by SpecFit in the wavelength range of λ = 250-400 nm based on a simple model involving two Cu(I)-promoted thiol deprotonation processes. ($c_{peptide}$ = 30 μM)

The spectral changes observed with decreasing pH suggest two consecutive protonation steps. The data were satisfactorily fitted with two apparent pK_a values with the computer program SpecFit according to the following equations.

$$CuL + H \rightleftharpoons CuLH \qquad logK_1^H = pK_{a2}$$

$$CuLH + H \rightleftharpoons CuLH_2 \qquad logK_2^H = pK_{a1}$$

Table 3. Apparent pK_a values of the Cu(I)-peptide complexes. Experimental errors in the last digits are indicated in parenthesis.

	pK_{a1}	pK_{a2}
EC	3.0(1)	5.5(3)
VC	1.3(2)	3.6(2)
HS	1.8(1)	4.3(2)

The first protonation steps take place with pK_{a2} values between 3.6 and 5.5 and result in half loss of intensity of the LMCT bands observed above pH = 7. This is consistent with the decoordination of one of the cysteines to give a Cu(I) complex with only one thiolate coordinating to the metal center. These apparent pK_a values of the Cu(I) complexes are lower than those reported for the Ag(I) complexes of **EC** and **VC**.[108] (De)protonation occurs significantly below physiological pH and therefore it is probably not relevant in the bacterial copper sequestration of CueR protein. pK_{a1} values determined for the second protonation step are in the range of 1.3-3.0 and lead to the complete loss of the LMCT absorbance to form of the $CuLH_2$ species with no thiolate bound to Cu(I). The latter species in acidic conditions may be low stability Cu(I) complexes in which the metal center is coordinated to other functions than thiolates, or may represent as well the total release of Cu(I) from the protonated ligands.

1.6. *Stability of the Cu(I) complexes at pH = 7.4*

The various spectroscopic technics applied for the characterization of the Cu(I) – **EC**, **VC**, **HS** systems demonstrated the CuP mononuclear complexes are the dominant species at pH = 7.4. Their apparent stabilities were determined in the presence of a well-characterized competitor. Previously studied peptide-Cu(I) complexes with two thiolate coordinating groups have stability in the range of logβ_{11} = 15-17 at physiological pH.[74, 100] Similar affinities were expected for our ligands as well and according to Wedd's recommendation [20, 145] bathocuproin disulfonate (BCS) is an appropriate choice of competitor for

determination of stabilities around $\log\beta_{11}$ ~ 17. ($[Cu(BCS)_2]^{3-}$ $\log\beta_2$ = 19.8). However, BCS turned out to be a too strong competitor in our systems and as Figure 33 shows only 2 equivalents were enough to withdraw nearly 50% of Cu(I) from the peptide complexes. Therefore, the weaker competitor bicinchoninate anion (BCA) was used to obtain the apparent $\log\beta_{11}$ values. Similarly to BCS, BCA forms the $[Cu(BCA)_2]^{3-}$ complex but with lower stability constant ($\log\beta_2$ = 17.2).

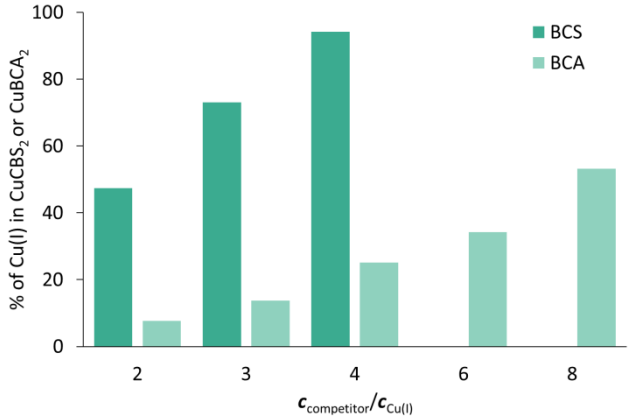

Figure 33. Comparison of the efficiency of BCS and BCA in the withdrawal of Cu(I) from the Cu(**EC**) complex in phosphate buffer (20 mM, pH =7.4). (c_{EC} ~ 65 µM, $c_{Cu(I)}$ = 0.9 c_{EC})

The addition of BCA resulted in the appearance of the intense absorption band centered at λ = 562 nm, ε = 7 900 $M^{-1}cm^{-1}$ as Cu(I) was transferred to $[Cu(BCA)_2]^{3-}$ from the CuP peptide complexes. The first indication on the magnitude of the affinities of the peptides towards Cu(I) is the number of BCA equivalents required for the 50% withdrawal of Cu(I). In case of **EC** only eight equivalents of BCA are enough for the 50% displacement, while with the two other peptides 16 (**VC**) and 24 (**HS**) equivalents are necessary, showing that affinity of the peptides for Cu(I) are in the order of **EC < VC < HS**. The calculated apparent stability constants are presented in Table 4.

Table 4. Apparent stability constants of the Cu(I)-peptide complexes at pH = 7.4. Experimental errors in the last digits are indicated in parenthesis

	$\log\beta_{11}^{pH\ 7.4}$
EC	15.3(1)
VC	15.8(1)
HS	16.3(1)

The lower stability of the Cu(**EC**) complex can be attributed to the charge repulsion between the negatively charged aspartate side chains. Similar effect was observed for other Cu(I) chelating ligands with negatively charged functional groups close to the CuS^{2-} or CuS^{3-} metal center.[76, 100] The somewhat higher affinity of the **HS** peptide may be the result of the missing prolines in the sequence, which makes this peptide more flexible to adopt an optimal geometry around Cu(I). Nevertheless, it is more likely that the contribution of the histidine in the coordination increases the stability of the complex. The Cu(I)-binding affinities obtained for the studied peptides are somewhat lower than those of the Atx1 model peptides incorporating the CxxC motif ($\log\beta_{11}^{pH7.4}$ = 17.4),[74] but compare well with more rigid cyclic decapeptides encompassing the CxxxxC motif ($\log\beta_{11}^{pH7.4}$ = 15.5-16.7).[100] This highlights that the affinity of peptide sequences with two cysteines for Cu(I) depends little on the flexibility of the loop and the number of amino acids between the two Cys residues. Therefore, the driving force for the coordination of the soft Cu(I) cation is expected to be mainly the formation of the two strong bonds with the soft thiolate donors. The stability constants determined in this study are very close to the affinity constant estimated for the Ag(I)-binding of **VC** ($\log\beta_{11}^{pH8.0}$ ~ 15–16), also by a competition experiment.[146] The comparison of the stabilities of the Cu(I) complexes with those determined previously for the Zn(II) complexes [108, 134] shows that these peptides display a large selectivity for Cu(I) vs. Zn(II).

However, the Cu(I)-binding affinities of these peptidic models are 5–6 orders of magnitude lower than that of the native CueR protein.[21] This is a possible consequence of a loss of entropy upon metal ion binding of the models [27] but also the lack of other potential stabilizing effects, e.g. hydrophobic interactions in the metal binding pocket or the overall charge neutralization that operate in the protein in contrast to the models, exemplifying the complexity of metal regulation processes in vivo, which cannot simply be described by thermodynamic equilibria. However, the studied model peptides still resemble the ability of the protein to exclusively accommodate one metal ion under ligand excess conditions.

In Summary

- similar Cu(I)-binding behavior of the three CueR model peptides
- mononuclear CuL complex formation in physiologically relevant conditions
- Cu(I)-coordinated via two Cys residues of the peptides and by the His of **HS**
- formation of polynuclear species in the presence of Cu(I) excess
- cysteine decoordination in two steps with decreasing pH, probably irrelevant in physiological Cu(I) sequestration
- large affinities to Cu(I) at pH = 7.4, in the range of other 2-Cys peptides
- similar affinity for Cu(I) and Ag(I), selectivity vs. Zn(II)
- models cannot reproduce the affinity of the native CueR

2. Cu(I) and Hg(II) binding of cysteine-rich decapeptides

2.1. *Ligand design*

The highly efficient Cu(I)-binding metallothioneins coordinate Cu(I) usually trigonally [23, 24] therefore model peptides containing 3 cysteine residues can be interesting form the viewpoint of Cu(I) chelation. The increase of the number of cysteines hopefully increases the Cu(I) binding affinity as well. In this aspect, the beneficial features of the tripodal and peptidic ligands of the Delangle lab also can be potentially combined. As described earlier, three-cysteine-containing tripodal pseudopeptide ligands form well-defined Cu(I) complexes with high stability, whilst peptide ligands are better internalized by hepatic cells.[102] The peptides studied in this chapter are presented in Figure 34.

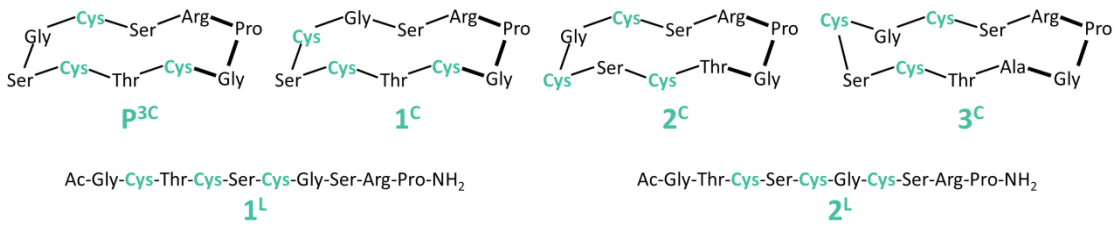

Figure 34. Schematic representation of the three-cysteine-containing peptides. The cysteine residues are highlighted in green and the bonds in the turn motif are indicated in bold.

The sequences are based on the metal binding loop of the copper chaperone Atx1 protein (MxCxxC). Investigation of the model peptide of this protein showed that although the methionine did not participate in the metal ion coordination, it was oriented towards the metal center.[74] Therefore the replacement of the Met residue by a Cys residue seemed to be an obvious choice to improve the metal binding properties in $\mathbf{P^{3C}}$ peptide.[109] The positions of the cysteines in the sequences of linear and cyclic peptides were systematically varied in the CxCxC motif, which can be found also in metallothioneins.[23, 24] The β turn inducer xPGx motif was introduced next to the metal binding sequence in $\mathbf{1^C}$ and one amino acid apart from it in $\mathbf{2^C}$ to rigidify the peptide scaffold. Linear analogues $\mathbf{1^L}$ and $\mathbf{2^L}$ were also synthesized to study the effect of the flexibility/cyclization on the metal binding properties. Finally, an extra amino acid, an alanine was inserted in the sequence of $\mathbf{3^C}$ to determine whether a larger flexibility in the cysteine sidechain orientation is beneficial or not.

2.2. *Copper(I) complexes: speciation*

Complex formation between Cu(I) ions and the peptides at pH = 7.4 was studied by UV-vis spectroscopy. During the titration of the peptides with Cu(I), the absorbances stabilized surprisingly slowly and the equilibrium was reached only after 2 hours. Such a long equilibration time was not observed before in similar three-thiolate-containing systems, neither in the case of simple nor complicated complex formation.[75-77] Therefore, samples were individually prepared by the addition of different equivalents of Cu(I) from 0.0 to 3.0 to the solutions of the peptides with 0.25 or 0.5 steps to ensure enough time for reaching the thermodynamic equilibrium. This long equilibration time might be the first indication of a complicated complex formation. Since all the six peptides display similar behavior, the metal binding of the peptides will be demonstrated by the results obtained with $\mathbf{1^C}$. The spectrum series recorded during the titration with Cu(I) is presented in Figure 35. The characteristic thiolate → Cu(I) LMCT band emerges around λ ~ 260 nm with increasing Cu(I) concentration. The absorbance increases linearly up to 2 equivalents of Cu(I) similarly to tripodal pseudopeptides encompassing 3 thiolates.[75-77] This breakpoint suggests the formation of polymetallic complex(es) with a $(Cu_2P)_n$ overall stoichiometry. The molar absorptions ε = 6-7000 $M^{-1}cm^{-1}$ per bound Cu(I) are in good agreement with previous results.[28, 75]

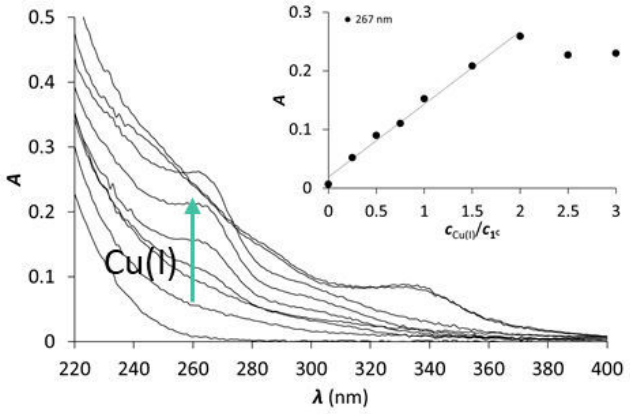

Figure 35. UV titration of $\mathbf{1^C}$ with Cu(I) after 2h of equilibration at pH = 7.4 (phosphate buffer, 20 mM). The inset shows the evolution of the absorbance as a function of the $c_{Cu(I)}/c_{peptide}$ ratio. ($c_{peptide}$ = 30 μM)

CD spectra were also recorded in the same individual samples. The LMCT bands (λ = 260-320 nm) appear as a result of Cu(I) addition (Figure 36), but the observed molar ellipticities ($[\Theta]$ = -2×10^4-1×10^4 deg cm^{-1} $dmol^{-1}$) are relatively low compared to other 3-thiolate systems ($[\Theta]$ = -4×10^4-8×10^4 deg cm^{-1} $dmol^{-1}$).[75-77] The most affected region of the spectra falls in the λ = 220-240 nm wavelength range displaying bands that are

characteristic for the peptide backbone structure. This indicates that the complex formation induces structural rearrangements. More significant changes in the spectrum occur after the addition of 2.0 equivalents of Cu(I). The series of the spectra do not display any clear tendency. These results suggest that the complex formation is rather complicated and the free peptides transform into more than one complex species.

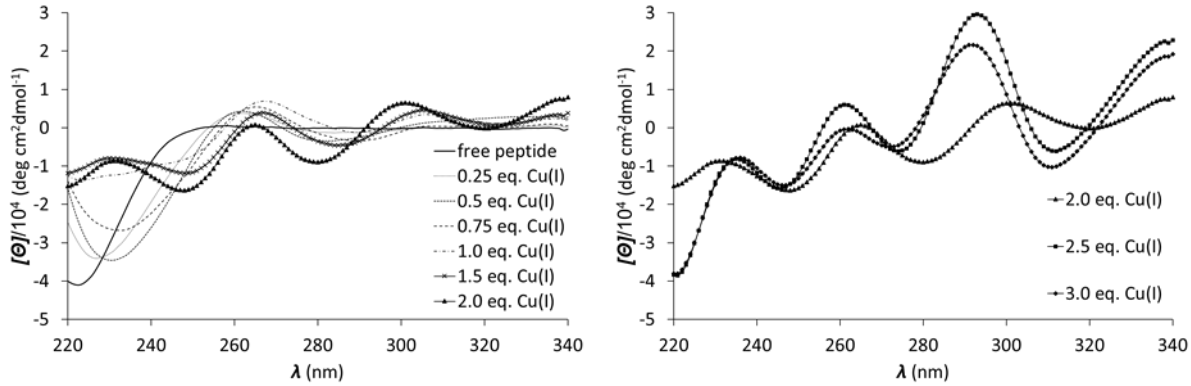

Figure 36. CD titration of $\mathbf{1}^{C}$ with Cu(I) from 0.0 to 2.0 equivalents (left) and from 2.0 to 3.0 equivalents (right) after 2h equilibration time at pH = 7.4 (phosphate buffer, 20 mM). ($c_{peptide}$ = 30 μM)

On the recorded ESI-MS spectra of the peptides with 0.9 Cu(I) equivalents, the formation of polynuclear species like Cu_4P_3, Cu_4P_2 can be observed besides the mononuclear CuP complex (Figure 37). At higher Cu(I) concentration further species with higher nuclearity, Cu_7P_3 and Cu_8P_4 are also detected.

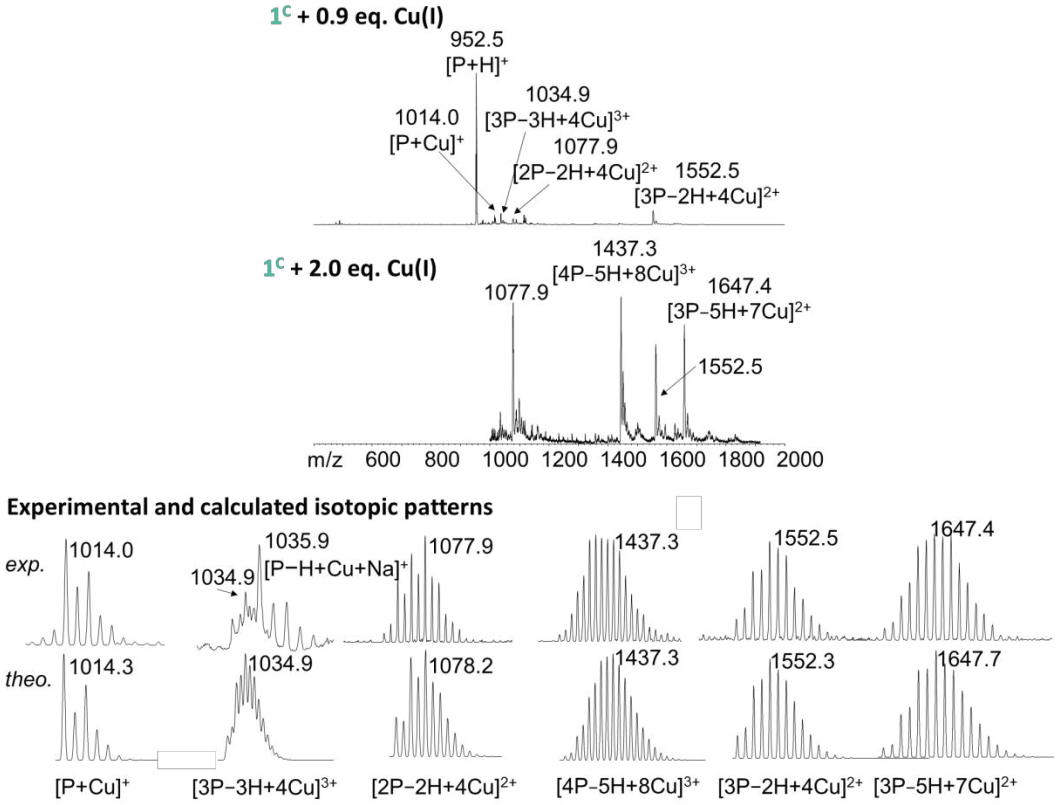

Figure 37. (+)ESI-MS spectra of $\mathbf{1^C}$ with 0.9 and 2.0 equivalents of Cu(I) at pH = 6.9 (acetate buffer, 20 mM) with the experimental and theoretical isotopic patterns of the detected species. ($c_{peptide}$ = 100 μM)

The evolution of the UV spectra is seemingly simple because intensity of the thiolate-Cu(I) LMCT band provides information only about the number of the Cu(I)-S bonds and not about the nature of the complexes. However, CD and ESI-MS results unambiguously show that the Cu(I) complex formation of the studied peptides is rather complicated and that many polymetallic species are present.

The comparison of these Cu(I)-peptide systems to tripodal pseudopeptides incorporating three thiolates reflects that despite the similar evolution of the UV spectra, the Cu(I) complex formation is completely different with the two types of ligands. The tripodal ligands have a well-defined metal binding cavity stabilized by a network of intramolecular hydrogen bonds and this structure is able to control the speciation of the Cu(I) complexes.[75, 76, 79] The sharp contrast between the two groups of ligands can be related to their different structures. The three-cysteine-containing peptides seem to be too flexible to arrange the Cys sidechains in a metal binding cavity appropriate for accommodating one Cu(I) ion, and thus cannot control the speciation of Cu(I) complexes.

2.3. *Copper(I) complexes: stability*

Apparent stability constants of the Cu(I)-peptide complexes were determined in the presence of the bathocuproine disulfonate (BCS) as a Cu(I)-binding competitor.[20] Because of the formation of several Cu(I)-peptide species, stabilities were calculated considering the formation of the CuP mononuclear complex, only to give an overall affinity of the peptides towards Cu(I) and hereby to allow a direct comparison between the peptides and to other values in the literature. The determined $\log\beta_{\mathrm{CuP}}^{\mathrm{pH7.4}}$ values presented in Table 5 show that all the peptides display high affinity for Cu(I) in the range of Cu(I) chaperone proteins, like Atx1.[11] Nevertheless, these values are close to each other, within the range of the experimental errors, indicating that the structural differences have no or little effect on the Cu(I) complex stabilities.

Table 5. The apparent stability constants of the Cu(I)-peptide complexes at pH = 7.4. Experimental errors in the last digits are indicated in parenthesis.

	$\log\beta_{\mathrm{CuP}}^{\mathrm{pH7.4}}$
$\mathbf{P^{3C}}$	18.1(1)
$\mathbf{1^{C}}$	17.3(3)
$\mathbf{1^{L}}$	17.4(2)
$\mathbf{2^{C}}$	17.8(4)
$\mathbf{2^{L}}$	17.8(2)
$\mathbf{3^{C}}$	17.9(4)

2.4. *Mercury(II) complexes: speciation*

Hg(II) is a metal ion with similar coordination properties to Cu(I) and therefore it is an often used probe of the oxygen and water sensitive Cu(I). To answer the question whether the complicated Cu(I) complexation behavior is originated from the peptide structure or it is specific for Cu(I) ion coordination, the interaction of the peptides with Hg(II) was also studied. Although, HgS_3 coordination geometry naturally occurs, for example in Hg(II)-bridged protein dimers, like those observed in the MerR metalloregulatory protein [147] or in the human copper chaperone Atox1,[17, 148] the formation of such a HgS_3 coordination in model systems was rather challenging for a long time, because of the strong preference of Hg(II) for the linear coordination.[149-152] It was first successfully achieved by Pecoraro

et al. applying single oligopeptide chain three-helix bundles [153] and three-stranded coiled coils.[154] However, the third cysteine thiolate coordinated at relatively high pH with pK_a of 8.6 and 7.6, respectively.

The simple $\mathbf{P^{3C}}$ compared to the three-stranded coiled coils is also able to stabilize the HgS_3 environment and the speciation of the Hg(II) complexes is already published,[109] but the stabilities were not determined.

In contrast to the RS^--Cu(I) UV LMCT bands, the LMCTs are good indicators of the coordination mode in the Hg(II)-thiolate systems. Bands characteristic for the HgS_3 environment are in the 240-320 nm wavelength range,[136, 155] while the di-thiolato Hg(II) complexes absorb only in higher energy region (< 230 nm).[74, 137, 138] Thus, the interaction between the peptides and Hg(II) was investigated by UV-vis spectroscopy. Stabilization of the absorbance was significantly faster than in case of Cu(I) complexation, which could be the result of a simpler speciation. Accordingly, continuous titration could be implemented by the addition of aliquots of Hg(II) solution from 0.0 to 3.0 equivalents at pH = 7.4. During the titration, intensive bands emerge on the UV spectra at λ = 240 and 280 nm with increasing Hg(II) concentration as presented by the Hg(II)-$\mathbf{1^C}$ system in Figure 38. The linear increase of the absorbances up to 1.0 equivalent of Hg(II) reflects the formation of a mononuclear HgP complex. The position of these bands clearly shows that all the three cysteine moieties of the peptide participate in the coordination of the metal ion. The absorbance of the bands characteristic for the HgS_3 geometry start to decrease beyond the 1:1 ratio, however the band at ~ 230 nm stays intact. These phenomena can be attributed to the transformation of the mononuclear complex into polymetallic species where the Hg(II) ion is bound to two thiolates.

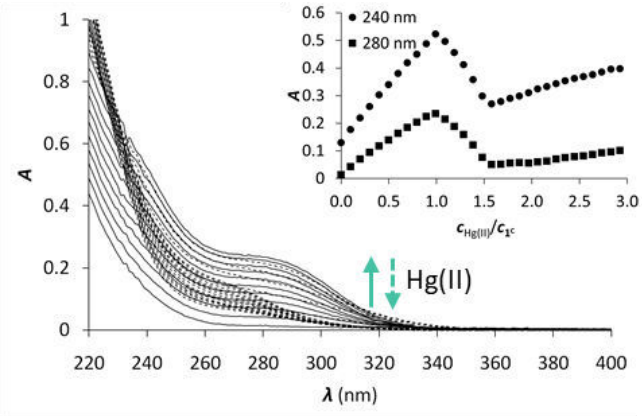

Figure 38. UV titration of $\mathbf{1^C}$ with Hg(II) at pH = 7.4 (phosphate buffer, 20 mM). The insets show the evolution of the absorbances at λ = 240 and 280 nm as a function of the $c_{Hg(II)}/c_{peptide}$ ratio. ($c_{peptide}$ = 30 μM)

ESI-MS measurements support well the conclusions drawn by UV spectroscopic results. Only the mononuclear HgP complex can be observed on the spectrum recorded for the peptides with 1.0 equivalent of Hg(II) in the form of mono- ($[P-H+Hg]^+$; m/z = 1152.3) and double charged ions ($[P+Hg]^{2+}$, m/z = 576.8) (Figure 39).

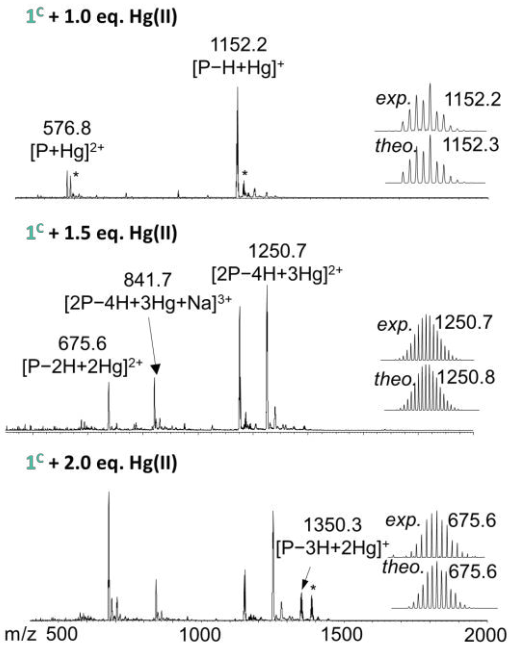

Figure 39. (+) ESI-MS spectra of **1**^{C} with 1.0, 1.5 and 2.0 equivalents of Hg(II) at pH = 6.9 (acetate buffer, 20 mM) with the experimental and theoretical isotopic patterns of the detected species. Asterisks mark the sodium adduct of the corresponding species. ($c_{peptide}$ = 100 μM)

In the presence of 1.5 Hg(II) equivalents, the Hg_3P_2 is the major detected species in the forms of the $[2P-4H+3Hg]^{2+}$ (m/z = 1250.8) and $[2P-4H+3Hg+Na]^{3+}$ (m/z = 841.7) ions. This seems to correlate with the HgS_2 coordination environment of the metal ion indicated by the observed changes of the UV spectra beyond the 1:1 Hg(II):peptide ratio (Figure 40). When 2.0 equivalents of Hg(II) are added, the Hg_3P_2 and Hg_2P ($[P-3H+2Hg]^+$, m/z = 1350.3) are detectable in similar amounts. This further transformation can be the explanation for the slight increase of the absorbance over 1.5 equivalents of Hg(II).

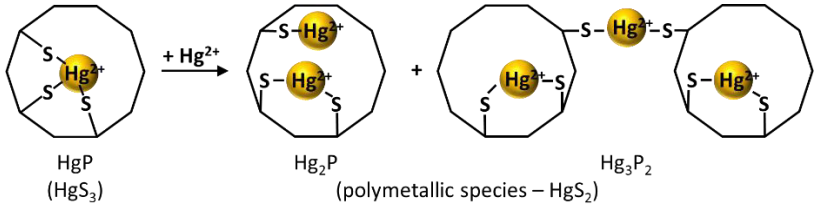

Figure 40. Schematic representation of the Hg(II)-peptide complexes

2.5. *The effect of pH on the Hg(II) complexation*

The effect of the pH on the Hg(II) complexion was also studied and the titration was followed by UV spectroscopy (Figure 41). The significant increase of the absorbance in the presence of 1.0 equivalent of Hg(II) compared to the free peptide at pH ~ 2.5 clearly shows that Hg(II) is already bound to the peptide even at this low pH.

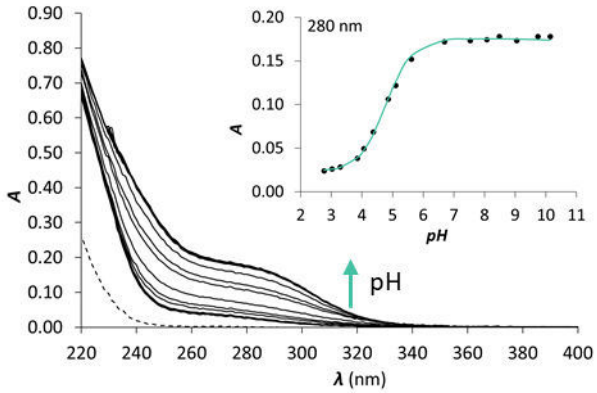

Figure 41. pH titration of $\mathbf{1^C}$ in the presence of 1.0 equivalent of Hg(II). The dashed line represents the spectrum of free $\mathbf{1^C}$ at pH = 2.5. The inset shows the evolution of the absorbances as a function of pH at 280 nm. Symbols represent the experimental points and the line shows the fitted absorbances obtained by SpecFit. ($c_{peptide}$ = 30 μM)

Following the changes in the absorbance at 280 nm characteristic for the HgS_3 geometry shows that the increase of the pH results in a significant increase of the intensity corresponding to the transformation of the HgS_2 species into the HgS_3 in parallel with the deprotonation of the third cysteine thiol moiety. The absorbance at 280 nm is stable over a wide pH range (pH = 6-11). Spectroscopic data were satisfactorily fitted by considering one pK_a value according to the following equation, where L represents the fully deprotonated form of the ligand.

$$HgLH \rightleftharpoons HgL + H \qquad pK_a$$

$$HgS_2 \rightleftharpoons HgS_3$$

The obtained pK_a values of the Hg(II)-peptide complexes are presented in Table 6 and follow the order of $\mathbf{P^{3C} < 3^C \approx 2^C < 1^C < 2^L \approx 1^L}$. Although, these values are in a quite narrow range, some tendency can be observed which may be related to some kind of weak influences. The lowest pK_a was determined for the peptide $\mathbf{P^{3C}}$, which indicates that the CxCxxC pattern of the coordinating Cys residues is probably more favorable for the formation of the HgS_3 geometry than the CxCxC motif. The separation of the metal binding fragment from the turn motif may be the explanation of the slightly lower pK_a of $\mathbf{2^C}$ and $\mathbf{3^C}$

relative to that of $\mathbf{1^C}$. The highest values of the two linear peptides may be the consequence of their larger flexibility and a more significant reorganization necessary for the coordination of the third Cys thiolate.

Table 6. Deprotonation constants of the HgHL complexes. Experimental errors in the last digits are indicated in parenthesis.

	$\mathbf{pK^{HgL}_{HgHL}}$
P^{3C}	4.3(1)[109]
1^C	4.8(1)
1^L	5.1(1)
2^C	4.5(1)
2^L	5.0(1)
3^C	4.5(1)

Interestingly, the values presented here are significantly lower than the pK_a observed for the relevant Hg(II)-complex of a tris-cysteine functionalized tripodal pseudopeptide bearing amidated carboxyl groups[136] or of the Hg(II)-binding three-stranded coiled coils.[153] The bulkiness or the electron-withdrawing effect of the carboxyl function of the tripods probably has an unfavorable effect on the $HgS_2 \rightleftharpoons HgS_3$ transformation. In our peptides the thiol functions are more solvent-exposed, which are expected to deprotonate more easily than similar functions found in the hydrophobic pocket of triple coiled coils complexes.

2.6. *Stability of the Hg(II) complexes*

The high thiophilicity of Hg(II) makes the determination of the complex stabilities challenging, and as a solution for this problem, competitions with iodide ions were performed. Preliminary studies indicate that the iodide was not able to withdraw Hg(II) from the peptide complexes at pH = 7.4, therefore titrations were implemented under acidic condition at pH = 2.0. According to the pH dependent transformation of the HgP complexes, the stabilities determined at pH = 2.0 should correspond to the species with HgS_2 geometry. As a first step, the molar absorption spectra of the Hg(II)-iodo complexes were determined by titrating the metal ion with I^- under the same condition used in the competition

experiments and applying the recalculated stability constants of Hg(II)-iodo complexes presented in Table 2 (Figure 42).

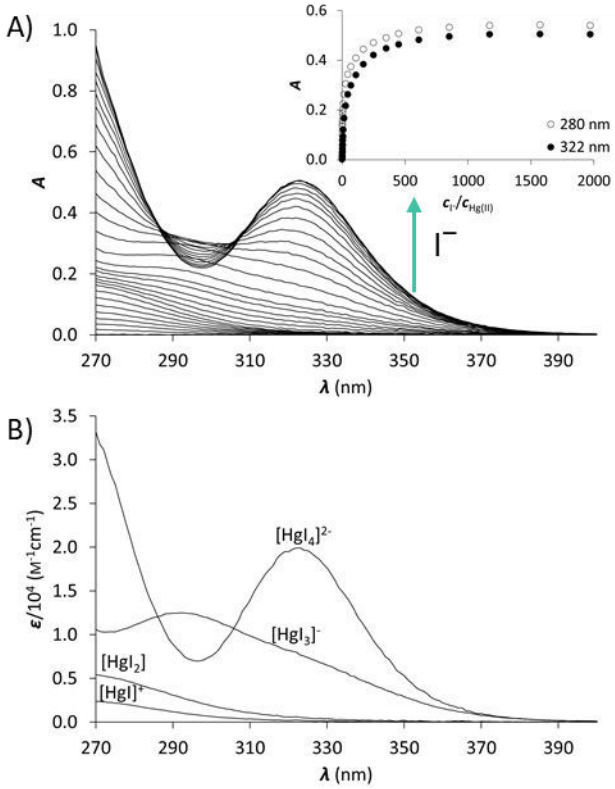

Figure 42. A) UV spectra recorded in the titration of Hg(II) with I^- at pH = 2.0. The inset shows the evolution of the absorbance at 322 nm (•) and 280 nm (◦) as a function of the $c_{I^-}/c_{Hg(II)}$ ratio. **B)** Molar absorption spectra of the Hg(II)-iodo complexes obtained in SpecFit. ($c_{Hg(II)}$ = 30 μM, I = 0.1 M $NaClO_4$)

UV spectra recorded in the titration of the Hg**1**^{C} complex with I^- are presented in Figure 43. At the beginning of the titration, up to ca. 10 equivalents of I^- no considerable spectral changes were observed. Further addition of I^- resulted in the appearance of new bands characteristic for the $[HgI_3]^-$ and $[HgI_4]^{2-}$ complexes. Complete displacement of the peptide was achieved by the addition of ca. 2000 equivalents of I^-.

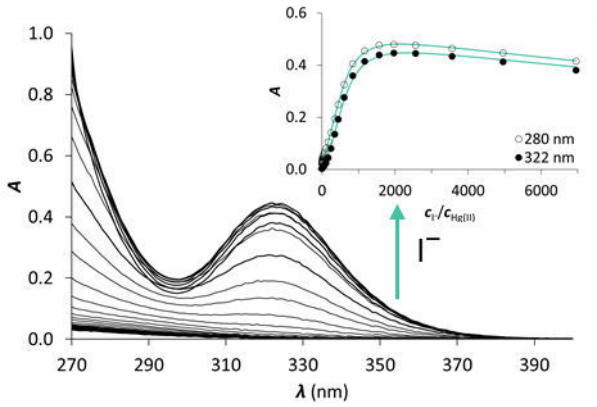

Figure 43. UV spectra recorded in the titration of Hg**1**^{C} with I^- at pH = 2.0. The inset shows the evolution of the absorbance at 322 nm (•) and 280 nm (◦) as a function of the $c_I/c_{Hg(II)}$ ratio. Symbols represent the experimental data, and solid lines represent the absorbances calculated by SpecFit. ($c_{Hg(II)} = c_{peptide} = 30$ μM)

To obtain the apparent stability constants of the HgP complexes, the recorded series of spectra were fitted by SpecFit. The molar spectra and the stability of the Hg(II)-iodo complexes (Table 2) were fixed in the fitting procedure. Best fits were obtained when the formation of a HgPI ternary complex was also considered. The appearance of such species is probably a consequence of the flexibility of the peptide structures. These complexes are present only in the early stages of the titration in ~20% relative proportion. In case of Hg**P**^{3C} a somewhat larger fraction of HgPI could be observed. The formation of the mixed ligand complexes, according to the HgP + I ⇌ HgPI equation, is characterized by stabilities falling in the range of log$K$ ~ 1.5-2.5. The determined apparent stability constants of the HgP complexes are presented in Table 7. These values are close to each other, indicating that all the six peptides have similar affinities for Hg(II) and that the differences in the peptide sequences do not notably affect the stabilities. Taken into account that at pH = 2.0 only two Cys thiolates are coordinated to the Hg(II), it is a possible explanation that the thiophilicity of Hg(II) easily governs the formation of the HgS_2 structure, independently from the preorientations of the donor groups.

Table 7. Apparent stability constants and estimated stability data of the Hg(II) complexes. Experimental errors in the last digits are indicated in parenthesis.

	$\log\beta_{HgP}^{pH2.0}$	$\log\beta_{HgP}^{pH7.4}$[a]	$\log\beta_{HgHL}$[a]	$\log\beta_{HgL}$[a]
P^{3C}	27.2(1)	40.9	48.7	44.4
1^{C}	27.3(1)	40.5	48.8	44.0
1^{L}	27.1(1)	40.0	48.6	43.5
2^{C}	27.2(1)	40.7	48.7	44.2
2^{L}	27.0(1)	40.0	48.5	43.5
3^{C}	27.5(1)	41.0	49.0	44.5

[a]Apparent stability constants for pH 7.4 and formation constants of the HgHL and HgL species were estimated from the apparent stabilities obtained at pH = 2.0

Formation constants were calculated for the protonated HgHL and the fully deprotonated HgL complexes from the relevant apparent stability constants applying the pK_a values corresponding to the HgLH ⇌ HgL + H process (Table 6) and the proton dissociation constants of one of the peptides, $\mathbf{1}^{L}$ ($pK_a^{H_3L}$= 7.67(1), $pK_a^{H_2L}$= 8.56(1), pK_a^{HL}= 9.26(1))[2] according to the following train of thoughts:

- The proton dissociation constants (K_a^{HL}, $K_a^{H_2L}$, $K_a^{H_3L}$) of the ligands can be expressed in the form of the overall formation constant of the fully protonated peptides (β_{H_3L}):

$$\frac{[H_3L]}{[L][H]^3} = \beta_{H_3L} = \frac{1}{K_a^{HL} \cdot K_a^{H_2L} \cdot K_a^{H_3L}} \quad (1)$$

- The apparent stability of the mononuclear complexes at pH = 2.0 is defined as:

$$\beta_{HgP}^{pH2.0} = \frac{[HgP]}{[Hg][P]} \quad (2)$$

- Since at pH = 2.0 Hg(II) binds to the monoprotonated ligand, the concentration of free peptide and the HgP complex can be estimated with the following concentrations:

$$[HgP] \approx [HgHL] \quad (3)$$

$$[P] \approx [HL] \quad (4)$$

- Then equation 2 transforms into:

$$\beta_{HgP}^{pH2.0} = \frac{[HgHL]}{[Hg][H_3L]} \quad (5)$$

[2] Acidic dissociation constants were determined by pH potentiometric titrations following a protocol describe earlier.[140]

- According to equation 1 [H_3L] can be substituted by:

$$[H_3L] = \beta_{H_3L}[L][H]^3 \quad (6)$$

- and then rearrange equation 5 to

$$\beta_{HgP}^{pH2.0} \cdot \beta_{H_3L} \cdot [H]^2 = \frac{[HgHL]}{[Hg][L][H]} \quad (7)$$

- This is not else than the formation constant of HgHL complex:

$$\beta_{HgHL} = \frac{[HgHL]}{[Hg][L][H]} \quad (8)$$

- The combination of (7) and (8) leads to an expression allowing the calculation of β_{HgHL} from the experimentally measured stability data:

$$\beta_{HgHL} = \beta_{HgP}^{pH2.0} \cdot \beta_{H_3L}[H]^2 \quad (9)$$

$$\log\beta_{HgHL} = \log\beta_{HgP}^{pH2.0} + \log\beta_{H_3L} - 2pH \quad (10)$$

- Formation constants for the parent HgL complexes can be obtained by using the spectrophotometrically determined deprotonation constants (pK_a^{HgHL}) for the HgHL ⇌ HgL+ H process:

$$\log\beta_{HgL} = \log\beta_{HgHL} - pK_a^{HgHL} \quad (11)$$

The calculated thermodynamic stability constants ($\log\beta_{HgHL}$ and $\log\beta_{HgL}$) are also presented in Table 7. These data also fall in a narrow range, confirming that the orientation of the Cys-sidechains has only a weak influence on the complex stabilities. Nevertheless, the slightly lower affinity of the linear peptides suggests the need for a more pronounced structure of the peptide backbone provided by the cyclization.

The thermodynamic stability constants of the HgL species of our peptides allow the comparison with Hg(II)-bisthiolate complexes of highly constrained bis-thiol ligands. Our peptides, indeed, display very similar Hg(II)-binding affinities to that of the well-known soft metal ion chelator BAL ($\log\beta_{HgL}$ = 44.8)[156] which forms a highly stable 5-membered chelate ring around the metal ion. Comparison of our data to the stability of the HgL species of the tetrapeptide Ac-Cys-DPro-Pro-Cys-NH_2 ($\log\beta_{HgL}$ = 40.0)[137] clearly indicates that the structure of our peptides are prone to easily rearrange to a suitable form for the tridentate coordination of Hg(II) and thus the larger number of Hg(II)-thiolate bonds is revealed in higher affinities.

Apparent stabilities of the HgP mono-complexes can be re-calculated for any desired pH values from the calculated thermodynamic stability constants (Table 7) allowing a direct

comparison of the Cu(I)- and Hg(II)-binding affinities of the studied peptides. The peptides show 20 orders of magnitude larger affinity for Hg(II) ($\log\beta_{HgP}^{pH7.4}$ ~ 41) than for Cu(I) ($\log\beta_{HgP}^{pH7.4}$ ~ 18) at physiological pH, due to the significantly softer character of Hg(II).

The three-cysteine containing peptides are found to be too flexible to control the Cu(I) complex speciation leading to the formation of several polymetallic species, but they are well adapted to accommodate one Hg(II) ion in a tri-thiolate environment. This significant difference between the behavior of the peptides towards Cu(I) and Hg(II) also indicate that the use of Hg(II) as a probe for Cu(I) coordination with sulfur-rich peptides or proteins in physiological conditions is not always fully appropriate.

IN SUMMARY

- different complex speciation of the peptides with Cu(I) and Hg(II)
- complicated Cu(I) complex speciation
- the peptide structure is too flexible to control the Cu(I) speciation
- affinity for Cu(I) is in the range of 10^{17}-10^{18}
- simple Hg(II) complex speciation: mononuclear complex with HgS_3 geometry at physiological pH
- pH dependent $HgS_2 \rightleftharpoons HgS_3$ transformation, with relatively low pK_a
- large Hg(II) complex stability ($\log\beta_{HgP}^{pH7.4}$ ~ 41)
- sequences are adapted for trithiolate Hg(II) coordination
- Hg(II) is not always an appropriate Cu(I) probe

3. Efficient Cu(I) binding of a rigid tetrapeptide incorporating two cysteines linked by a β turn

3.1. *Rational peptide design to control the metal binding*

Studies of the series of the relatively long 3-cysteine-containing peptides demonstrated that Cu(I) complexation with quite flexible peptides could be complicated. Therefore, rational ligand design can be a logical solution to control the speciation of Cu(I) complexes. Introducing amino acids that induce β turns is one of the options to rigidify peptide scaffolds and enhance metal binding affinity.[157] β turn is the simplest defined loop structure with conformational characteristics.[158] It consists of four amino acid residues (from i to i+3) and defined by a hydrogen bond between the C=O of the residues i and the NH of the i+3. There are four types of beta turns depending on the Φ and Ψ torsion angles of residues i+1 and i+2. These torsion angles are the following $\Phi_{i+1} = -60$, $\Psi_{i+1} = -30$, $\Phi_{i+2} = -90$ and $\Psi_{i+2} = 0$ in type I, and $\Phi_{i+1} = -60$, $\Psi_{i+1} = 120$, $\Phi_{i+2} = 80$ and $\Psi_{i+2} = 0$ in type II. Type I' and II' are the mirror images of type I and II.[159, 160]

The cyclic proline (Pro) is the most constrained natural amino acid, which can induce a turn. As it was presented in the Literature review, simple Cu(I) complex speciation was achieved with cyclic peptides encompassing β turn inducer xPGx motifs by the Delangle group.[74, 100] Similarly, it was demonstrated that β sheet like peptide scaffold was a key element in achieving high affinity for uranyl cation.[161] Mononuclear UO_2^{2+} complexes of constrained structured peptides with two PG motifs had significantly higher stability than complexes formed with the more flexible ones containing only one turn, while the completely unstructured linear peptide formed nondefined polymetallic species of low affinity. Iranzo and co-workers proved that cyclization had a remarkable effect on the Cu^{2+} coordination properties of decapeptides bearing two prolylglycine units. The cyclic peptides had a higher affinity for Cu^{2+} than the linear ones at all studied pH values. Difference in Cu^{2+} exchange rate was also observed between the two structures.[162, 163]

Some amino acids of D configuration were also shown to stabilize peptide structures.[158, 164-166] Iranzo's team also demonstrated that the introduction of the DPro-Pro motif into a short peptide sequence was very favorable for heavy metal chelation.[137] The tetrapeptide Ac-Cys-DPro-Pro-Cys-NH_2 (CDPPC) incorporating two cysteines at the two termini was designed to mimic the CxxC consensus sequence found in metallochaperones or metal transporters.[167-169] This peptide forms a mononuclear Hg(II)-complex with a large stability ($\log K = 40.0$). The favorable effect of the DPro-Pro

motif on Hg(II) coordination was proven by comparison to the CPPC peptide incorporating two natural proline residues. A three orders of magnitude lower stability constant was estimated for the dithiolatomercury(II) complex of CPPC underscoring the significance of the preorganized DPro-Pro containing sequence.

The outstanding Hg(II)-sequestering features of CDPPC suggest that this short sequence may also be interesting in view of chelating Cu(I), a soft metal ion with coordination preferences resembling those of Hg(II). We also studied the behavior of a less rigid structure introduced by the more flexible Xxx-Pro-Gly-Xxx motif in the peptide Ac-Cys-Pro-Gly-Cys-NH_2 (CPGC). The schematic structures of the peptides are presented in Figure 44.

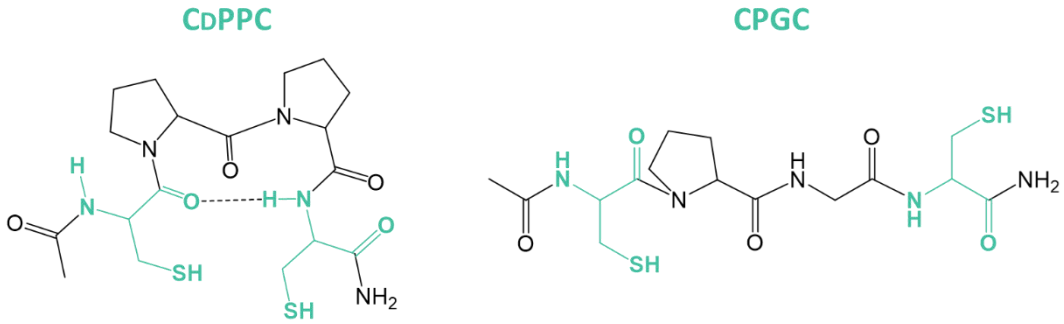

Figure 44. Schematic structures of the tetrapeptides with *β* turn inducing motifs. The dashed line symbolizes the H-bond in the turn present in CDPPC

3.2. *Characterization of the apopeptides*

The solution structures of the peptides were investigated by ^{1}H NMR. Complete assignment of the proton resonances (Table 8) was achieved by the combination of 1D (Figure 45) and 2D (COSY, TOCSY, NOESY) methods. The ^{1}H NMR spectrum of CDPPC recorded at 298 K in water reflects the presence of peptides with different structures. The major conformation represents 73% of the total peptide concentration. The resonances attributed to the minor components disappear upon Cu(I) addition (discussed later), which suggests that the corresponding minor species are in a relatively slow exchange with the major one at the NMR timescale and that Cu(I) restricts the peptide into one specific conformation in the complex.

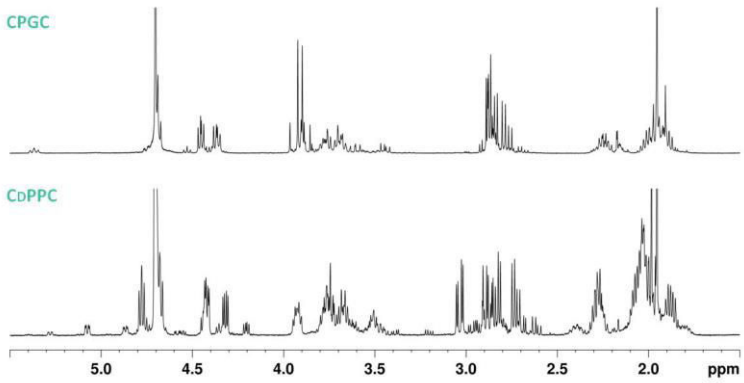

Figure 45. ^{1}H NMR spectra of the free peptides in phosphate buffer in D_2O (20mM, pD = 7.4). ($c_{peptide}$ ~ 1.00-2.00 mM)

Table 8. Assignments of the ^{1}H NMR resonances (δ, ppm) of the free peptides (major conformation) in phosphate buffer (20 mM, pD = 7.4, D_2O). Amide protons were identified in H_2O/D_2O, 9/1, v/v.

CPGC	NH	$C_\alpha H$	$C_\beta H$	Others
Cys1	8.28	4.67	2.82	(Ac) 1.97
Pro2	–	4.38	1.93; 2.26	(γ) 2.00 (δ) 3.70; 3.78
Gly3	8.46	3.93	–	
Cys4	8.09	4.47	2.88	(NH_2) 7.14; 7.63

CDPPC	NH	$C_\alpha H$	$C_\beta H$	Others
Cys1	8.21	4.77	2.77	(Ac) 1.95
DPro2	–	4.41	2.01; 2.23	(γ) 2.02 (δ) 3.64; 3.89
Pro3	–	4.64	1.86; 2.28	(γ) 2.03 (δ) 3.74
Cys4	7.87	4.32	2.87; 3.02	(NH_2) 7.07; 7.14

Since β turns are characterized by a hydrogen bond between the $C{=}O_i$ and $NH_{(i+3)}$ groups, the temperature coefficients of the amide proton resonances were measured since they are good indication of the presence or absence of H-bonds. Weaker intermolecular hydrogen bonds formed with the solvent molecules are more easily cleaved with increasing temperature, therefore the chemical shifts of solvent exposed NH display higher temperature dependence. On the other hand, it is generally assumed that NH resonances owing temperature gradient less negative than −4.5 ppb/K are solvent-shielded and participate in strong intramolecular hydrogen bonds providing a constrained peptide structure.[170-174]

Table 9 compares the measured temperature coefficients of the Cys amide proton resonances in the two peptides. These values show that the NH of the Cys4 residue is significantly more solvent shielded than that of the Cys1 in both cases.

Table 9. Temperature coefficients of the amide proton resonances of the Cys residues

	$\Delta\delta/\Delta T$ (ppb/K)			
	CDPPC		CPGC	
	Cys1	Cys4	Cys1	Cys4
Free L	−9.3	–4.0	–8.2	–6.3
Cu_4L_3	–6.7	–2.5		

The temperature coefficient determined for the NH resonance of the Cys4 residue in CDPPC (−4.0 ppb/K) strongly supports the hydrogen bond between the C=O of Cys1 and the NH of Cys4 characteristic for a β turn. This value in CPGC is significantly smaller ($\Delta\delta/\Delta T$ = −6.3 ppb/K) indicating the absence of such a H-bond as a consequence of the less structured backbone.

3.3. *Copper(I) ion complexes of CDPPC: spectroscopic results*

The interaction between CDPPC and Cu(I) was investigated by UV-vis spectroscopy (Figure 46). The appearance of the characteristic RS^- to Cu(I) LMCT transition at 263 nm [133] in parallel with increasing Cu(I) concentration proves the coordination of the cysteine thiolates to Cu(I). The absorbance at this wavelength increases linearly up to 1.3 equivalents of Cu(I) with a molar absorbance value consistent with the previous results (ε ~ 7000 $M^{-1}cm^{-1}$).

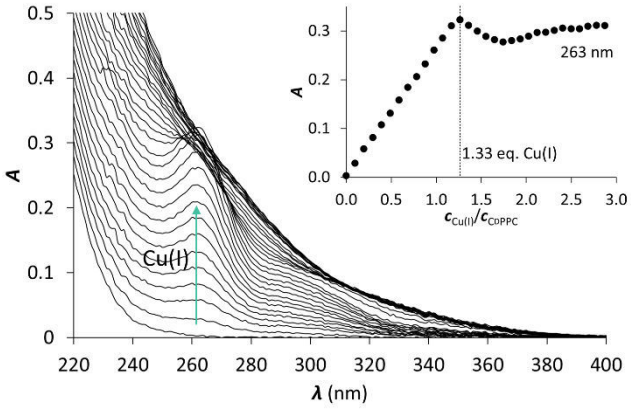

Figure 46. UV titration of CDPPC with Cu(I) at pH = 7.4 (phosphate buffer, 20 mM). The inset shows the evolution of absorbance as a function of the $c_{Cu(I)}/c_{CDPPC}$ ratio. ($c_{peptide}$ = 30 μM)

Intense bands appear in the LMCT region on the recorded CD spectra as a result of Cu(I) addition, characterized with extrema at λ = 237 (+), 256 (+), 290 (−) and 340 (+) nm (Figure 47). Similarly to UV spectroscopic observations, the intensity of these bands increase linearly with increasing Cu(I) concentration until a sharp breakpoint at 1.3 Cu(I) equivalents. The two isodichroic points were observed at λ = 277 and 321 nm demonstrating the transformation of the free peptide into a single Cu(I) complex before the breakpoint.

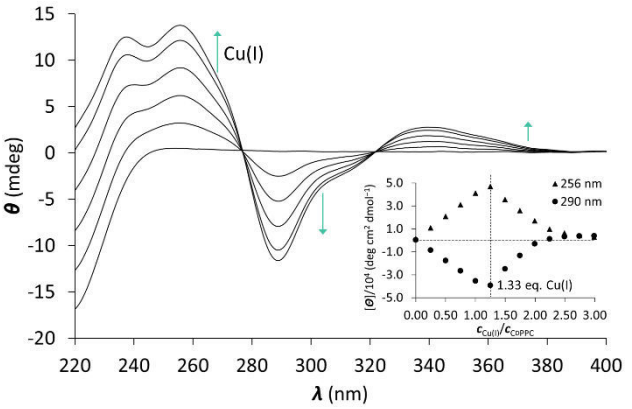

Figure 47. CD titration of CDPPC with Cu(I) from 0.0 to 1.3 equivalents at pH = 7.4 (phosphate buffer, 20 mM). The inset shows the evolution of the molar ellipticity at λ = 256 and 290 nm as a function of the $c_{Cu(I)}/c_{CDPPC}$ ratio. ($c_{peptide}$ = 30 μM)

During the ^{1}H NMR titration of CDPPC with Cu(I) the signals of the free peptide gradually transformed to new, narrow signals and completely disappeared by the addition of 1.33 equivalents of Cu(I) as presented in Figure 48. The well-resolved signals support the formation of a unique species. The proton resonances in the Cu(I)-peptide complex (highlighted in green in Figure 48) were assigned by TOCSY and ROESY experiments (Table 10).

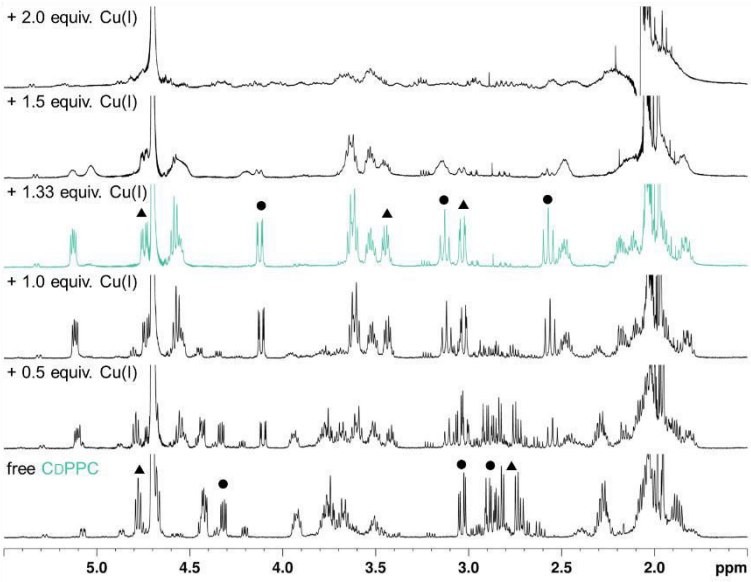

Figure 48. ^{1}H NMR spectra of the aliphatic region of CDPPC with increasing amounts of Cu(I) in phosphate buffer in D_2O (20 mM, pD = 7.4,). ($c_{peptide}$ = 1.58 mM)

Table 10. Assignments of the ^{1}H NMR resonances (δ, ppm) of Cu_4(CDPPC) in phosphate buffer (20 mM, pD = 7.4, D_2O) at 298 K, 500 MHz. Amide protons were identified in H_2O/D_2O, 9/1, v/v.

Cu_4(CDPPC)$_3$	NH	$C_\alpha H$	$C_\beta H$	Others
Cys1	7.81	4.74	3.12; 3.44	(Ac) 2.02
DPro2	–	4.54	2.04; 2.11	(γ) 1.85 (δ) 3.62
Pro3	–	5.08	2.18; 2.50	(γ) 1.87; 2.02 (δ) 3.52; 3.61
Cys4	9.24	4.10	2.54; 3.10	(NH_2) 6.96; 7.45

As it was seen earlier UV-data alone does not provide information about the speciation. However, the three spectroscopic results together, where the endpoint of the titration was observed at 1.33 equivalents of Cu(I), indicate the formation of a Cu:peptide complex of a 1.33:1.00 stoichiometry. This may be reminiscent of a Cu_4S_6 cluster in a Cu_4(Peptide)$_3$ complex.

In all the three cases the continuation of the titrations shows the transformation of this assumed cluster into other species in the presence of more than 1.33 Cu(I) equivalents. Further evolution of the LMCT bands in UV and CD titrations was observed until 2.5 equivalents of Cu(I). The ^{1}H NMR resonances become broad indicating the formation of more than one species. These species formed with an excess of Cu(I) are likely to be Cu(I)-thiolate clusters too, with higher nuclearity.

Further analysis of the NMR spectra of the Cu_4P_3 complex reveal that the coordination of the Cu(I) ion mainly affect the signals of the cysteine residues. The $C_\alpha H$ resonances of the Cu(I) complex are systematically upfield shifted compared to the free peptide. The $C_\beta H_2$ resonances are shifted downfield in Cys1 and upfield in Cys4. These protons are detected as an ABX systems, with a significant difference between the chemical shifts of the two protons belonging to the same carbon atom [$\Delta\delta_{AB}$ = 0.32 and 0.56 ppm for the $C_\beta H_2$ protons of Cys1 and Cys4, respectively]. This is an indication of a significantly different chemical environment and therefore a well-ordered and rigid structure of the Cu(I)-thiolate cluster.

The temperature coefficients of the amide proton resonances were also measured in the complex. The −2.5 Δppb/K value determined for the NH of Cys4 shows that this signal is less affected by the temperature compared to the free ligand (see Table 9). This indicates the H-bond between the amide oxygen of the first Cys residue and the amide proton of the fourth Cys is stronger in the complex and it provides a tighter structure.

3.4. *Copper(I) ion complexes of CDPPC: molecularity*

ESI-MS spectra were acquired to confirm the composition of the Cu(I)-CDPPC complex. Samples containing the peptide and 0.9, 1.33 and 2.0 equivalents of Cu(I) were analyzed. In the first two samples the same species were detected with different relative abundance. The spectrum of the sample containing 1.33 Cu(I) equivalents reflects the presence of three complexes (Figure 49). The Cu_4P_3 is the major detected species in the form of the $[3P-6H+4Cu]^{2-}$ ion (*m/z* = 812.3). The two other observed species are the Cu_3P_2 ($[P-4H+3Cu]^-$; *m/z* = 1104.8) and CuL ($[P-2H+Cu]^-$; *m/z* = 520.1). A tandem MS/MS experiment on the ion of *m/z* = 812.3 proves that these two other species are produced by fragmentation. This confirms the formation of a single Cu_4P_3 complex when the Cu(I)/peptide ratio is below 1.33. The characteristic peaks of the $[3P-6H+4Cu]^{2-}$ ion do not appear in the ESI-MS spectrum of the sample containing 2.0 equivalents of Cu(I). Although the quality of the recorded spectrum is relatively poor with low signal intensities, the formation of several polymetallic species including Cu_4P_2, Cu_5P_2, Cu_9P_5 or Cu_7P_3 can be evidenced.

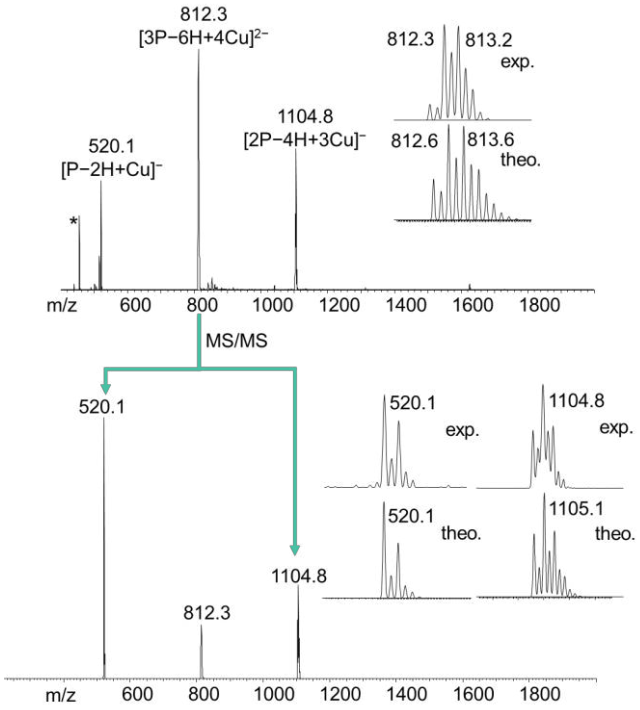

Figure 49. Top. (−)ESI-MS spectrum of CDPPC in NH_4AcO buffer (20 mM, pH = 6.9) in the presence of 1.33 equiv. Cu(I). ($c_{peptide}$ = 100 µM) **Down.** Fragmentation of the $[3P-6H+4Cu]^{2-}$ ion at m/z = 812.3. Insets give the comparison of the experimental and theoretical isotopic patterns of the detected species. * indicates the oxidized peptide

ESI-MS experiments provide information about the metal complex speciation only under specific experimental conditions in gas phase, which is only indicative of species found in solution. Nevertheless, the well-resolved ^{1}H NMR spectrum of the Cu(I)-CDPPC complex made it possible to measure the diffusion coefficient (D) by pulse gradient spin echo (PGSE) NMR to gain deeper insights about the molecularity of the species in solution. According to the Einstein-Stokes equation, the diffusion coefficient (D) is related to the r_H hydrodynamic radius (also called as Stokes radius) of the molecule considered as a hard sphere.

$$D = \frac{kT}{6\pi\eta r_H}$$

where k is the Boltzmann's constant, T is the absolute temperature and η is the viscosity. As the Stokes radius is related to the cube root of the molecular weight ($r_H \sim \sqrt[3]{M}$), the molecular weight (M_i) of the species under interest can be deduced from the ratio of its experimental diffusion coefficient (D_i) and that of a closely-related reference molecule (D_r) with a known molecular weight (M_r).[113]

$$\frac{D_i}{D_r} = \sqrt[3]{\frac{M_r}{M_i}}$$

For a sample containing CDPPC and 1.33 equivalents of Cu(I) $D_i = 1.95 \cdot 10^{-9}$ m^2/s diffusion coefficient was determined in phosphate buffer in D_2O containing 7.9 % CD_3CN in volume originated from the solvent of the Cu(I) solution. The free peptide, as a molecule with known molecular weight (M = 459 g/mol), was used as a reference. Its diffusion coefficient ($D_r = 2.99 \cdot 10^{-10}$ m^2/s) was measured in the same solvent mixture to provide the same viscosity. From these data, a molecular mass M_i = 1645 g/mol was calculated for the Cu(I) complex, which is in a very good agreement with the theoretical molecular weight of the $[Cu_4P_3H_{-6}]^{2-}$ cluster (M = 1625 g/mol). These data are in total accordance with other spectroscopic studies and point to the exclusive formation of the Cu_4P_3 cluster with the constrained peptide CDPPC for Cu(I)/P ratios lower than 1.33.

Among proteins that participate in copper homeostasis many form the same Cu_4S_6 type cluster. Such a cluster can be found, among others, in the cytosolic C-terminal domain of the Ctr1 copper transporter,[11] the fully reduced form of the Cox17 chaperone of cytochrome c oxidase,[12, 13, 175] the metal-responsive transcription factor of Drosophila [176] or the transcription factor Amt1.[177] Interestingly, the simple CDPPC peptide can mimic the behavior of these proteins and forms the cluster in a so-called all-or-nothing, cooperative manner under physiologically relevant condition.

It is also worthy to note, that the two soft metal ions, Cu(I) and Hg(II), interact differently with CDPPC. Hg(II) was observed to form mononuclear complex with a linear coordination geometry, whereas the exclusive formation of the Cu_4P_3 species incorporating trigonally coordinated metal ions was proved for Cu(I). This supports our conclusion in the previous chapter that the analogy between these two metal ions has to be handled with extreme care.

3.5. *Copper(I) ion complexes of CPGC: spectroscopic results*

The Cu(I) binding of the less rigid CPGC peptide was also analyzed by means of UV-vis, CD and NMR spectroscopy and ESI-MS. The complex formation turned out to be more complicated compared to CDPPC. Although the UV titration shows the linear increase of the RS^- to Cu(I) LMCT band centered at 236 nm up to ca. 1.5 Cu(I) equivalents (Figure 50), the evolution of the CD features is rather characteristic for the formation of several species (Figure 51). ESI-MS spectra are of rather poor quality with low signal intensities

regardless of the applied Cu(I)/P ratio, as often observed with thiolate ligands forming a mixture of Cu(I) species. The broad signals in the ^{1}H NMR spectra, observed after Cu(I) addition, may be due to an equilibrium between several species coexisting in an intermediate exchange rate at the NMR timescale. Therefore, in agreement with other spectroscopic results, the formation of a mixture of several species is highly probable with this more flexible compound.

These results unambiguously reveal the importance of the rigid, pre-organized structure of CDPPC peptide in controlling the speciation of Cu(I) complexes in water at pH = 7.4.

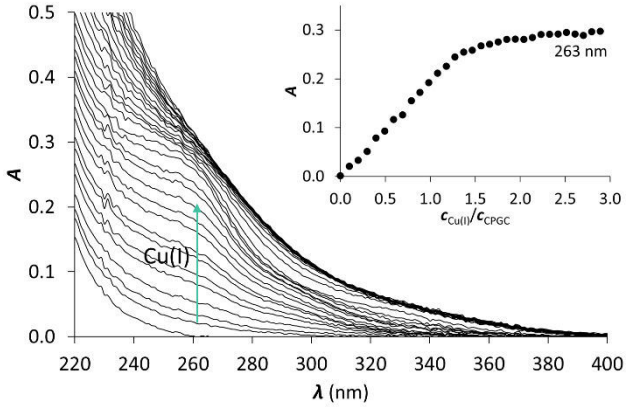

Figure 50. UV titration of CPGC with Cu(I) at pH = 7.4 (phosphate buffer, 20 mM). The inset shows the evolution of the absorbance at λ = 263 nm as a function of the $c_{Cu(I)}/c_{CPGC}$ ratio. ($c_{peptide}$ = 30 µM)

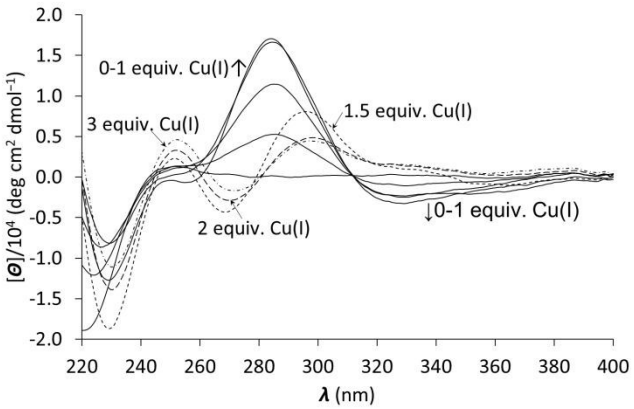

Figure 51. CD titration of CPGC with Cu(I) at pH = 7.4 (phosphate buffer, 20 mM). ($c_{peptide}$ = 30 µM)

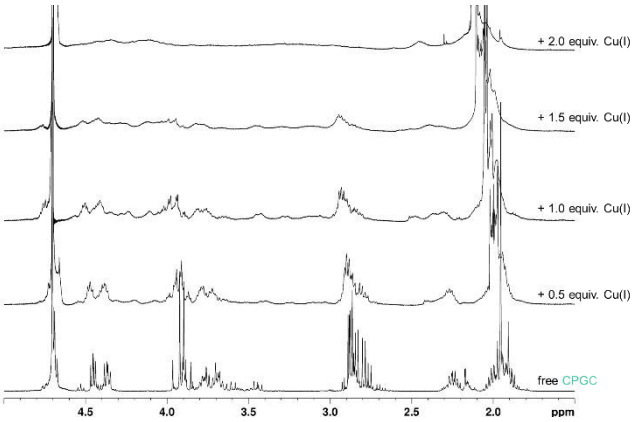

Figure 52. ^{1}H NMR spectra of the aliphatic region of CPGC with increasing amounts of Cu(I) in phosphate buffer in D_2O (20 mM, pD = 7.4). ($c_{peptide}$ = 1.91 mM)

3.6. *The stability of the copper(I) complexes*

Apparent stability constants of the Cu(I) complexes of CDPPC and CPGC peptides at pH = 7.4 were also determined in the presence of the competitor BCS. However, when the samples were prepared in the regular way (CuP + BCS), the equilibration time was too long (weeks) in the case of CDPPC. Therefore, we decided to change the mixing order of the components and attempted to withdraw the Cu(I) from $[Cu(BCS)_2]^{3-}$ complex with the peptides. The stabilization was still slower in the system of CDPPC than with CPGC. This explains the fewer points recorded in the former system (Figure 53). The different equilibration times might reflect the different structures of the complexes formed with the two peptides.

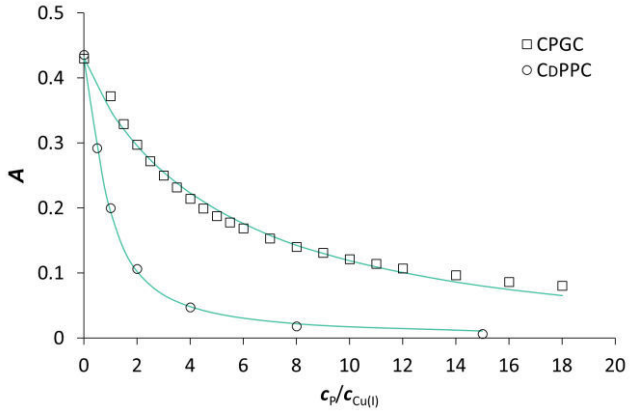

Figure 53. Absorbance at λ = 483 nm recorded during the titration of $Cu(BCS)_2$ with CDPPC (○) and CPGC (□) at pH = 7.4 (phosphate buffer, 20 mM). The solid lines represent the absorbances calculated by SpecFit. ($c_{Cu(I)}$ = 30 μM; c_{BCS} = 300 μM)

Figure 53 clearly presents the striking difference between the affinities of the two peptides for Cu(I). 15 equivalents of CDPPC relative to Cu(I) displace all the metal ion from

the BCS complex leading to the total loss of absorbance at λ = 483 nm. In contrast, 45 equivalents of CPGC (not shown) were not enough for a complete displacement. The UV-vis spectra recorded during the titration with CDPPC were satisfactorily fitted by considering only the Cu_4P_3 cluster and $\log\beta_{43}^{pH7.4}$ = 78.9 was determined. The complicated speciation of the Cu(I)-CPGC complexes prevented a fully appropriate fitting. Therefore, apparent affinity constants were calculated considering the formation of the 1:1 mononuclear complex for both peptides to allow a direct comparison. Data shown in Table 11 display a one order of magnitude difference in favor of CDPPC giving a further advantage of the preorganized peptide backbone. CDPPC not only mimics the structural features of some Cu proteins, but its affinity for Cu(I) is also in the range of previously reported stabilities of proteins involved in Cu homeostasis.[11]

Table 11. Apparent stability constants of the Cu(I) and Zn(II) complexes of CDPPC and CPGC at pH = 7.4

	CDPPC		CPGC	
	Cu(I)	Zn(II)	Cu(I)	Zn(II)
$\log\beta_{11}^{pH\ 7.4}$	17.5(1)	6.3(1)[a]	16.4(1)	5.6(1)[a]
		6.4(1)[b]		7.4(2)[b]
$\log\beta_{12}^{pH\ 7.4}$				13.1(2)[b]
$\log\beta_{43}^{pH\ 7.4}$	78.9(3)			

[a]Calculated from competition experiments with zincon.

[b]Calculated from UV titrations with Zn(II).

3.7. *Zinc(II) complexes: spectroscopy and stability*

Zinc(II), as an abundant metal ion in cells, is a potential competitor in Cu(I) binding. Therefore, the Zn(II) complexation of CDPPC and CPGC was also studied by UV titrations and ESI-MS experiments. The addition of Zn(II) aliquots to the solution of the lignads results in the increase of absorbance in the wavelength range characteristic for the RS^- to Zn(II) LMCT (λ < 240 nm).[178, 179] The CDPPC reacts with Zn(II) in a quite simple manner and the absorbance reaches the maximum around 1.0 equivalent of Zn(II) added. The recorded ESI-MS spectra showed the formation of only the mononuclear complex (Figure 55). ZnP_2 can be detected only under ligand excess condition, but in negligible amount. In contrast, the increase of absorbance has a breakpoint at 0.5 equivalent of Zn(II) during the titration of CPGC indicating the formation of ZnP_2 complex where the metal ion is coordinated by four

thiolate donor groups. The further evolution of absorbance at 240 nm probably reflects the transformation of ZnP_2 to ZnP. Accordingly, ESI-MS shows the significant contribution of ZnP_2 besides the ZnP complex both in the presence of 0.5 and 1.0 equivalent of Zn(II).

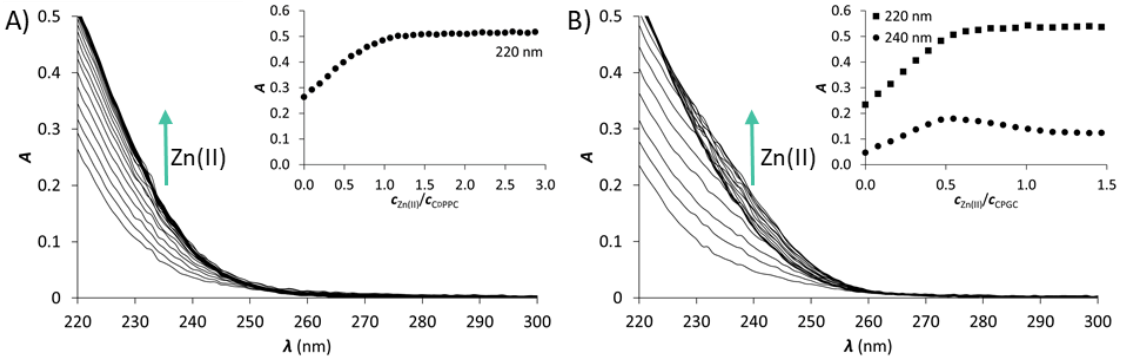

Figure 54. UV titration of CDPPC (A) and CPGC (B) with Zn(II) at pH = 7.4 (phosphate buffer, 20 mM). The insets show the evolution of the absorbance at chosen wavelengths as a function of the $c_{Zn(II)}/c_{peptide}$ ratio. ($c_{peptide}$ ~ 30 μM)

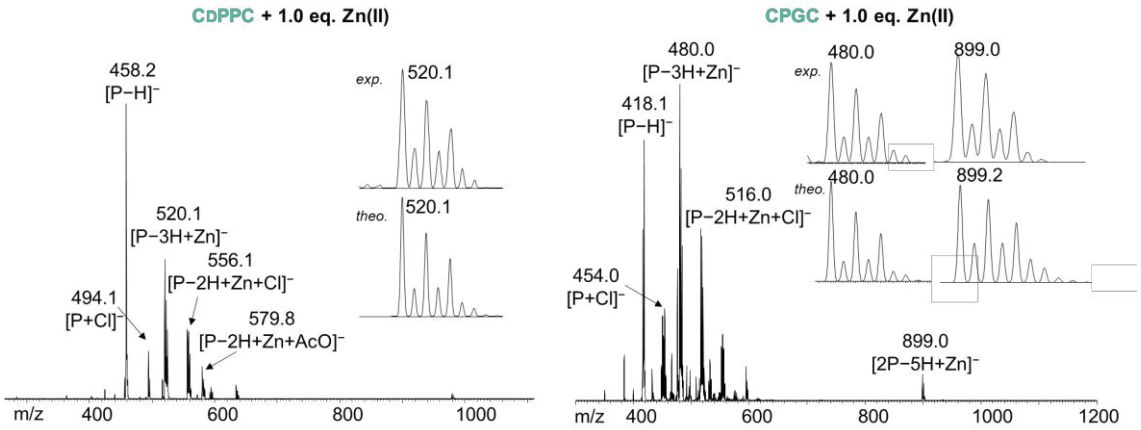

Figure 55. (−)ESI-MS spectra of CDPPC and CPGC with 1.0 equivalent of Zn(II) at pH = 6.9 (NH_4AcO buffer, 20 mM) with the experimental and theoretical isotopic patterns of the detected species. ($c_{peptide}$ = 100 μM)

Apparent stability constants of the ZnP complexes were determined by two different methods. UV titrations of the peptides with Zn(II) were fitted by considering the formation of only the ZnP complex in the sample of CDPPC and the ZnP and ZnP_2 with CPGC. The results reported in Table 11 show significantly lower Zn(II)-binding affinity compared to Cu(I). Competition studies with zincon, a well-known Zn(II) chelator,[123] confirm affinities in the same range. The good agreement between the two independent determination in case of CDPPC confirms the simple speciation with the formation of the ZnP complex.

IN SUMMARY

- DPro-Pro motif induces more rigid backbone than Pro-Gly
- CDPPC forms a Cu_4P_3 cluster involving a Cu_4S_6 core with high stability
- CDPPC mimics the cluster formation and stability of natural Cu(I) proteins under physiological conditions
- CPGC forms several Cu(I) species with lower stability
- Pre-organization of the metal binding groups is essential for the control of Cu(I) complex speciation
- Both peptides display large selectivity for Cu(I) vs. Zn(II)

SUMMARY

VI. Summary

The essential micronutrient copper participates in several biological processes, like respiration, iron homeostasis, antioxidant defense or pigment formation. However, excess of copper can promote ROS formation and thus induce oxidative damages. Therefore, intracellular copper concentration is under strict control. Menkes and Wilson's diseases are genetic disorders causing impairment in copper homeostasis leading to copper deficiency or overload, respectively. Wilson's disease is treated by chelation therapy, but the presently used drugs have several adverse side effects. New peptide or tripodal pseudopeptide ligands that display high affinity for the intracellular Cu(I) and target hepatic cells have been developed by Delangle *et al*. Some of them are currently proposed as highly specific drugs for localized copper chelation therapy in Wilson's disease.

My Ph.D. work consisted of the design of three groups of cysteine containing peptides and the characterization of their Cu(I) complexes to determine whether they are appropriate candidates for the treatment of Wilson's disease. The interaction of some peptides with Hg(II), which is a metal ion possessing similar coordination properties to Cu(I) and therefore an often used probe of the oxygen and water sensitive Cu(I), or with the ubiquitous Zn(II), which is a potential intracellular competitor, was also studied.

The peptides were designed following three different approaches. In a first strategy, we attempted to take advantage of the outstanding selectivity and sensitivity of the bacterial copper efflux regulator protein CueR by studying oligopeptides based on the metal binding motif of CueR involving two cysteine residues. Second, three-cysteine containing linear and cyclic peptides were designed with the aim of merging the better internalization of peptides by hepatocytes and the high Cu(I) affinity of tripods previously studied in the Delangle's lab. Finally, the advantages of a highly preorganized peptide structure were exploited in a short, rigid tetrapeptide where two cysteines were linked by a turn motif (CDPPC). For comparative purposes studies were also performed with another, less rigid tetrapeptide ligand containing the PG unit as a turn inducing motif

Terminally protected linear peptides were synthesized by solid phase peptide synthesis following the Fmoc protocol. For the cyclic peptides, linear precursors with unprotected termini were assembled by the same method. After the cleavage off the resin, cyclization was performed. The crude products were purified by reversed phase HPLC. The purity was checked by analytical HPLC and ESI-MS.

Since the cysteine moieties and Cu(I) are sensitive for oxidation, all sample manipulations were performed in a glovebox under argon atmosphere. The majority of the experiments were carried out at pH = 7.4 in buffered media. In a few cases, pH titrations were also executed at constant metal-to-ligand concentration ratios. The interaction of the peptides with the metal ion was studied by UV-vis, CD and NMR spectroscopy and ESI-MS. The stability of the peptide-metal ion complexes was determined by competition reaction with well-known ligands.

The three CueR model peptides, **EC**, **VC** and **HS** display very similar behavior towards Cu(I). Mononuclear complexes are formed in excess of the ligands and they transform into polynuclear species in the presence of Cu(I) excess. Based on the observed thiolate to Cu(I) charge transfer transitions in the UV and CD spectra, Cu(I) is bound by the two cysteine residues. For **HS**, ^{1}H NMR spectra show the involvement of the histidine residue in metal ion coordination. Analysis of a series of pH dependent UV spectra reveals that the complex formation is complete above pH = 7.0 and decrease of pH induces the decoordination of cysteines in two steps leading to the complete loss of LMCT absorbances. The pK_a values belonging to these processes are significantly below the physiological pH indicating that they are probably not relevant in biological Cu(I) sequestration.

The stabilities of the mononuclear complexes at pH = 7.4 determined in the presence of the competitor ligand BCA are quite large ($\log\beta_{11}^{pH7.4}$ ~ 16) and similar to those obtained for peptides incorporating the CxxC or the CxxxxC motif. This result shows that the length of the spacer between the Cys residues affects little the affinity towards Cu(I). Therefore, the driving force for the coordination of the soft Cu(I) cation is expected to be mainly the formation of the two strong bonds with the soft thiolate donors. Comparison of stability constants with previous results shows that the peptides are highly selective for Cu(I) against Zn(II), but have similar affinity for Ag(I). Although, the Cu(I)-binding affinities of these peptide models are 5–6 orders of magnitude lower than that of the native CueR protein, they still resemble the ability of the protein to exclusively accommodate one metal ion under ligand excess conditions. This, combined with the large affinity and high selectivity vs. Zn(II), are the features that are advantageous in the view of the development of new Cu(I) chelators.

In the three-cysteine-containing cyclic peptides $\mathbf{P^{3C}}$, $\mathbf{1^{C}}$, $\mathbf{2^{C}}$ and $\mathbf{3^{C}}$ and their linear derivatives $\mathbf{1^{L}}$ and $\mathbf{2^{L}}$, the Cys residues are arranged in CxCxxC or CxCxC motifs, found in

metallothioneins. With this series, the effects of different structural influencing modifications on the metal ion binding were also studied.

The Cu(I) complex formation of all the six peptides was found to be rather complicated. This was first indicated by UV-vis studies when the LMCT absorbances stabilized only after 2 hours of equilibration during the titration of the peptides with Cu(I). Therefore, the use of independently prepared samples was necessary. Although, the UV titrations reveal a seemingly simple evolution of absorbances with an endpoint that refers to the formation of polymetallic species of an overall $(Cu_2P)_n$ stoichiometry, the recorded CD spectra and ESI-MS experiments evidence the presence of a mixture of polymetallic species. Consequently, the peptides proved to be too flexible to control the speciation and hereby leading to the formation of several species.

Because of the undefined speciation, the average affinity of the peptides for Cu(I) at pH = 7.4 was determined. Therefore, the UV spectroscopic results of the competition with BCS were evaluated by considering the formation of only the mononuclear CuP complex. All peptides display high affinity towards Cu(I) in the range typical of Cu(I) chaperone proteins. The similar $\log\beta_{11}^{pH7.4}$ ~ 18 values indicate that the structural differences have minor effect on the stability of the Cu(I) complexes.

To reveal whether this complicated behavior is originated from the peptide structure or it is specific for Cu(I), the interaction with Hg(II), a soft metal ion possessing similar chemical properties, was also studied. Mononuclear HgP complexes are formed when the ligands are in excess and the complex formation is significantly faster compared to Cu(I). The position of the thiolate to Hg(II) LMCT at λ = 280 and 240 nm clearly demonstrates that Hg(II) is coordinated by all the three Cys residues of the peptides at pH = 7.4. In the presence of Hg(II) excess, the mononuclear complexes transform into polymetallic species adopting the more favorable HgS_2 coordination mode. The results of the UV titrations and MS experiments strongly support the formation of Hg_2P_3 complexes up to 1.5 equivalents of Hg(II), that transform into other species with an increasing metal ion excess.

UV-pH titrations showed an $HgS_2 \rightleftharpoons HgS_3$ transformation with pK_a = 4.3-5.1 values characterizing the deprotonation of the third cysteine thiol. These values are relatively close to each other for the six peptides, indicating that the structural differences affect little the stability of the HgS_3 species. However, the observed tendency reveal that the CxCxxC motif in $\mathbf{P^{3C}}$ is more favorable, just like the longer distance from the turn motif in $\mathbf{2^C}$ and $\mathbf{3^C}$ compared to $\mathbf{1^C}$, and the cyclic against the linear structure. Interestingly, these pK_a values

are significantly lower than those obtained for the three-stranded coiled coils, which is probably related to the very different water-accessibility of the thiol groups.

The apparent stability of the HgP complexes was determined at pH = 2.0 by competition with I^- ions. All peptides display rather similar affinities for Hg(II) showing that the preorientation of the donor groups has only a modest influence on the stabilities and the high thiophilicity of Hg(II) easily governs the formation of the favored HgS_2 structures. The apparent stability constants estimated for pH = 7.4 show a more than 20 orders of magnitude larger affinity of the peptides for Hg(II) than for Cu(I) due to the significantly larger thiophilicity of Hg(II). Stabilities of the HgP complexes are of the same magnitude as the Hg(II) complex of the well-known heavy metal chelator BAL, which forms a highly stable five member chelate ring by the coordination of two thiolate groups. Our peptides display higher affinity for Hg(II) than the highly constrained CDPPC peptide as a consequence of the higher number of coordinating donor groups. The large stability constants together with the low pK_a values clearly indicate that all these three-cysteine-containing peptides are adapted for an efficient trithiolate coordination of the thiophilic cation Hg(II).

The striking difference in the behavior of the peptides towards the two soft metal ions demonstrate that the use of Hg(II) as a probe for Cu(I) coordination with sulfur-rich peptides or proteins in physiological conditions may not always be fully appropriate.

The effect of the preorganization on the metal binding properties was studied on two tetrapeptides where two cysteines were linked by a β turn inducer motif, the DPro-Pro (CDPPC) or Pro-Gly (CPGC). CDPPC was confirmed to possess a more rigid structure by measuring the ^1H NMR temperature coefficient of the amide proton of the Cys4 residue that indicates the presence of a hydrogen bond between the C=O group of Cys1 and NH of Cys4. The UV, CD and NMR titration reveal that CDPPC form a single Cu(I) complex until 1.33 equivalents of Cu(I) and the results of DOSY NMR and ESI-MS experiments prove that this species is a Cu_4P_3 cluster with a Cu_4S_6 core where a Cu(I) ion is in a highly favorable trithiolate coordination. It is worthy to note, that this simple peptide is able to mimic the cluster formation that are typical in proteins like Ctr1 or Cox17. In contrast, all experimental data refer to a more complicated Cu(I) complex formation of CPGC. The observed difference emphasizes the importance of a well-defined, preorganized structure in the control of Cu(I) complex speciation. Furthermore, the apparent stability constant calculated for a theoretical CuP mononuclear complexes is one order of magnitude larger for CDPPC ($\log\beta_{11}^{pH7.4}$ = 17.5) than for CPGC ($\log\beta_{11}^{pH7.4}$ = 16.4).

The Zn(II) complexes of CDPPC and CPGC were demonstrated to be mononuclear ZnP or ZnP_2 species. The apparent stability constants at physiological pH calculated for the ZnP complexes are in a magnitude of 10^6, and the selectivity in favor of Cu(I) with respect to Zn(II) is therefore extremely large.

The Cu(I) complexation by CDPPC is strikingly different compared to what was previously observed with Hg(II). This supports that the use of Hg(II) as a probe of Cu(I) must be handled with extreme care.

Since CDPPC forms a single Cu_4P_3 cluster with high stability and displays large selectivity for Cu(I) with respect to the ubiquitous Zn(II), it is an interesting simple peptide candidate to be targeted to the liver cells for the localized treatment of Cu overload in Wilson's disease.

VII. References

1. R. R. Conry, in *Encyclopedia of Inorganic Chemistry*, John Wiley & Sons, Ltd, 2006, DOI: 10.1002/0470862106.ia052.
2. D. Huster, Wilson disease, *Best Pract. Res., Clin. Gastroenterol.*, 2010, **24**, 531-539.
3. M. Tegoni, D. Valensin, L. Toso and M. Remelli, Copper Chelators: Chemical Properties and Bio-medical Applications, *Curr. Med. Chem.*, 2014, **21**, 3785-3818.
4. P. Delangle and E. Mintz, Chelation therapy in Wilson's disease: from D-penicillamine to the design of selective bioinspired intracellular Cu(I) chelators, *Dalton Trans.*, 2012, **41**, 6359-6370.
5. R. G. Pearson, Hard and Soft Acids and Bases, *J. Am. Chem. Soc.*, 1963, **85**, 3533-3539.
6. K. A. Koch, M. M. O. Peña and D. J. Thiele, Copper-binding motifs in catalysis, transport, detoxification and signaling, *Chemistry & Biology*, 1997, **4**, 549-560.
7. S. Lutsenko, Copper trafficking to the secretory pathway, *Metallomics*, 2016, **8**, 840-852.
8. J. Jiang, I. A. Nadas, M. A. Kim and K. J. Franz, A Mets Motif Peptide Found in Copper Transport Proteins Selectively Binds Cu(I) with Methionine-Only Coordination, *Inorg. Chem.*, 2005, **44**, 9787-9794.
9. M. J. Pushie, K. Shaw, K. J. Franz, J. Shearer and K. L. Haas, Model Peptide Studies Reveal a Mixed Histidine-Methionine Cu(I) Binding Site at the N-Terminus of Human Copper Transporter 1, *Inorg. Chem.*, 2015, **54**, 8544-8551.
10. K. L. Haas, A. B. Putterman, D. R. White, D. J. Thiele and K. J. Franz, Model Peptides Provide New Insights into the Role of Histidine Residues as Potential Ligands in Human Cellular Copper Acquisition via Ctr1, *J. Am. Chem. Soc.*, 2011, **133**, 4427-4437.
11. Z. Xiao, F. Loughlin, G. N. George, G. J. Howlett and A. G. Wedd, C-Terminal Domain of the Membrane Copper Transporter Ctr1 from Saccharomyces cerevisiae Binds Four Cu(I) Ions as a Cuprous-Thiolate Polynuclear Cluster: Sub-femtomolar Cu(I) Affinity of Three Proteins Involved in Copper Trafficking, *J. Am. Chem. Soc.*, 2004, **126**, 3081-3090.
12. P. Palumaa, L. Kangur, A. Voronova and R. Sillard, Metal-binding mechanism of Cox17, a copper chaperone for cytochrome c oxidase, *Biochem. J*, 2004, **382**, 307.
13. A. Voronova, W. Meyer-Klaucke, T. Meyer, A. Rompel, B. Krebs, J. Kazantseva, R. Sillard and P. Palumaa, Oxidative switches in functioning of mammalian copper chaperone Cox17, *Biochem. J*, 2007, **408**, 139.
14. F. Arnesano, L. Banci, I. Bertini, D. L. Huffman and T. V. O'Halloran, Solution Structure of the Cu(I) and Apo Forms of the Yeast Metallochaperone, Atx1, *Biochemistry*, 2001, **40**, 1528-1539.
15. R. A. Pufahl, C. P. Singer, K. L. Peariso, S. J. Lin, P. J. Schmidt, C. J. Fahrni, V. C. Culotta, J. E. Penner-Hahn and T. V. Halloran, Metal Ion Chaperone Function of the Soluble Cu(I) Receptor Atx1, *Science*, 1997, **278**, 853.
16. Z. Xiao and A. G. Wedd, The challenges of determining metal-protein affinities, *Natural Product Reports*, 2010, **27**, 768-789.

17. M. Łuczkowski, B. A. Zeider, A. V. H. Hinz, M. Stachura, S. Chakraborty, L. Hemmingsen, D. L. Huffman and V. L. Pecoraro, Probing the Coordination Environment of the Human Copper Chaperone HAH1: Characterization of Hg^{II}-Bridged Homodimeric Species in Solution, *Chem. Eur. J.*, 2013, **19**, 9042-9049.
18. S. Lutsenko, K. Petrukhin, M. J. Cooper, C. T. Gilliam and J. H. Kaplan, N-terminal Domains of Human Copper-transporting Adenosine Triphosphatases (the Wilson's and Menkes Disease Proteins) Bind Copper Selectively in Vivo and in Vitro with Stoichiometry of One Copper Per Metal-binding Repeat, *J. Biol. Chem.*, 1997, **272**, 18939-18944.
19. C. Ariöz, Y. Li and P. Wittung-Stafshede, The six metal binding domains in human copper transporter, ATP7B: molecular biophysics and disease-causing mutations, *BioMetals*, 2017, **30**, 823-840.
20. Z. Xiao, J. Brose, S. Schimo, S. M. Ackland, S. La Fontaine and A. G. Wedd, Unification of the Copper(I) Binding Affinities of the Metallo-chaperones Atx1, Atox1, and Related Proteins: Detection Probes and Affinity Standards, *J. Biol. Chem.*, 2011, **286**, 11047-11055.
21. M. T. Morgan, L. A. H. Nguyen, H. L. Hancock and C. J. Fahrni, Glutathione limits aquacopper(I) to sub-femtomolar concentrations through cooperative assembly of a tetranuclear cluster, *J. Biol. Chem.*, 2017, **292**, 21558-21567.
22. M. Margoshes and B. L. Vallee, A Cadmium Protein from Equine Kidney Cortex, *J. Am. Chem. Soc.*, 1957, **79**, 4813-4814.
23. C. A. Blindauer and O. I. Leszczyszyn, Metallothioneins: unparalleled diversity in structures and functions for metal ion homeostasis and more, *Nat. Prod. Rep.*, 2010, **27**, 720-741.
24. M. Capdevila, R. Bofill, Ò. Palacios and S. Atrian, State-of-the-art of metallothioneins at the beginning of the 21st century, *Coord. Chem. Rev.*, 2012, **256**, 46-62.
25. M. J. Stillman, Metallothioneins, *Coord. Chem. Rev.*, 1995, **144**, 461-511.
26. K. B. Nielson, C. L. Atkin and D. R. Winge, Distinct metal-binding configurations in metallothionein, *J. Biol. Chem.*, 1985, **260**, 5342-5350.
27. J. Byrd, R. M. Berger, D. R. McMillin, C. F. Wright, D. Hamer and D. R. Winge, Characterization of the copper-thiolate cluster in yeast metallothionein and two truncated mutants, *J. Biol. Chem.*, 1988, **263**, 6688-6694.
28. D. L. Pountney, I. Schauwecker, J. Zarn and M. Vasak, Formation of Mammalian Cu_8-Metallothionein in vitro: Evidence for the Existence of Two $Cu(I)_4$-Thiolate Clusters, *Biochemistry*, 1994, **33**, 9699-9705.
29. P. Faller and M. Vašák, Distinct Metal−Thiolate Clusters in the N-Terminal Domain of Neuronal Growth Inhibitory Factor, *Biochemistry*, 1997, **36**, 13341-13348.
30. Ò. Palacios, A. Pagani, S. Pérez-Rafael, M. Egg, M. Höckner, A. Brandstätter, M. Capdevila, S. Atrian and R. Dallinger, Shaping mechanisms of metal specificity in a family of metazoan metallothioneins: evolutionary differentiation of mollusc metallothioneins, *BMC Biology*, 2011, **9**, 4.
31. U. Weser and H.-J. Hartmann, Differently bound copper(I) in yeast Cu_8-thionein, *Biochim. Biophys. Acta, Protein Struct. Mol. Enzymol.*, 1988, **953**, 1-5.

32. A. Presta, A. R. Green, A. Zelazowski and M. J. Stillman, Copper Binding to Rabbit Liver Metallothionein, *Eur. J. Biochem.*, 1995, **227**, 226-240.
33. V. Calderone, B. Dolderer, H.-J. Hartmann, H. Echner, C. Luchinat, C. Del Bianco, S. Mangani and U. Weser, The crystal structure of yeast copper thionein: The solution of a long-lasting enigma, *Proc. Natl. Acad. Sci. U. S. A.*, 2005, **102**, 51-56.
34. Y. J. Li and U. Weser, Circular dichroism, luminescence, and electronic absorption of copper binding sites in metallothionein and its chemically synthesized .alpha. and .beta. domains, *Inorg. Chem.*, 1992, **31**, 5526-5533.
35. R. B. Martin, in *Encyclopedia of Inorganic Chemistry*, John Wiley & Sons, Ltd, 2006, DOI: 10.1002/0470862106.ia136.
36. B. Halliwell and J. M. C. Gutteridge, [1] Role of free radicals and catalytic metal ions in human disease: An overview, *Methods Enzymol.*, 1990, **186**, 1-85.
37. M. Valko, H. Morris and M. T. D. Cronin, Metals, Toxicity and Oxidative Stress, *Current Medicinal Chemistry*, 2005, **12**, 1161-1208.
38. A. N. Pham, G. Xing, C. J. Miller and T. D. Waite, Fenton-like copper redox chemistry revisited: Hydrogen peroxide and superoxide mediation of copper-catalyzed oxidant production, *J. Catal.*, 2013, **301**, 54-64.
39. E. Atrián-Blasco, P. Gonzalez, A. Santoro, B. Alies, P. Faller and C. Hureau, Cu and Zn coordination to amyloid peptides: From fascinating chemistry to debated pathological relevance, *Coord. Chem. Rev.*, 2018, **371**, 38-55.
40. O. Bandmann, K. H. Weiss and S. G. Kaler, Wilson's disease and other neurological copper disorders, *The Lancet Neurology*, 2015, **14**, 103-113.
41. B. Sarkar, in *Neurodegenerative Diseases and Metal Ions*, eds. A. Sigel, H. Sigel and R. K. Sigel, 2006, vol. 1, pp. 207-225.
42. S. G. Kaler, C. S. Holmes, D. S. Goldstein, J. Tang, S. C. Godwin, A. Donsante, C. J. Liew, S. Sato and N. Patronas, Neonatal Diagnosis and Treatment of Menkes Disease, *New England Journal of Medicine*, 2008, **358**, 605-614.
43. A. Donsante, L. Yi, P. M. Zerfas, L. R. Brinster, P. Sullivan, D. S. Goldstein, J. Prohaska, J. A. Centeno, E. Rushing and S. G. Kaler, ATP7A Gene Addition to the Choroid Plexus Results in Long-term Rescue of the Lethal Copper Transport Defect in a Menkes Disease Mouse Model, *Molecular Therapy*, 2011, **19**, 2114-2123.
44. M. Patil, K. A. Sheth, A. C. Krishnamurthy and H. Devarbhavi, A Review and Current Perspective on Wilson Disease, *J. Clin. Exp. Hepatol.*, 2013, **3**, 321-336.
45. T. Müller, H. Feichtinger, H. Berger and W. Müller, Endemic Tyrolean infantile cirrhosis: an ecogenetic disorder, *The Lancet*, 1996, **347**, 877-880.
46. D. L. de Romaña, M. Olivares, R. Uauy and M. Araya, Risks and benefits of copper in light of new insights of copper homeostasis, *J. Trace Elem. Med Biol.*, 2011, **25**, 3-13.
47. K. J. Franz, Clawing back: broadening the notion of metal chelators in medicine, *Curr. Opin. Chem. Biol.*, 2013, **17**, 143-149.
48. J. A. Vilensky and K. Redman, British anti-Lewisite (dimercaprol): An amazing history, *Annals of Emergency Medicine*, 2003, **41**, 378-383.
49. A. Członkowska and T. Litwin, in *Handbook of Clinical Neurology*, eds. A. Członkowska and M. L. Schilsky, Elsevier, 2017, vol. 142, pp. 181-191.

50. P. V. Ioannou and R. Purchase, Interaction of British Anti-Lewisite (BAL) with Copper(I) and Copper(II) compounds in conjunction with Wilson's disease, *Main Group Chem.*, 2018, **17**, 1-16.
51. J. M. Walshe, Penicillamine, a new oral therapy for Wilson's disease, *Am. J. Med.*, 1956, **21**, 487-495.
52. P. Ferenci, Diagnosis and current therapy of Wilson's disease, *Alimentary Pharmacology & Therapeutics*, 2004, **19**, 157-165.
53. G. Crisponi, V. M. Nurchi, D. Fanni, C. Gerosa, S. Nemolato and G. Faa, Copper-related diseases: From chemistry to molecular pathology, *Coord. Chem. Rev.*, 2010, **254**, 876-889.
54. J. Peisach and W. E. Blumberg, A Mechanism for the Action of Penicillamine in the Treatment of Wilson's Disease, *Mol. Pharmacol.*, 1969, **5**, 200.
55. Y. Sugiura and H. Tanaka, Studies on the Sulfur-containing Chelating Agents. XXV. Chelate Formation of Penicillamine and Its Related Compounds with Copper (II), *CHEMICAL & PHARMACEUTICAL BULLETIN*, 1970, **18**, 368-373.
56. Y. Sugiura and H. Tanaka, Evidence for a Ternary Complex Containing Albumin, Copper, and Penicillamine, *Mol. Pharmacol.*, 1972, **8**, 249.
57. K. Várnagy, I. Sóvágó and H. Kozłowski, Transition metal complexes of amino acids and derivatives containing disulphide bridges, *Inorg. Chim. Acta*, 1988, **151**, 117-123.
58. J. M. Walshe, Management of Penicillamine Nephropathy In Wilson's Disease: A New Chelating Agent, *The Lancet*, 1969, **294**, 1401-1402.
59. S. Boga, D. Jain and M. L. Schilsky, Trientine induced colitis during therapy for Wilson disease: a case report and review of the literature, *BMC Pharmacol. Toxicol.*, 2015, **16**, 4.
60. I. H. Scheinberg, M. E. Jaffe and I. Sternlieb, The Use of Trientine in Preventing the Effects of Interrupting Penicillamine Therapy in Wilson's Disease, *New England Journal of Medicine*, 1987, **317**, 209-213.
61. V. M. Nurchi, G. Crisponi, M. Crespo-Alonso, J. I. Lachowicz, Z. Szewczuk and G. J. S. Cooper, Complex formation equilibria of CuII and ZnII with triethylenetetramine and its mono- and di-acetyl metabolites, *Dalton Trans.*, 2013, **42**, 6161-6170.
62. S. H. Laurie and B. Sarkar, Potentiometric and spectroscopic study of the equilibria in the aqueous copper(II)–3,6-diazaoctane-1,8-diamine system and an equilibrium-dialysis examination of the ternary system of human serum albumin–copper(II)–3,6-diazaoctane-1,8-diamine, *Dalton Trans.*, 1977, 1822-1827.
63. R. Tremmel, P. Uhl, F. Helm, D. Wupperfeld, M. Sauter, W. Mier, W. Stremmel, G. Hofhaus and G. Fricker, Delivery of Copper-chelating Trientine (TETA) to the central nervous system by surface modified liposomes, *Int. J. Pharm.*, 2016, **512**, 87-95.
64. R. Purchase, The treatment of Wilson's disease, a rare genetic disorder of copper metabolism, *Sci. Prog.*, 2013, **96**, 19-32.
65. L. Zhang, J. Lichtmannegger, K. H. Summer, S. Webb, I. J. Pickering and G. N. George, Tracing Copper−Thiomolybdate Complexes in a Prospective Treatment for Wilson's Disease, *Biochemistry*, 2009, **48**, 891-897.
66. J. Smirnova, E. Kabin, I. Järving, O. Bragina, V. Tõugu, T. Plitz and P. Palumaa, Copper(I)-binding properties of de-coppering drugs for the treatment of Wilson

disease. α-Lipoic acid as a potential anti-copper agent, *Scientific Reports*, 2018, **8**, 1463.
67. G. C. Sturniolo, C. Mestriner, P. Irato, V. Albergoni, G. Longo and R. D'Incà, Zinc therapy increases duodenal concentrations of metallothionein and iron in Wilson's disease patients, *Am. J. Gastroenterol.*, 1999, **94**, 334.
68. J. Condomina, T. Zornoza-Sabina, L. Granero and A. Polache, Kinetics of zinc transport in vitro in rat small intestine and colon: interaction with copper, *European Journal of Pharmaceutical Sciences*, 2002, **16**, 289-295.
69. T. U. Hoogenraad, J. Van Hattum and C. J. A. Van den Hamer, Management of Wilson's disease with zinc sulphate: Experience in a series of 27 patients, *Journal of the Neurological Sciences*, 1987, **77**, 137-146.
70. J. Rautio, H. Kumpulainen, T. Heimbach, R. Oliyai, D. Oh, T. Järvinen and J. Savolainen, Prodrugs: design and clinical applications, *Nature Reviews Drug Discovery*, 2008, **7**, 255.
71. V. Oliveri and G. Vecchio, Prochelator strategies for site-selective activation of metal chelators, *J. Inorg. Biochem.*, 2016, **162**, 31-43.
72. C. Gateau and P. Delangle, Design of intrahepatocyte copper(I) chelators as drug candidates for Wilson's disease, *Ann. N.Y. Acad. Sci.*, 2014, **1315**, 30-36.
73. A. Meister and M. E. Anderson, Glutathione, *Annu. Rev. Biochem*, 1983, **52**, 711-760.
74. P. Rousselot-Pailley, O. Sénèque, C. Lebrun, S. Crouzy, D. Boturyn, P. Dumy, M. Ferrand and P. Delangle, Model Peptides Based on the Binding Loop of the Copper Metallochaperone Atx1: Selectivity of the Consensus Sequence MxCxxC for Metal Ions Hg(II), Cu(I), Cd(II), Pb(II), and Zn(II), *Inorg. Chem.*, 2006, **45**, 5510-5520.
75. A. M. Pujol, C. Gateau, C. Lebrun and P. Delangle, A Cysteine-Based Tripodal Chelator with a High Affinity and Selectivity for Copper(I), *J. Am. Chem. Soc.*, 2009, **131**, 6928-6929.
76. A. M. Pujol, C. Gateau, C. Lebrun and P. Delangle, A Series of Tripodal Cysteine Derivatives as Water-Soluble Chelators that are Highly Selective for Copper(I), *Chem. Eur. J.*, 2011, **17**, 4418-4428.
77. A.-S. Jullien, C. Gateau, C. Lebrun, I. Kieffer, D. Testemale and P. Delangle, D-Penicillamine Tripodal Derivatives as Efficient Copper(I) Chelators, *Inorg. Chem.*, 2014, **53**, 5229-5239.
78. A.-S. Jullien, C. Gateau, C. Lebrun and P. Delangle, Pseudo-peptides Based on Methyl Cysteine or Methionine Inspired from Mets Motifs Found in the Copper Transporter Ctr1, *Inorg. Chem.*, 2015, **54**, 2339-2344.
79. A.-S. Jullien, C. Gateau, I. Kieffer, D. Testemale and P. Delangle, X-ray Absorption Spectroscopy Proves the Trigonal-Planar Sulfur-Only Coordination of Copper (I) with High-Affinity Tripodal Pseudopeptides, *Inorg. Chem.*, 2013, **52**, 9954-9961.
80. P. Faller, Neuronal growth-inhibitory factor (metallothionein-3): reactivity and structure of metal–thiolate clusters, *FEBS Journal*, 2010, **277**, 2921-2930.
81. G. Hefter, P. M. May and P. Sipos, A general method for the determination of copper(I) equilibria in aqueous solution, *J. Chem. Soc., Chem. Commun.*, 1993, DOI: 10.1039/C39930001704, 1704-1706.

82. J. T. Rubino, P. Riggs-Gelasco and K. J. Franz, Methionine motifs of copper transport proteins provide general and flexible thioether-only binding sites for Cu(I) and Ag(I), *JBIC Journal of Biological Inorganic Chemistry*, 2010, **15**, 1033-1049.
83. J. Wu, M. H. Nantz and M. A. Zern, Targeting hepatocytes for drug and gene delivery: emerging novel approaches and applications.*Journal*, 2002, **7**, d717-725.
84. K. Poelstra, J. Prakash and L. Beljaars, Drug targeting to the diseased liver, *J. Controlled Release*, 2012, **161**, 188-197.
85. A. A. D'Souza and P. V. Devarajan, Asialoglycoprotein receptor mediated hepatocyte targeting — Strategies and applications, *J. Controlled Release*, 2015, **203**, 126-139.
86. M. Spiess, The asialoglycoprotein receptor: a model for endocytic transport receptors, *Biochemistry*, 1990, **29**, 10009-10018.
87. G. Ashwell and J. Harford, Carbohydrate-Specific Receptors of the Liver, *Annu. Rev. Biochem*, 1982, **51**, 531-554.
88. J. U. Baenziger and Y. Maynard, Human hepatic lectin. Physiochemical properties and specificity, *J. Biol. Chem.*, 1980, **255**, 4607-4613.
89. M. C. Torrani, L. Fiume, W. B. V. De, B. Lavezzo, M. Brunetto, A. Ponzetto, G. S. Di, C. Busi, A. Mattioli and G. Gervasi, Adenine arabinoside monophosphate coupled to lactosaminated human albumin administered for 4 weeks in patients with chronic type B hepatitis decreased viremia without producing significant side effects, *Hepatology (Baltimore, Md.)*, 1996, **23**, 657-661.
90. G. D. Stefano, F. P. Colonna, A. Bongini, C. Busi, A. Mattioli and L. Fiume, Ribavirin conjugated with lactosaminated poly-l-lysine: Selective delivery to the liver and increased antiviral activity in mice with viral hepatitis, *Biochem. Pharmacol.*, 1997, **54**, 357-363.
91. G. Di Stefano, L. Fiume, M. Baglioni, L. Bolondi, C. Busi, P. Chieco, F. Kratz, F. Manaresi and M. Pariali, A conjugate of doxorubicin with lactosaminated albumin enhances the drug concentrations in all the forms of rat hepatocellular carcinomas independently of their differentiation grade, *Liver International*, 2006, **26**, 726-733.
92. L. Fiume, L. Bolondi, C. Busi, P. Chieco, F. Kratz, M. Lanza, A. Mattioli and G. Di Stefano, Doxorubicin coupled to lactosaminated albumin inhibits the growth of hepatocellular carcinomas induced in rats by diethylnitrosamine, *Journal of Hepatology*, 2005, **43**, 645-652.
93. A. David, P. Kopečková, T. Minko, A. Rubinstein and J. Kopeček, Design of a multivalent galactoside ligand for selective targeting of HPMA copolymer–doxorubicin conjugates to human colon cancer cells, *European Journal of Cancer*, 2003, **40**, 148-157.
94. K. G. Rajeev, J. K. Nair, M. Jayaraman, K. Charisse, N. Taneja, J. O'Shea, J. L. S. Willoughby, K. Yucius, T. Nguyen, S. Shulga-Morskaya, S. Milstein, A. Liebow, W. Querbes, A. Borodovsky, K. Fitzgerald, M. A. Maier and M. Manoharan, Hepatocyte-Specific Delivery of siRNAs Conjugated to Novel Non-nucleosidic Trivalent N-Acetylgalactosamine Elicits Robust Gene Silencing in Vivo, *ChemBioChem*, 2015, **16**, 903-908.

95. D. J. Peng, J. Sun, Y. Z. Wang, J. Tian, Y. H. Zhang, M. H. M. Noteborn and S. Qu, Inhibition of hepatocarcinoma by systemic delivery of Apoptin gene via the hepatic asialoglycoprotein receptor, *Cancer Gene Therapy*, 2006, **14**, 66.
96. H. L. Jiang, J. T. Kwon, Y. K. Kim, E. M. Kim, R. Arote, H. J. Jeong, J. W. Nah, Y. J. Choi, T. Akaike, M. H. Cho and C. S. Cho, Galactosylated chitosan-graft-polyethylenimine as a gene carrier for hepatocyte targeting, *Gene Ther.*, 2007, **14**, 1389.
97. M. Nishikawa, S. Takemura, Y. Takakura and M. Hashida, Targeted Delivery of Plasmid DNA to Hepatocytes In Vivo: Optimization of the Pharmacokinetics of Plasmid DNA/Galactosylated Poly(L-Lysine) Complexes by Controlling their Physicochemical Properties, *J. Pharmacol. Exp. Ther.*, 1998, **287**, 408.
98. E.-M. Kim, H.-J. Jeong, I.-K. Park, C.-S. Cho, H.-B. Moon, D.-Y. Yu, H.-S. Bom, M.-H. Sohn and I.-J. Oh, Asialoglycoprotein receptor targeted gene delivery using galactosylated polyethylenimine-graft-poly(ethylene glycol): In vitro and in vivo studies, *J. Controlled Release*, 2005, **108**, 557-567.
99. D. Boturyn, E. Defrancq, G. T. Dolphin, J. Garcia, P. Labbe, O. Renaudet and P. Dumy, RAFT Nano-constructs: surfing to biological applications, *J. Pept. Sci.*, 2008, **14**, 224-240.
100. A. M. Pujol, M. Cuillel, O. Renaudet, C. Lebrun, P. Charbonnier, D. Cassio, C. Gateau, P. Dumy, E. Mintz and P. Delangle, Hepatocyte Targeting and Intracellular Copper Chelation by a Thiol-Containing Glycocyclopeptide, *J. Am. Chem. Soc.*, 2011, **133**, 286-296.
101. A. M. Pujol, M. Cuillel, A.-S. Jullien, C. Lebrun, D. Cassio, E. Mintz, C. Gateau and P. Delangle, A Sulfur Tripod Glycoconjugate that Releases a High-Affinity Copper Chelator in Hepatocytes, *Angew. Chem. Int. Ed.*, 2012, **51**, 7445-7448.
102. M. Monestier, P. Charbonnier, C. Gateau, M. Cuillel, F. Robert, C. Lebrun, E. Mintz, O. Renaudet and P. Delangle, ASGPR-Mediated Uptake of Multivalent Glycoconjugates for Drug Delivery in Hepatocytes, *ChemBioChem*, 2016, **17**, 590-594.
103. M. Vetrik, J. Mattova, H. Mackova, J. Kucka, P. Pouckova, O. Kukackova, J. Brus, S. Eigner-Henke, O. Sedlacek, L. Sefc, P. Stepanek and M. Hruby, Biopolymer strategy for the treatment of Wilson's disease, *J. Controlled Release*, 2018, **273**, 131-138.
104. R. B. Merrifield, Solid Phase Peptide Synthesis. I. The Synthesis of a Tetrapeptide, *J. Am. Chem. Soc.*, 1963, **85**, 2149-2154.
105. G. B. Fields and R. L. Noble, Solid phase peptide synthesis utilizing 9-fluorenylmethoxycarbonyl amino acids, *Int. J. Pept. Protein Res.*, 1990, **35**, 161-214.
106. E. Kaiser, R. L. Colescott, C. D. Bossinger and P. I. Cook, Color test for detection of free terminal amino groups in the solid-phase synthesis of peptides, *Anal. Biochem.*, 1970, **34**, 595-598.
107. A. Jancso, D. Szunyogh, F. H. Larsen, P. W. Thulstrup, N. J. Christensen, B. Gyurcsik and L. Hemmingsen, Towards the role of metal ions in the structural variability of proteins: CdII speciation of a metal ion binding loop motif, *Metallomics*, 2011, **3**, 1331-1339.

108. D. Szunyogh, H. Szokolai, P. W. Thulstrup, F. H. Larsen, B. Gyurcsik, N. J. Christensen, M. Stachura, L. Hemmingsen and A. Jancsó, Specificity of the Metalloregulator CueR for Monovalent Metal Ions: Possible Functional Role of a Coordinated Thiol?, *Angew. Chem. Int. Ed.*, 2015, **54**, 15756-15761.
109. O. Sénèque, P. Rousselot-Pailley, A. Pujol, D. Boturyn, S. Crouzy, O. Proux, A. Manceau, C. Lebrun and P. Delangle, Mercury Trithiolate Binding (HgS_3) to a de Novo Designed Cyclic Decapeptide with Three Preoriented Cysteine Side Chains, *Inorg. Chem.*, 2018, **57**, 2705-2713.
110. P. Kamau and R. B. Jordan, Complex Formation Constants for the Aqueous Copper(I)−Acetonitrile System by a Simple General Method, *Inorg. Chem.*, 2001, **40**, 3879-3883.
111. G. L. Ellman, Tissue sulfhydryl groups, *Arch. Biochem. Biophys.*, 1959, **82**, 70-77.
112. P. W. Riddles, R. L. Blakeley and B. Zerner, in *Methods Enzymol.*, Academic Press, 1983, vol. Volume 91, pp. 49-60.
113. A. R. Waldeck, P. W. Kuchel, A. J. Lennon and B. E. Chapman, NMR diffusion measurements to characterise membrane transport and solute binding, *Prog. Nucl. Magn. Reson. Spectrosc.*, 1997, **30**, 39-68.
114. A. Jerschow and N. Müller, Suppression of Convection Artifacts in Stimulated-Echo Diffusion Experiments. Double-Stimulated-Echo Experiments, *J. Magn. Reson.*, 1997, **125**, 372-375.
115. D. Sinnaeve, The Stejskal–Tanner equation generalized for any gradient shape — an overview of most pulse sequences measuring free diffusion, *Concepts in Magnetic Resonance Part A*, 2012, **40A**, 39-65.
116. H. Gampp, M. Maeder, C. J. Meyer and A. D. Zuberbühler, Calculation of equilibrium constants from multiwavelength spectroscopic data—I, *Talanta*, 1985, **32**, 95-101.
117. H. Gampp, M. Maeder, C. J. Meyer and A. D. Zuberbu¨hler, Calculation of equilibrium constants from multiwavelength spectroscopic data—II, *Talanta*, 1985, **32**, 257-264.
118. H. Gampp, M. Maeder, C. J. Meyer and A. D. Zuberbühler, Calculation of equilibrium constants from multiwavelength spectroscopic data—III, *Talanta*, 1985, **32**, 1133-1139.
119. H. Gampp, M. Maeder, C. J. Meyer and A. D. Zuberbühler, Calculation of equilibrium constants from multiwavelength spectroscopic data—IV, *Talanta*, 1986, **33**, 943-951.
120. L. G. Sillen, Electrometric Investigation of Equilibria between Mercury and Halogen Ions. Vlll. Survey and Conclusions, *Acta Chem. Scand.*, 1949, **3**, 539-553.
121. I. Grenthe, A. V. Plyasunov and K. Spahiu, Estimations of medium effects on thermodynamic data, *Modelling in aquatic chemistry*, 1997, **325**.
122. J. Powell Kipton, L. Brown Paul, H. Byrne Robert, T. Gajda, G. Hefter, S. Sjöberg and H. Wanner, Chemical speciation of environmentally significant heavy metals with inorganic ligands. Part 1: The Hg^{2+}, Cl^{-}, OH^{-}, CO_3^{2-}, SO_4^{2-}, and PO_4^{3-} aqueous systems (IUPAC Technical Report).*Journal*, 2005, **77**, 739.
123. C. F. Shaw, J. E. Laib, M. M. Savas and D. H. Petering, Biphasic kinetics of aurothionein formation from gold sodium thiomalate: a novel metallochromic technique to probe zinc(2+) and cadmium(2+) displacement from metallothionein, *Inorg. Chem.*, 1990, **29**, 403-408.

124. F. W. Outten, C. E. Outten, J. Hale and T. V. O'Halloran, Transcriptional Activation of an Escherichia coliCopper Efflux Regulon by the Chromosomal MerR Homologue, CueR, *J. Biol. Chem.*, 2000, **275**, 31024-31029.
125. C. Petersen and L. B. Møller, Control of copper homeostasis in Escherichia coli by a P-type ATPase, CopA, and a MerR-like transcriptional activator, CopR, *Gene*, 2000, **261**, 289-298.
126. J. V. Stoyanov, J. L. Hobman and N. L. Brown, CueR (YbbI) of Escherichia coli is a MerR family regulator controlling expression of the copper exporter CopA, *Mol. Microbiol.*, 2001, **39**, 502-512.
127. N. L. Brown, J. V. Stoyanov, S. P. Kidd and J. L. Hobman, The MerR family of transcriptional regulators, *FEMS Microbiology Reviews*, 2003, **27**, 145-163.
128. J. L. Hobman, MerR family transcription activators: similar designs, different specificities, *Mol. Microbiol.*, 2007, **63**, 1275-1278.
129. J. L. Hobman, J. Wilkie and N. L. Brown, A Design for Life: Prokaryotic Metal-binding MerR Family Regulators, *Biometals*, 2005, **18**, 429-436.
130. Z. Ma, F. E. Jacobsen and D. P. Giedroc, Metal Transporters and Metal Sensors: How Coordination Chemistry Controls Bacterial Metal Homeostasis, *Chem. Rev.*, 2009, **109**, 4644-4681.
131. A. Changela, K. Chen, Y. Xue, J. Holschen, C. E. Outten, T. V. Halloran and A. Mondragón, Molecular Basis of Metal-Ion Selectivity and Zeptomolar Sensitivity by CueR, *Science*, 2003, **301**, 1383.
132. K. Chen, S. Yuldasheva, J. E. Penner-Hahn and T. V. O'Halloran, An Atypical Linear Cu(I)−S_2 Center Constitutes the High-Affinity Metal-Sensing Site in the CueR Metalloregulatory Protein, *J. Am. Chem. Soc.*, 2003, **125**, 12088-12089.
133. M. Beltramini and K. Lerch, Spectroscopic studies on Neurospora copper metallothionein, *Biochemistry*, 1983, **22**, 2043-2048.
134. D. Szunyogh, B. Gyurcsik, F. H. Larsen, M. Stachura, P. W. Thulstrup, L. Hemmingsen and A. Jancso, ZnII and HgII binding to a designed peptide that accommodates different coordination geometries, *Dalton Transactions*, 2015, **44**, 12576-12588.
135. M. A. Kihlken, A. P. Leech and N. E. Le Brun, Copper-mediated dimerization of CopZ, a predicted copper chaperone from Bacillus subtilis, *Biochem. J*, 2002, **368**, 729.
136. A. M. Pujol, C. Lebrun, C. Gateau, A. Manceau and P. Delangle, Mercury-Sequestering Pseudopeptides with a Tris(cysteine) Environment in Water, *Eur. J. Inorg. Chem.*, 2012, **2012**, 3835-3843.
137. S. Pires, J. Habjanič, M. Sezer, C. M. Soares, L. Hemmingsen and O. Iranzo, Design of a Peptidic Turn with High Affinity for HgII, *Inorg. Chem.*, 2012, **51**, 11339-11348.
138. G. R. Dieckmann, D. K. McRorie, D. L. Tierney, L. M. Utschig, C. P. Singer, T. V. O'Halloran, J. E. Penner-Hahn, W. F. DeGrado and V. L. Pecoraro, De Novo Design of Mercury-Binding Two- and Three-Helical Bundles, *J. Am. Chem. Soc.*, 1997, **119**, 6195-6196.
139. S. M. Kelly and N. C. Price, The Use of Circular Dichroism in the Investigation of Protein Structure and Function, *Curr. Protein Pept. Sci.*, 2000, **1**, 349-384.

140. A. Jancsó, B. Gyurcsik, E. Mesterházy and R. Berkecz, Competition of zinc(II) with cadmium(II) or mercury(II) in binding to a 12-mer peptide, *J. Inorg. Biochem.*, 2013, **126**, 96-103.
141. L. Zhang, M. Koay, M. J. Maher, Z. Xiao and A. G. Wedd, Intermolecular Transfer of Copper Ions from the CopC Protein of Pseudomonas syringae. Crystal Structures of Fully Loaded CuICuII Forms, *J. Am. Chem. Soc.*, 2006, **128**, 5834-5850.
142. M. Sendzik, M. J. Pushie, E. Stefaniak and K. L. Haas, Structure and Affinity of Cu(I) Bound to Human Serum Albumin, *Inorg. Chem.*, 2017, **56**, 15057-15065
143. R. Bogumil, P. Faller, D. L. Pountney and M. Vašák, Evidence for Cu(I) Clusters and Zn(II) Clusters in Neuronal Growth-Inhibitory Factor Isolated from Bovine Brain, *Eur. J. Biochem.*, 1996, **238**, 698-705.
144. K. Fujisawa, S. Imai, N. Kitajima and Y. Moro-oka, Preparation, Spectroscopic Characterization, and Molecular Structure of Copper(I) Aliphatic Thiolate Complexes, *Inorg. Chem.*, 1998, **37**, 168-169.
145. Z. Xiao, L. Gottschlich, R. van der Meulen, S. R. Udagedara and A. G. Wedd, Evaluation of quantitative probes for weaker Cu(I) binding sites completes a set of four capable of detecting Cu(I) affinities from nanomolar to attomolar, *Metallomics*, 2013, **5**, 501-513.
146. A. Jancso, *unpublished results*, 2015.
147. S. P. Watton, J. G. Wright, F. M. MacDonnell, J. W. Bryson, M. Sabat and T. V. O'Halloran, Trigonal mercuric complex of an aliphatic thiolate: A spectroscopic and structural model for the receptor site in the mercury (II) biosensor MerR, *J. Am. Chem. Soc.*, 1990, **112**, 2824-2826.
148. A. K. Wernimont, D. L. Huffman, A. L. Lamb, T. V. O'Halloran and A. C. Rosenzweig, Structural basis for copper transfer by the metallochaperone for the Menkes/Wilson disease proteins, *Nature Structural Biology*, 2000, **7**, 766.
149. R. A. Steele and S. J. Opella, Structures of the Reduced and Mercury-Bound Forms of MerP, the Periplasmic Protein from the Bacterial Mercury Detoxification System, *Biochemistry*, 1997, **36**, 6885-6895.
150. E. Rossy, O. Sénèque, D. Lascoux, D. Lemaire, S. Crouzy, P. Delangle and J. Covès, Is the cytoplasmic loop of MerT, the mercuric ion transport protein, involved in mercury transfer to the mercuric reductase?, *FEBS Lett.*, 2004, **575**, 86-90.
151. R. Ledwidge, B. Patel, A. Dong, D. Fiedler, M. Falkowski, J. Zelikova, A. O. Summers, E. F. Pai and S. M. Miller, NmerA, the Metal Binding Domain of Mercuric Ion Reductase, Removes Hg^{2+} from Proteins, Delivers It to the Catalytic Core, and Protects Cells under Glutathione-Depleted Conditions, *Biochemistry*, 2005, **44**, 11402-11416.
152. A. C. Rosenzweig, D. L. Huffman, M. Y. Hou, A. K. Wernimont, R. A. Pufahl and T. V. O'Halloran, Crystal structure of the Atx1 metallochaperone protein at 1.02 Å resolution, *Structure*, 1999, **7**, 605-617.
153. S. Chakraborty, J. Yudenfreund Kravitz, P. W. Thulstrup, L. Hemmingsen, W. F. DeGrado and V. L. Pecoraro, Design of a Three-Helix Bundle Capable of Binding Heavy Metals in a Triscysteine Environment, *Angew. Chem. Int. Ed.*, 2011, **50**, 2049-2053.

154. O. Iranzo, P. W. Thulstrup, S.-b. Ryu, L. Hemmingsen and V. L. Pecoraro, The Application of ^{199}Hg NMR and ^{199m}Hg Perturbed Angular Correlation (PAC) Spectroscopy to Define the Biological Chemistry of Hg^{II}: A Case Study with Designed Two- and Three-Stranded Coiled Coils, *Chem. Eur. J.*, 2007, **13**, 9178-9190.
155. M. Łuczkowski, M. Stachura, V. Schirf, B. Demeler, L. Hemmingsen and V. L. Pecoraro, Design of Thiolate Rich Metal Binding Sites within a Peptidic Framework, *Inorg. Chem.*, 2008, **47**, 10875-10888.
156. J. S. Casas and M. M. Jones, Mercury(II) complexes with sulfhydryl containing chelating agents: Stability constant inconsistencies and their resolution, *Journal of Inorganic and Nuclear Chemistry*, 1980, **42**, 99-102.
157. B. Imperiali and T. M. Kapoor, The reverse turn as a template for metal coordination, *Tetrahedron*, 1993, **49**, 3501-3510.
158. J. Venkatraman, S. C. Shankaramma and P. Balaram, Design of Folded Peptides, *Chem. Rev.*, 2001, **101**, 3131-3152.
159. G. D. Rose, L. M. Glerasch and J. A. Smith, Turns in peptides and proteins, *Adv. Protein Chem.*, 1985, **37**, 1-109.
160. J. A. Smith, L. G. Pease and K. D. Kopple, Reverse turns in peptides and protein, *Critical Reviews in Biochemistry*, 1980, **8**, 315-399.
161. C. Lebrun, M. Starck, V. Gathu, Y. Chenavier and P. Delangle, Engineering Short Peptide Sequences for Uranyl Binding, *Chem. Eur. J.*, 2014, **20**, 16566-16573.
162. A. Fragoso, P. Lamosa, R. Delgado and O. Iranzo, Harnessing the Flexibility of Peptidic Scaffolds to Control their Copper(II)-Coordination Properties: A Potentiometric and Spectroscopic Study, *Chem. Eur. J.*, 2013, **19**, 2076-2088.
163. A. Fragoso, R. Delgado and O. Iranzo, Copper(II) coordination properties of decapeptides containing three His residues: the impact of cyclization and Asp residue coordination, *Dalton Trans.*, 2013, **42**, 6182-6192.
164. A. Borics, R. F. Murphy and S. Lovas, Molecular Dynamics Simulations of β-turn Forming Tetra- and Hexapeptides, *J. Biomol. Struct. Dyn.*, 2004, **21**, 761-770.
165. D. K. Chalmers and G. R. Marshall, Pro-D-NMe-Amino Acid and D-Pro-NMe-Amino Acid: Simple, Efficient Reverse-Turn Constraints, *J. Am. Chem. Soc.*, 1995, **117**, 5927-5937.
166. S. Rao Raghothama, S. Kumar Awasthi and P. Balaram, β-Hairpin nucleation by Pro-Gly β-turns. Comparison of D-Pro-Gly and L-Pro-Gly sequences in an apolar octapeptide, *Perkin Trans. 2*, 1998, 137-144
167. S. J. Opella, T. M. DeSilva and G. Veglia, Structural biology of metal-binding sequences, *Curr. Opin. Chem. Biol.*, 2002, **6**, 217-223.
168. A. C. Rosenzweig, Copper Delivery by Metallochaperone Proteins, *Acc. Chem. Res.*, 2001, **34**, 119-128.
169. M. S. Shoshan and E. Y. Tshuva, The MXCXXC class of metallochaperone proteins: model studies, *Chem. Soc. Rev.*, 2011, **40**, 5282-5292.
170. H. Kessler, Conformation and Biological Activity of Cyclic Peptides, *Angew. Chem. Int. Ed.*, 1982, **21**, 512-523.

171. E. Schievano, A. Bisello, M. Chorev, A. Bisol, S. Mammi and E. Peggion, Aib-Rich Peptides Containing Lactam-Bridged Side Chains as Models of the 310-Helix, *J. Am. Chem. Soc.*, 2001, **123**, 2743-2751.
172. H. J. Dyson, M. Rance, R. A. Houghten, R. A. Lerner and P. E. Wright, Folding of immunogenic peptide fragments of proteins in water solution, *J. Mol. Biol.*, 1988, **201**, 161-200.
173. N. J. Baxter and M. P. Williamson, Temperature dependence of 1H chemical shifts in proteins, *J. Biomol. NMR*, 1997, **9**, 359-369.
174. T. Cierpicki and J. Otlewski, Amide proton temperature coefficients as hydrogen bond indicators in proteins, *J. Biomol. NMR*, 2001, **21**, 249-261.
175. C. Srinivasan, M. C. Posewitz, G. N. George and D. R. Winge, Characterization of the Copper Chaperone Cox17 of Saccharomyces cerevisiae, *Biochemistry*, 1998, **37**, 7572-7577.
176. X. Chen, H. Hua, K. Balamurugan, X. Kong, L. Zhang, G. N. George, O. Georgiev, W. Schaffner and D. P. Giedroc, Copper sensing function of Drosophila metal-responsive transcription factor-1 is mediated by a tetranuclear Cu(I) cluster, *Nucleic Acids Res.*, 2008, **36**, 3128-3138.
177. J. A. Graden, M. C. Posewitz, J. R. Simon, G. N. George, I. J. Pickering and D. R. Winge, Presence of a Copper(I)−Thiolate Regulatory Domain in the Copper-Activated Transcription Factor Amt1, *Biochemistry*, 1996, **35**, 14583-14589.
178. M. Vasak, J. H. R. Kaegi and H. A. O. Hill, Zinc(II), cadmium(II), and mercury(II) thiolate transitions in metallothionein, *Biochemistry*, 1981, **20**, 2852-2856.
179. J. H. Kägi, M. Vasák, K. Lerch, D. E. Gilg, P. Hunziker, W. R. Bernhard and M. Good, Structure of mammalian metallothionein, *Environ. Health Perspect.*, 1984, **54**, 93-103.

Összefoglalás

A réz, mint létfontosságú nyomelem számos biológiai folyamatban vesz részt. Ilyen a légzés, a vas-háztartás, az oxidatív stressz elleni védelem vagy a pigment képződés. Azonban ha a réz feleslegbe kerül, ő maga is képes oxidatív károk okozására. Ezért sejten belüli koncentrációja szigorú szabályozás alatt áll. A Menkes és a Wilson betegségek genetikai elváltozások, melyek a szervezet réz-háztartásának felborulásához vezetnek és rézhiány ill., -felhalmozódás alakul ki. A Wilson betegség kelát-terápiával kezelhető, azonban a jelenleg alkalmazott gyógyszerek számos súlyos mellékhatást váltanak ki.

Pascale Delangle kutatócsoportjának célja olyan új peptid vagy tripodális ligandumok kifejlesztése, melyek egyrészt nagy affinitást mutatnak a sejten belüli Cu(I) ionok iránt, másrészt célzottan a májsejtekbe képesek felszívódni, ezáltal csökkentve a mellékhatások kockázatát.

Doktori munkám céljaként új peptid típusú, cisztein tartalmú ligandumok tervezését, valamint előállítását és Cu(I) ionokkal való kölcsönhatásának vizsgálatát tűztük ki célul, annak érdekében, hogy kiderüljön, a megtervezett és vizsgált vegyületek megfelelő kelátorok lennének-e a Wilson betegség kezelésére. Egyes esetekben a peptidek Hg(II) és Zn(II) ionokkal való kölcsönhatását is tanulmányoztuk, mert a Hg(II) hasonló koordinációs kémiai tulajdonságokkal rendelkezik, mint a Cu(I) és emiatt gyakorta használják az oxidációra érzékeny Cu(I) helyett próbaionként, illetve a Zn(II) ion a szervezetben nagy mennyiségben fordul elő és így a Cu(I) potenciális vetélytársa lehet.

A peptideket három különböző stratégia alapján terveztük meg. Az első csoport ligandumaiban a bakteriális rézháztartás-szabályozó CueR fehérje nagyfokú érzékenységét és szelektivitását igyekeztünk kihasználni. Ennek érdekében a CueR fehérjének a két ciszteint tartalmazó fémkötő szakaszát modellező peptideket állítottunk elő. A következő megközelítésben három ciszteint tartalmazó lineáris és ciklikus peptidek segítségével próbáltuk egyesíteni a Delangle csoportban korábban tanulmányozott ligandumok kedvező tulajdonságait, azaz a tripodális ligandumok nagy Cu(I) affinitását, illetve a peptid kelátorok azon tulajdonságát, hogy glikokonjugátumaikat a májsejtek nagyobb hatékonysággal képesek felvenni. Végül, a peptid szerkezetének nagyfokú preorganizációjából fakadó előnyöket terveztük kihasználni egy rövid, merev tetrapeptid segítségével, melyben két ciszteint egy turn motívum köt össze. Összehasonlíthatóság érdekében egy kevésbé merev vázú peptiddel végeztünk vizsgálatokat (CPGC).

A terminálisan védett lineáris peptideket szilárd fázisú peptidszintézissel állítottuk elő az Fmoc stratégiát követve. A ciklikus peptidek előállítása során először hasonló módon lináris prekurzorokat szintetizáltunk, melyeket a gyantáról való hasítás után híg oldatban, standard kapcsolószerek jelenlétében ciklizáltunk. A nyers termékeket fordított fázisú HPLC-vel tisztítottuk, majd tisztaságukat analitikai HPLC-vel és ESI-MS segítségével ellenőriztük.

Mivel mind a cisztein tiolcsoportjai, mind a Cu(I) ion oxidációra érzékeny, a minták előkészítése és további kezelése inert atmoszférában, egy gloveboxban történt. A kísérletek többségét pufferelt közegben, 7,4-es pH-n hajtottuk végre. Néhány esetben pH függő UV spektrumsorozatot is felvettünk állandó fémion:peptid arány mellett. A peptidek fémionokkal való kölcsönhatását UV-látható, CD és NMR spektroszkópiával, valamint ESI-MS segítségével vizsgáltuk. A peptid-fémion komplexek stabilitását minden esetben az adott fémiont hatékonyan kötő, jól ismert ligandummal végrehajtott kiszorításos reakcióval határoztuk meg.

A CueR három modell peptidje, az **EC**, **VC** és **HS** nagyon hasonlóan viselkednek Cu(I) ionokkal történő kölcsönhatásuk során. Ligandum felesleg jelenlétében egymagvú komplexek képződnek, melyek átalakulnak többmagvú részecskékké, ha a fémion kerül feleslegbe. Az UV és CD spektrumokon a Cu(I)-ligandum arány növelésével párhuzamosan megjelenő tiolát-Cu(I) töltésátviteli sávok intenzitásának alakulása arra utal, hogy 7,4-es pH-n a Cu(I) a két cisztein oldalláncán keresztül koordinálódik a peptidekhez. A **HS** esetében ^{1}H NMR vizsgálatokkal igazoltuk, hogy a hisztidin oldallánca is részt vesz a fémion megkötésében. A pH változtatásával felvett UV spektrumok azt mutatják, hogy a komplexek pH = 7 felett teljes mértékben kialakulnak, valamint, hogy a pH csökkenésével a cisztein tiolátok két lépésben dekoordinálódnak a fémiontól. Az ezen folyamatokra meghatározott pK_s értékek jelentősen kisebbek a fiziológiás pH-nál, ami arra utal, hogy a pH indukálta tiol-disszociációs folyamatok feltehetőleg nem játszanak szerepet a CueR működése során.

Az egymagvú komplexek BCA ligandummal való kiszorítási reakció segítségével meghatározott látszólagos stabilitása pH = 7,4-en meglehetősen nagy ($\log\beta_{11}^{pH7,4}$ ~ 16) és azonos nagyságrendű a CxxC vagy CxxxxC motívumot tartalmazó peptidek Cu(I)-affinitásával. Ez arra utal, hogy a ciszteinek szekvencián belüli távolsága nem befolyásolja számottevően a peptidek Cu(I)-kötő hatékonyságát és a komplexek stabilitását elsősorban a két Cu(I)-tiolát kötés erőssége határozza meg. Korábbi stabilitási eredményekkel való összehasonlítás alapján a peptidek jelentős szelektivitást mutatnak a Cu(I) ionok irányába a

Zn(II) ionokkal szemben, azonban a CuP komplexek stabilitása hasonló, mint a megfelelő Ag(I) komplexeké. Habár a modell peptidek affinitása 5-6 nagyságrenddel elmarad a natív CueR fehérjéhez képest, ligandum felesleg jelenlétében a fehérjével megegyező módon csak egyetlen fémiont kötnek meg. Ez, valamint a nagy Cu(I) affinitás, ill. a Zn(II) ionokkal szemben mutatott szelektivitás együttesen a Cu(I)-kelátorként való alkalmazás szempontjából kedvező tulajdonságok.

A három ciszteint tartalmazó ciklikus $\mathbf{P^{3C}}$, $\mathbf{1^{C}}$, $\mathbf{2^{C}}$ és $\mathbf{3^{C}}$ peptidekben, valamint lineáris megfelelőikben, $\mathbf{1^{L}}$-ben és $\mathbf{2^{L}}$-ben, a cisztein aminosavak a metallotioneinekben is megtalálható CxCxxC és CxCxC motívumok szerint helyezkednek el. A peptidek ezen sorozatával azt is tanulmányoztuk, hogy a szekvenciát és a ligandum szerkezetet érintő kisebb változtatások miként befolyásolják a fémion megkötését.

Mind a hat peptid Cu(I) ionokkal való reakciója meglehetősen összetett rendszer kialakulásához vezetett. Ennek első előjele az abszorbancia lassú stabilizálódása volt az UV spektroszkópiás vizsgálatok során, mikor a peptideket Cu(I)-oldattal titrálva az LMCT sávok intenzitása csak ~2 óra elteltével állandósult. Ezért további méréseinkhez egyedi mintákat alkalmaztunk. Az abszorbancia lineáris változása látszólag egyszerű folyamatra utal, melynek végpontja 2 ekvivalens Cu(I) hozzáadásakor figyelhető meg. Ennek alapján a $(Cu_2P)_n$ általános összetétellel egyszerűen leírható részecske képződése feltételezhető. Ezzel szemben a CD- és ESI-MS spektrumok különböző többmagvú részecskék bonyolult keverékének képződését támasztja alá. A vizsgált peptidek szerkezete tehát túlságosan flexibilisnek bizonyult ahhoz, hogy egy jól definiált szerkezetbe kényszerítse a Cu(I) iont, amelynek következménye számos, elsősorban többmagvú részecske együttes jelenléte a rendszerekben.

Mivel a képződő komplexek összetétele nem meghatározott, csak a peptidek átlagos Cu(I)-kötő affinitását tudtuk meghatározni. Ehhez a BCS ligandummal elvégzett kiszorításos reakció UV spektrumainak értékelésekor egy 1:1 összetételű, CuP általános képlettel leírható komplex képződését vettük figyelembe. Minden peptid Cu(I)-affinitása jelentős és nagyságrendileg megegyezik a dajka fehérjékre jellemző Cu(I)-kötő képességgel. A hasonló $\log\beta_{11}^{pH7,4}$ ~ 18 értékek arra utalnak, hogy a szerkezeti különbségek csak csekély mértékben befolyásolják a peptidek Cu(I)-affinitását.

Annak felderítése érdekében, hogy a komplexképződési folyamatok összetettsége a peptid szerkezetéből adódik vagy az kifejezetten a Cu(I) ionokra jellemző, a peptidek kölcsönhatását egy másik szoft fémionnal, a Hg(II)-vel is megvizsgáltuk. Az első

szembetűnő különbség a Hg(II) komplexek jóval gyorsabb kialakulása. Ligandum felesleg jelenlétében HgP összetételű komplexek képződnek. A tiolát-Hg(II) töltésátviteli sávok pozíciója λ = 280 és 240 nm-nél egyértelműen mutatja, hogy 7,4-es pH-n a peptidek mindhárom tiolát-csoportja részt vesz a fémion megkötésében. Hg(II) felesleget alkalmazva az egymagvú komplexek többmagvú részecskékké alakulnak át, melyekben a Hg(II) a kedvezőbb HgS_2 módon koordinálódik. Az UV és ESI-MS mérések eredményei 1,5 ekvivalens Hg(II) hozzáadásáig a Hg_2P_3 összetételű komplex képződését valószínűsítik, majd a Hg(II) felesleg további növelésével összetettebb részecskék alakulnak ki.

A pH függvényében felvett UV spektrumok változása HgS_2 és HgS_3 koordinációs módú komplexek pH-függő egyensúlyára utal, ahol a harmadik tiol-csoport deprotonálódására az egyes Hg(II)-peptid rendszerekben pK_s = 4,3-5,1 értékeket határoztunk meg. Mivel ezek az értékek viszonylag közel esnek egymáshoz, a szerkezeti különbségek csak kis mértékben befolyásolják a HgS_3 részecske stabilitását. A pK_s értékek sorrendje alapján megállapítható, hogy a $\mathbf{P^{3C}}$ peptid CxCxxC szekvenciája a HgS_3 geometria kialakulásának szempontjából kedvezőbb, mint a többi ligandum CxCxC motívuma, csakúgy, mint a $\mathbf{2^C}$ és $\mathbf{3^C}$ peptidekben a kötőhely az $\mathbf{1^C}$ ligandumhoz képest nagyobb távolsága a PG motívumtól, illetve a ciklikus szerkezet a lineárishoz képest. A meghatározott pK_s értékek mindegyike jelentősen kisebb, mint a háromszálú, ún. „coiled-coil” peptidek Hg(II)-komplexeire publikált deprotonálódási állandók, melynek valószínű oka a tiol-csoportok eltérő oldószer-hozzáférhetősége a különböző struktúrákban.

A HgP komplexek látszólagos stabilitását pH = 2,0-n határoztuk meg I^- ionokkal való kiszorítás segítségével. A hasonló stabilitási értékek azt mutatják, hogy a donor csoportok pozíciója és irányítottsága csekély mértékben befolyásolja a peptidek Hg(II)-kötő képességét, és a fémion nagy tiofilicitása elegendő hajtóerő a pH = 2,0-n megfigyelt HgS_2 szerkezet kialakulásához. A 7,4-es pH-ra átszámolt látszólagos stabilitási állandók 20 nagyságrenddel nagyobbak, mint a Cu(I) komplexek azonos körülmények között meghatározott stabilitása, ami a Hg(II) ionok jelentősebb tiofil karakterének tulajdonítható. A HgP komplexek stabilitási állandói hasonlóak, mint a jól ismert nehézfém-kelátor BAL Hg(II) komplexéé, melyben kiemelten stabilis, öttagú kelátgyűrű képződik a fémion koordinálódása során. Ugyanakkor peptidjeink HgS_3 típusú komplexeinek stabilitása nagyobb annál, mint amit a merev szerkezetű CDPPC peptid Hg(II) komplexére meghatároztak, mely a koordinálódó donorcsoportok növekvő számának logikus következménye. A nagy stabilitási állandók és az alacsony pK_s értékek bizonyítják, hogy

ezek a három ciszteint tartalmazó peptidek kiválóan alkalmasak a Hg(II) ionok tritiolát koordinációs környezetben való megkötésére.

A peptidek a két szoft karakterű fémionnal szembeni viselkedésében megmutatkozó markáns különbségek azt tükrözik, hogy a Hg(II) nem minden esetben alkalmazható modell ionként a Cu(I) tiol-tartalmú peptidekkel vagy fehérjékkel fiziológiás körülmények között való kölcsönhatásának tanulmányozására.

A peptidszerkezet preorganizáltságának fémion megkötésére gyakorolt hatását két olyan rövid tetrapeptid segítségével vizsgáltuk, melyekben két ciszteint egy β turn kialakítására képes motívum köt össze. Ezek a motívumok a CDPPC peptidben alkalmazott DPro-Pro, illetve a CPGC Pro-Gly egysége voltak. A cisztein egységek amid nitrogénjeinek ^{1}H NMR jeleinek hőmérsékletfüggését vizsgálva meggyőződtünk arról, hogy a DPro-Pro motívum merevebb peptidszerkezetet képes biztosítani. UV, CD és NMR spektroszkópiás titrálások alapján megállapítottuk, hogy a CDPPC csupán egyfajta Cu(I) komplexet képez 1,33 ekvivalens fémion hozzáadásáig. ESI-MS és DOSY NMR mérések bizonyították, hogy ez a részecske egy Cu_4P_3 összetételű klaszter Cu_4S_6 maggal, melyben egy fémiont három tiolátcsoport vesz körbe. Ez az egyszerű rövid peptid figyelemre méltó módon utánozza számos Cu(I)-kötő fehérje, pl. a Ctr1 vagy Cox17 réz-tiolát klaszterképző képességét. Ezzel ellentétben, a CPGC peptiddel elvégzett kísérletek jóval összetettebb, komplikáltabb komplexképződési folyamatra utalnak. A CDPPC Cu(I) komplexének stabilitása ($\log\beta_{11}^{pH7,4}$ = 17,5) körülbelül egy nagyságrenddel nagyobb, mint a PG motívumot tartalmazó rokon ligandumé ($\log\beta_{11}^{pH7,4}$ = 16,4). A két peptid viselkedésének összevetése alapján elmondható, hogy a jól meghatározott, preorganizált szerkezet kulcsfontosságú a Cu(I) komplex speciációjának szabályozásában.

A CDPPC és CPGC peptidek Zn(II) ionnal való kölcsönhatása során ZnP és ZnP_2 komplexek képződését figyeltük meg. Fiziológiás pH-n a ZnP komplexek látszólagos stabilitási állandói a 10^6-os nagyságrendbe esnek, ami a peptidek kimagasló Cu(I)-szelektivitását mutatja Zn(II) ionokkal szemben.

CDPPC Cu(I) komplexképző sajátságai jelentősen különböznek a korábban vizsgált Hg(II) komplexekétől, ami újabb bizonyíték arra vonatkozóan, hogy a Hg(II), mint Cu(I)-próbaion, csak nagy körültekintés mellett alkalmazható.

A CDPPC peptid jól definiált Cu(I) koordinációja és a Zn(II) ionnal szemben mutatott jelentős szelektivitása alapján ígéretes vegyület a májsejteket célzó funkcionalizálásra, és ennek révén alkalmas lehet a Wilson betegség során felhalmozódó Cu(I) célzott eltávolítására is.

Résumé

Le cuivre est un micronutriment essentiel qui participe à de nombreux processus biologiques, comme par exemple la respiration, l'homéostasie du fer, la lutte contre le stress oxydant ou la production de pigments. Cependant, le cuivre libre est toxique pour l'organisme parce qu'il catalyse une réaction de type Fenton formant des espèces réactives de l'oxygène. Par conséquent la concentration en cuivre est finement régulée dans tous les organismes vivants. Les maladies de Menkes et de Wilson sont dues à des dérèglements de l'homéostasie du cuivre qui se manifestent respectivement par une déficience ou une accumulation de cuivre dans l'organisme. La maladie de Wilson est traitée avec des chélateurs du cuivre, qui provoquent des effets secondaires importants chez certains patients. C'est pourquoi, l'équipe CIBEST propose de nouveaux chélateurs sélectifs du cuivre(I) et ciblés vers le foie qui est le premier organe touché.

Mon projet de doctorat consiste en l'élaboration de trois familles de peptides qui contiennent des acides aminés cystéines et en l'étude de leurs complexes de Cu(I) pour déterminer s'ils sont des candidats adaptés pour le traitement de la maladie de Wilson. L'interaction de certains peptides avec les ions Hg(II) ou Zn(II) a également été étudiée. En effet, le Hg(II) est un cation métallique possédant des propriétés similaires au Cu(I) et donc souvent utilisé pour modéliser le Cu(I) qui est sensible à l'oxygène et se dismute dans l'eau. Le Zn(II) est quant à lui omniprésent dans les cellules et un compétiteur intracellulaire potentiel du Cu().

Les séquences des peptides ont été choisies selon trois stratégies différentes. Dans la première, des séquences inspirées de la boucle de liaison du cuivre de la protéine bactérienne CueR (copper efflux regulator), contenant deux cystéines, ont été étudiées afin de bénéficier de la sélectivité et de la sensibilité de ce régulateur. Dans une deuxième approche, des peptides contenant trois cystéines dans les motifs CxCxxC et CxCxC ont été étudiés pour combiner les avantage des peptides (bonne internalisation dans les cellules hépatiques quand ils sont judicieusement fonctionnalisés) et des tripodes (très forte affinité pour le Cu(I)) de l'équipe CIBEST. Finalement, la pré-organisation a été exploitée dans un tétrapeptide rigide où les deux cysteines sont liées dans un coude β préformé.

La synthèse des peptides linéaires, protégés en N-ter et C-ter, a été réalisée par synthèse peptidique en phase solide (SPPS) en utilisant la stratégie « Fmoc ». Pour obtenir les peptides cycliques, les précurseurs linéaires protégés sur leurs chaînes latérales et avec

des extrémités N-ter et C-ter libres ont été synthétisés par SPPS. Après avoir décroché le peptide de la résine, la cyclisation a été réalisée dans une solution diluée. Les peptides obtenus ont été purifiés par HPLC et leur pureté a été vérifiée par HPLC analytique et ESI-MS.

Pour obtenir la stabilité, la composition et le mode de liaison des complexes, des mesures par spectroscopie UV-visible, dichroïsme circulaire, RMN et ESI-MS ont été réalisées. Les mesures ont été préférentiellement effectuées en boîte à gants car les ligands et l'ion Cu(I) sont sensibles à l'oxydation. La plupart des expériences ont été réalisées à pH = 7.4 en milieu tamponné. Dans certains cas, l'effet du pH a été analysé pour des rapports métal:ligand constants. Afin de déterminer la stabilité des complexes, des compétiteurs dont l'affinité pour les ions métalliques est connue, ont été utilisés.

Les trois peptides modèles du régulateur CueR, **EC**, **VC** et **HS**, étudiés lors de ma thèse, se comportent de la même façon avec le Cu(I). Ils forment des complexes 1:1 en excès de ligand, qui se transforment en espèce polynucléaire en excès de Cu(I). L'analyse des bandes LMCT sur les spectres UV et CD montre que le Cu(I) est lié par les deux groupes thiolates des cystéines. Le spectre de RMN du proton indique également la coordination de l'histidine du peptide **HS**. L'analyse des spectres UV en fonction du pH révèle que la formation des complexes est complète au-dessus de pH = 7.0 et que la diminution de pH provoque la décoordination des cystéines en deux étapes en menant à la perte totale de l'absorbance des bandes LMCT. Les pK_a obtenus pour ces deux processus sont significativement en dessous du pH physiologique, ce qui indique qu'ils ne sont probablement pas pertinents pour la séquestration biologique du Cu (I).

Les stabilités des complexes mononucléaire à pH = 7.4, déterminées en présence du compétiteur BCA, sont élevées ($\log\beta_{11}^{pH7.4} \sim 16$) et similaires à la stabilité des complexes avec des peptides incorporant le motif CxxC ou le CxxxxC. Ce résultat montre que la distance entre les résidus Cys dans le peptide affecte peu l'affinité pour le Cu(I). Par conséquent, la force motrice de la coordination du cation mou Cu(I) est principalement due à la formation des deux liaisons fortes avec les donneurs thiolates mous. La comparaison des constantes de stabilité avec les résultats précédents montre que les peptides sont fortement sélectifs pour le Cu(I) par rapport au Zn(II), mais ont une affinité similaire pour l'Ag(I). Les affinités pour le Cu(I) de ces peptides modèles sont plus faibles, de 5 à 6 ordres de grandeur, que celle de la protéine CueR native. Néanmoins, ces peptides miment la capacité de la protéine à accueillir exclusivement un ion Cu(I) dans des conditions d'excès de ligand et une

forte affinité et sélectivité par rapport au Zn(II). Ces caractéristiques sont avantageuses dans la perspective du développement de nouveaux chélateurs du Cu(I).

Dans les peptides contenant trois cystéines, $\mathbf{P^{3C}}$, $\mathbf{1^{C}}$, $\mathbf{2^{C}}$, $\mathbf{3^{C}}$, $\mathbf{1^{L}}$ et $\mathbf{2^{L}}$, les résidus Cys sont placés dans les motifs CxCxxC ou CxCxC identifiés dans les métallothionéines. Cette série de peptides a permis d'évaluer les effets des modifications structurales sur la coordination des ions métalliques Hg(II) et Cu(I).

La complexation du Cu(I) s'est avérée compliquée avec les six peptides. Une première difficulté a été les longs temps d'équilibration (supérieurs à 2 heures) lors de la formation des complexes. Par conséquent, les échantillons de stœchiométries données ont été préparés individuellement. Malgré l'évolution simple des spectre UV, qui indique la formation des complexes avec la stœchiométrie $(Cu_2P)_n$, les spectres CD et ESI-MS démontrent la présence de plusieurs espèces polymétalliques. Ces peptides s'avèrent donc trop flexibles pour contrôler la spéciation des complexes du Cu(I). Une affinité moyenne de ces peptides pour le Cu(I) a été déterminée à pH = 7.4. Le résultat des compétitions avec le ligand BCS a été évalué en considérant la formation d'un seul complexe 1:1 mononucléaire. Tous les peptides ont une forte affinité pour le Cu(I), typique des protéines chaperonnes du Cu(I). Les valeurs des constantes de stabilité ($\log\beta_{11}^{pH7.4}$ ~ 18) sont similaires sur la série, ce qui indique que la structure des peptides influence peu la stabilité des complexes de Cu(I) formés.

Afin de comprendre si le comportement complexe observé avec le Cu(I) provenait de la séquence peptidique ou des propriétés de coordination du Cu(I), l'interaction avec le Hg(II), un ion métallique mou aux propriétés similaires à celles du Cu(I), a également été étudiée. Des complexes mononucléaires de Hg(II) se forment quand le ligand est en excès. Leur formation est significativement plus rapide qu'avec le Cu(I). La position des bandes LMCT pour λ = 280 et 240 nm démontre que le Hg(II) est coordonné par les trois cystéines à pH = 7.4. En excès de Hg(II), les complexes mononucléaires se transforment en espèces polymétalliques pour adopter une coordination de type HgS_2, très favorable. Les dosages UV et les expériences de spectrométrie de masse confirment la formation de complexes Hg_2P_3 en excès de Hg(II).

L'équilibre de transformation $HgS_2 \rightleftharpoons HgS_3$ est mis en évidence par l'évolution des spectres UV avec le pH, avec des pK_a = 4.3-5.1, qui caractérisent la déprotonation d'un troisième thiol. Ces valeurs sont relativement proches pour les six peptides, ce qui indique que la structure des peptides affecte peu la stabilité des complexes de Hg(II). Cependant, la

tendance observée révèle que le motif CxCxxC dans le peptide cyclique **P^{3C}** est plus favorable que le motif CxCxC, et que les structures cycliques sont plus favorables que les linéaires. Il est intéressant de noter que ces pK_a ont des valeurs significativement en dessous de celles obtenues avec les « three-stranded coiled coils » (pK_a = 7-9), probablement grâce à une hydratation plus forte des groupes thiols accessibles à l'eau dans nos peptides de structures exposées.

Les constantes apparentes de stabilité des complexes HgP ont été déterminées à pH = 2.0 par compétition avec I^-. Les six peptides ont des affinités similaires pour le Hg(II), ce qui montre que la pré-orientation des groupes donneurs n'a qu'une influence modeste sur les stabilités et que la forte affinité du Hg(II) pour les groupes thiolates gouverne la formation de la coordination HgS_2 préférée. Les constantes de stabilité apparentes estimées à pH = 7.4 montrent une affinité pour le Hg(II) plus forte de 20 ordres de grandeurs que pour le Cu(I) en raison du caractère plus mou du Hg(II). Les stabilités des complexes HgP sont similaires à celles mesurées avec des chélateurs classiques des métaux lourds comme le BAL, qui forme un cycle chélate à cinq chaînons très stable par la coordination de deux groupes thiolates. Par ailleurs, nos peptides à 3 cystéines ont une affinité pour le Hg(II) plus grande que le peptide rigide CDPPC portant 2 cystéines, car le nombre de groupes thiolates coordonnés à pH 7.4 est plus élevé. La stabilité élevée et les valeurs faibles des pK_a indiquent que ces peptides sont bien adaptés pour une coordination efficace du Hg(II) par trois groupes thiolates.

La différence dans la coordination des peptides vis-à-vis des deux ions mous Hg(II) et Cu(I) démontre que l'utilisation du Hg(II) comme ion modèle pour la coordination du Cu(I) avec des peptides ou des protéines riches en soufre dans des conditions physiologiques n'est pas toujours appropriée.

Dans une dernière partie, l'effet de la pré-organisation sur la coordination d'ion métallique a été étudié avec deux tétrapeptides dans lesquels les deux cystéines sont liés dans un motif de type coude β : DPro-Pro (CDPPC) et Pro-Gly (CPGC). La structure plus rigide de CDPPC a été confirmée par des études en température par RMN du proton, qui montrent l'existence d'une liaison hydrogène intramoléculaire entre groupe C=O de la Cys1 et le groupe NH de la Cys4. Les dosages UV, CD et RMN révèlent que CDPPC forme un seul complexe de Cu(I) jusqu'à l'addition de 1.33 équivalents de Cu(I). La RMN DOSY et l'ESI-MS prouvent que c'est un cluster de type Cu_4P_3 avec un cœur Cu_4S_6 dans lequel les ions Cu(I) sont liés dans la coordination favorable trithiolate. Il est intéressant de noter que ce

peptide simple est capable d'imiter la formation des clusters Cu(I)-thiolates identifiés dans de nombreuses protéines impliquées dans l'homéostasie du cuivre, comme Cox17 ou Ctr1. Au contraire, les données expérimentales avec le tétrapeptide plus flexible CPGC montrent la formation d'un mélange de complexes polymétalliques de Cu(I). Les différences observées démontrent l'importance de la structure du peptide et de sa pré-organisation dans le contrôle de la spéciation des complexes de Cu(I). De plus, la constante apparente de stabilité calculée pour un complexe 1:1 CuP est plus grande d'un ordre de grandeur pour le peptide rigide CDPPC ($\log\beta_{11}^{pH7.4} = 17.5$) que pour le peptide plus flexible CPGC ($\log\beta_{11}^{pH7.4} = 16.4$).

Les complexes de Zn(II) formés avec CDPPC et CPGC sont des espèces mononucléaires ZnP ou ZnP_2. Les constantes apparentes de stabilité calculées pour le complexe ZnP sont de l'ordre de 10^6 et la sélectivité pour le Cu(I) par rapport au Zn(II) est donc extrêmement élevée.

A nouveau, les complexes du Cu(I) avec CDPPC sont très différents de ceux observés précédemment dans la littérature avec le Hg(II). Cela confirme que l'utilisation du Hg(II) comme modèle du Cu(I) doit être traitée prudemment.

Le peptide CDPPC forme uniquement le cluster Cu_4P_3 avec une grande stabilité et une bonne sélectivité Cu(I)/Zn(II) ; il est donc intéressant pour mettre au point un chélateur intracellulaire du Cu(I), et sa fonctionnalisation afin de pouvoir cibler les cellules hépatiques pour le traitement de maladie Wilson sera donc pertinente dans le futur.

List of publications

Identification number in the Hungarian Collection of Scientific Publications (MTMT): 10054976

Publications related to the dissertation

1. **E. Mesterházy**, B. Boff, C. Lebrun, P. Delangle and A. Jancsó, Oligopeptide models of the metal binding loop of the bacterial copper efflux regulator protein CueR as potential Cu(I) chelators, *Inorg. Chim. Acta*, 2018, **472**, 192-198.
   IF = 2.264
2. **E. Mesterházy**, C. Lebrun, A. Jancsó and P. Delangle, A Constrained Tetrapeptide as a Model of Cu(I) Binding Sites Involving Cu_4S_6 Clusters in Proteins, *Inorg. Chem.*, 2018, **57**, 5723-5731.
   IF = 4.700
3. **E. Mesterházy**, C. Lebrun, S. Crouzy, A. Jancsó and P. Delangle, Short oligopeptides with three cysteine residues as models of sulphur-rich Cu(I)- and Hg(II)-binding sites in proteins, *Metallomics*, 2018, DOI: 10.1039/C8MT00113H. *published online*
   IF = 4.069

   ΣIF = 11.033

Further publication

1. A. Jancsó, B. Gyurcsik, **E. Mesterházy** and R. Berkecz, Competition of zinc(II) with cadmium(II) or mercury(II) in binding to a 12-mer peptide, *J. Inorg. Biochem.*, 2013, **126**, 96-103.
   IF = 3.274

Oral presentations and posters

1. **Mesterházy, E.**, Jancsó, A., Lebrun, C., Tömösi, F., Delangle, P., A Wilson betegség kezelésére potenciálisan alkalmas Cu(I) kelátorok
   50. Komplexkémiai Kollokvium, Balatonvilágos, 2016.
2. **Mesterházy, E.**, Jancsó, A., Lebrun, C., Tömösi, F., Delangle, P., New peptidic Cu(I) chelators as potential candidates for the treatment of Wilson's disease
   13th European Biological Inorganic Chemistry Conference, Budapest, 2016.
3. **Mesterházy**, **E.,** Jancsó, A., Lebrun, C., Delangle, P., Interaction of copper(I) with 12-mer peptides mimicking the metal binding domain of CueR, a copper-efflux regulator
   Journées de Chimie de Coordination de la SCF, Grenoble, 2017
4. **Mesterházy, E.**, Lebrun, C., Jancsó, A., Delangle, P., An Efficient Peptidic Copper(I) Chelator with Two Cysteines Linked by a Strong Turn
   14th International Symposium on Applied Bioinorganic Chemistry , Toulouse, 2017
5. **Mesterházy, E.**, Lebrun, C., Jancsó, A., Delangle, P., Cu(I)ionok hatékony megkötésére alkalmas β-turn motívumot és két ciszteint tartalmazó tetrapeptid
   52. Komplexkémiai Kollokvium, Balatonvilágos, 2018.

6. **Mesterházy, E.**, Lebrun, C., Crouzy, S., Jancsó, A., Delangle, P., Metalloproteinek cisztein-gazdag Cu(I)- és Hg(II)-kötőhelyeit utánzó modellpeptidek
52. Komplexkémiai Kollokvium, Balatonvilágos, 2018.
7. **Mesterházy, E.**, Lebrun, C., Crouzy, S., Jancsó, A., Delangle, P., Oligopeptide models of cysteine-rich Cu(I)- and Hg(II)-binding metal sites of metalloproteins
14th European Biological Inorganic Chemistry Conference, Birmingham, 2018.
8. **Mesterházy, E.**, Jancsó, A., Gyurcsik, B., Berkecz, R., Zinc(II) interaction of a 12-mer peptide and competition of group 12 ions in binding to the ligand
REGIONAL CONFERENCE "Heavy metal as contaminants of the environments". Timisoara, Romania, 2013
9. Balogh, R.K., **Mesterházy. E.**, Gyurcsik, B., Jancsó, A., Christensen, H. E. M., Asaka, M.N., Kato, K., Nagata, K., Réz(I)ionok szelektív kimutatása a CueR fémszabályzó fehérje segítségével
XXXVIII. KÉMIAI ELŐADÓI NAPOK, Szeged, 2015.
10. Balogh, R.K., **Mesterházy. E.**, Kato, K., Nagata, K Jancsó, A., Gyurcsik, B. Detection of toxic metal ions by the CueR metalloregulator
14th European Biological Inorganic Chemistry Conference, Birmingham, 2018.

Acknowledgement

I wish to express my deepest gratitude to my supervisors, Dr. Pascale Delangle and Dr. Attila Jancsó for assisting my scientific development and their valuable help during the years of the PhD and for that they did not give up in the labyrinth of the administration of the co-tutelle.

Many thanks to the Queen of MS, Colette Lebrun for performing the ESI-MS experiments and for her help in the peptide synthesis and HPLC experiments.

I would like to thank Pierre-Alan Bayle his guide with NMR experiments.

I say thank you to Dr. Béla Gyurcsik for giving me the opportunity for the little trips to the field of molecular biology and to Japan.

I owe thanks to my family and to those wonderful people I met in the “PhD room” and in the SyMMES group for their support in the past years.

I kindly acknowledge the financial support providing by the French Government and Campus France enabling the co-tutelle PhD program.